

AN ABSTRACT OF THE THESIS OF

Roger Timothy Kovacic for the degree of Doctor of Philosophy

in BIOCHEMISTRY/BIOPHYSICS presented on June 14, 1976

Title: HYDRODYNAMIC PROPERTIES OF HOMOGENEOUS

DOUBLE-STRANDED DNA

Abstract approved: *Redacted for Privacy*
K. E. Van Holde

Endonuclease R HaeIII was isolated from Haemophilus aegyptius and superhelical circular DNA was isolated from PM2 bacteriophage. The cleavage of PM2 DNA by HaeIII results in 17 restriction fragments. Fifteen of these fragments are unique in both size and sequence and range in size from 94 to 1740 basepairs. These fragments have been isolated by preparative electrophoresis. In addition a mixture of two unique fragments with an average size of 50 basepairs was also isolated. These 16 DNA preparations were the materials used in the experiments which followed.

Moving boundary sedimentation velocity measurements were made on each of the 16 DNA preparations to provide a measure of DNA conformation in solution. There was no concentration or speed effect observed for the largest fragment over a concentration range of 7.5 to 15 μ g/ml and speeds of 34,000 to 48,000 rpm. The maximum deviation in $s_{20,w}^0$ from the mean for any particular preparation was 1.6%. Deviations were usually less than 1.0%.

The molecular weights of the fragments were determined by analytical electrophoresis. SV40-Hind, SV40-HaeIII, SV40-Hind-HaeIII, λ -Hind and PM2-HaeIII restriction digests were coelectrophoresed in a 3.0% acrylamide slab gel in order to establish the size of the PM2-HaeIII restriction fragments. To best fit the data a sigmoidal curve fitting procedure was developed and applied. The procedure provides a curve which is consistent with the data over the full size range. Short column sedimentation equilibrium measurements carried out to determine the molecular weights of several of the fragments by independent means verify the molecular weights from gel electrophoresis. However, the equilibrium method was not reproducible enough to unequivocally establish the molecular weights of the fragments.

From the results of the above experiments it was found that the $s_{20,w}^0$ was a monotonically increasing function of the molecular weight. This is consistent with a unique Kuhn statistical length. The data are also consistent with the Yamakawa-Fujii theory for wormlike cylinders. In the range of sizes which DNA is well modeled by a rigid rod experiment agrees with theory if a helix diameter of 27 \AA and $\bar{v} \rho_0$ of 0.5385 are assumed. In the region of transition from rigid rod to wormlike coil behavior the agreement is good if a statistical length of 1200 \AA and the same diameter and $\bar{v} \rho_0$ are assumed. Comparison of the results presented here with other

theories for the wormlike coil would also prove interesting. The conclusion that the Kuhn statistical length is independent of sequence should be verified by measurement of the rotational diffusion coefficient for these fragments. The dependence of the Kuhn statistical length on temperature and ionic strength would also clarify the relationship of sequence to Kuhn statistical length. It is important, however, to study fragments which range in size from 1 to 4 Kuhn statistical lengths since their hydrodynamic properties should be the most sensitive to the effects of sequence heterogeneity.

© 1976

ROGER TIMOTHY KOVACIC

ALL RIGHTS RESERVED

Hydrodynamic Properties of Homogeneous
Double-Stranded DNA

by

Roger Timothy Kovacic

A THESIS

submitted to

Oregon State University

in partial fulfillment of
the requirements for the
degree of

Doctor of Philosophy

Completed June 14, 1976

Commencement June 1977

APPROVED:

Redacted for Privacy

Professor of Biophysics
in charge of major

Redacted for Privacy

Acting Chairman Department of Biochemistry and Biophysics

Redacted for Privacy

Dean of Graduate School

0

Date thesis is presented June 14, 1976

Typed by Susie Kozlik for Roger Timothy Kovacic

ACKNOWLEDGEMENTS

I especially thank Professor K. E. Van Holde for his guidance and understanding during the course of this work. Professor Lyle R. Brown of the Department of Microbiology was very helpful in providing me with advice, help and laboratory space while I grew the Haemophilus aegyptius from which Endonuclease R HaeIII was isolated. I also thank Professor George D. Pearson for his advice and encouragement during the course of this work.

Ms. Maureen Drury provided excellent technical assistance with the sedimentation studies carried out in this thesis. Mrs. Georgia Riedel prepared many DNA gels and provided general technical assistance.

I thank Dr. Dennis Lohr and Dr. Barbara Shaw for many interesting discussions and for their encouragement. I very much appreciate the support which I received from my fellow students, Chintamen Sahasrabuddhe, Neal Eldred, Jeff Corden, Kelly Tatchell, Don Blair, George Rose and Fumio Arisaka.

TABLE OF CONTENTS

	<u>Page</u>
INTRODUCTION	1
MATERIALS AND METHODS	11
Permanent Stock Cultures	11
Preparation of PM2 Stocks	12
Large Scale Lysates	13
Large Scale Harvest	15
Concentration of PM2 Lysates	15
PM2 DNA Isolation	17
Large Scale Growth of <u>Haemophilus aegyptius</u>	18
Isolation of Endonuclease R <u>HaeIII</u>	20
Analytical Gel Electrophoresis	23
Acrylamide Gels	23
Agarose Gels	24
Agarose-Ethidium Bromide Gels	25
Preparative Gel Electrophoresis	25
Sedimentation Analysis	28
Corrections to Standard Conditions	31
Computer Aided Calculations	32
RESULTS	35
PM2- <u>HaeIII</u> Fragments	35
Sedimentation Equilibrium Studies	40
Calibration of Molecular Weights by Gel Electrophoresis	49
Sedimentation Velocity Results	72
DISCUSSION	86
CONCLUSIONS	96
BIBLIOGRAPHY	99
APPENDICES	
Appendix I: Media, Standard Solutions and Special Procedures	105
Appendix II: Polyacrylamide Gel Electrophoresis	113
Appendix III: Programs for the Hewlett Packard 9821A Calculator	121

LIST OF FIGURES

<u>Figure</u>		<u>Page</u>
1	Analytical Electrophoresis Pattern of Whole PM2- <u>Hae</u> III Digest and the Isolated Fragments D, E, F, G and H	36
2	Scan of a Gel Containing PM2- <u>Hae</u> III Digest Stained with Toluidine Blue 0	37
3	Scan of a PM2- <u>Hae</u> III Digest Electrophoresed Under Denaturing Conditions	39
4	Upward Curvature in the Plot of $\ln c$ vs $r^2 - r_o^2$ for Sedimentation Equilibrium Data	41
5	Normal Plot of $\ln c$ vs $r^2 - r_o^2$ for Sedimentation Equilibrium Data	42
6	Plot of $\ln c$ vs $r^2 - r_o^2$ for a Sedimentation Equilibrium Experiment with Alkali Denatured DNA	43
7	Calibration of the PM2- <u>Hae</u> III Digest with SV40- <u>Hae</u> III Fragments	52
8	Ferguson Plot for PM2- <u>Hae</u> III Fragments Electrophoresed in 3 to 6% Acrylamide (20:1) Gels	62
9	Sigmoidal Fit for PM2- <u>Hae</u> III Fragments Electrophoresed in 3 to 6% Acrylamide (20:1) Gels	63
10	Sigmoidal Fit for PM2- <u>Hae</u> III Fragments Electrophoresed in 0.7 to 2.0% Agarose-Ethidium Bromide Gels	64
11	Sigmoidal Fit for PM2- <u>Hae</u> III Fragments Electrophoresed in 4 to 6% Acrylamide (40:1) Gels	65
12	Calibration of the PM2- <u>Hae</u> III Digest by Coelectrophoresis with 4 Other Restriction Digests in a 3% Acrylamide (20:1) Slab Gel	70
13	Effect of $\bar{v}p_o$ and η_o on the Shape of the Yamakawa-Fujii Theoretical Curve	81

<u>Figure</u>		<u>Page</u>
14	Effect of d and λ^{-1} on the Shape of the Yamakawa-Fujii Theoretical Curve	83
15	Comparison of the Empirical Relationship Between $s_{20,w}^0$ and M_w with the Predictions of the Yamakawa-Fujii Theory	84

LIST OF TABLES

<u>Table</u>	<u>Page</u>
1 Molecular Weights of PM2- <u>Hae</u> III Fragments Determined from Sedimentation Equilibrium Experiments	44
2 Calibration of PM2- <u>Hae</u> III Fragments by Comparison With SV40- <u>Hae</u> III Fragments	53
3 Calibration of PM2- <u>Hae</u> III Fragments by Comparison With Ad2-RI Fragments	55
4 Phillipsen's Calibration of PM2- <u>Hae</u> III Fragments by Comparison With PM2- <u>Hind</u> Fragments	56
5 The V_m , Slope, Intercept and Relative V_m for the Sigmoidal Fits Shown in Figures 9, 10, 11	66
6 Sizes of PM2- <u>Hae</u> III Fragments Calculated From the Sigmoidal Fit in Several Gel Systems	68
7 Sizes of PM2- <u>Hae</u> III Fragments From Sigmoidal and Linear Fits to the Data for Five Restriction Digests Coelectrophoresed in a 3.0% Acrylamide (20:1) Slab Gel	71
8 Molecular Weight and Average $s_{20,w}^0$ for PM2- <u>Hae</u> III Fragments	73
9 Coefficients of Yamakawa-Fujii Equation 1 for Several Combinations of the Helix Diameter and the Kuhn Statistical Length	76
10 Coefficients of the Modified Yamakawa-Fujii Equation 2 for Several Combinations of the Helix Diameter and the Kuhn Statistical Length	77
11 Coefficients of Yamakawa-Fujii Equation 3 for Several Combinations of the Helix Diameter and the Kuhn Statistical Length	79
12 Coefficients of the Modified Yamakawa-Fujii Equation 4 for Several Combinations of the Helix Diameter and the Kuhn Statistical Length	80

HYDRODYNAMIC PROPERTIES OF HOMOGENEOUS DOUBLE-STRANDED DNA

INTRODUCTION

Interest in the conformation of DNA molecules in solution has been rekindled by new questions raised in the process of extending our knowledge of the mechanisms of genetic structure and control to the molecular level. Of particular interest are the relationship between DNA conformation in solution and in chromatin and the role played by DNA tertiary structure in genetic recognition events. Unfortunately the conformational states of DNA cannot be measured directly and so indirect measures of the conformation must be found. The simplest measure of conformational state is the translational diffusion coefficient. From a combination of the diffusion coefficient and the molecular weight one may simply determine if a polymer like DNA has an extended or compact conformation. In practice, however, translational diffusion coefficients for macromolecules are difficult to measure directly. The usual approach, therefore, is to combine measurements of the molecular weight with the Svedberg coefficient which is determined from the sedimentation of the macromolecule in an ultracentrifuge.

The Svedberg coefficient, s , can be shown to be

$$s = \frac{M(1 - \bar{v}\rho)}{N_A f}$$

where M is the molecular weight in grams/mole, \bar{v} is the partial specific volume of the polymer in the buffer of choice, ρ is the density of the buffer, N_A is Avogadro's number and f is a function of the conformation of the polymer (1). The factor f is called the translational friction coefficient and is defined if s , M , \bar{v} and ρ can be determined. Alternatively f can be determined by reference to available semiempirical theories which relate the shape of a molecule in solution to its frictional properties. These theoretical considerations are considerably simplified for double-stranded DNA by the information already available about DNA structure. Double-stranded DNA is extended and highly asymmetric. Base stacking and the two helically interwound backbones impart a good deal of rigidity to the structure. Therefore, a simple model for relatively short DNA might be a rigid rod. For extremely high molecular weight DNA the overall conformation is thought to be that of a random coil. Kuhn first suggested that the DNA random coil could be mathematically described as a series of rigid segments of uniform length separated by entirely flexible joints (2). The length of one segment has been called the Kuhn statistical length (λ^{-1}) and is a measure of the flexibility of the polymer. More recent work has focused on the conformational state which is intermediate between the rigid rod and the random coil states. This conformational state has been called the stiff coil or wormlike coil because it is modeled on a

flexible cylinder with a constant cross section. The Kuhn statistical length is retained as a measure of flexibility even though the nature of the model has changed (3-5). It should be emphasized, however, that these models provide a mathematical framework within which to construct a description of the behavior of DNA in solution. The physical changes at the molecular level which produce the observed conformation need not be the same as those postulated by either model.

The Yamakawa-Fujii theory for the behavior of polymers which may be modeled by wormlike cylinders is probably the most sophisticated theory yet described (5). In the formulation of the Yamakawa and Fujii theory the frictional coefficient f is related to λ^{-1} and Ξ by the equation:

$$f = \Xi \lambda^{-1}$$

If f in the Svedberg equation is replaced by $\Xi \lambda^{-1}$ the equation is

$$s = \frac{\lambda M(1 - \bar{v}\rho)}{N_A \Xi}$$

For polymers of uniform mass per unit length, M_L , and length, L , where L is in units of λ^{-1}

$$\lambda M = M_L L$$

and the Svedberg equation may be rewritten

$$s = \frac{M_L L (1 - \bar{v} \rho)}{N_A \Xi}$$

Since the relationship $3\pi \eta L / \Xi$ has been calculated by Yamakawa and Fujii a third equation may be written

$$s = \frac{M_L (1 - \bar{v} \rho)}{N_A (3\pi \eta)} \frac{3\pi \eta L}{\Xi}$$

where η is the solvent viscosity in poise. As a rule sedimentation velocity data are corrected to hypothetical conditions of zero polymer concentration and sedimentation in water at 20° C. Under the standard conditions the equation can be written

$$s_{20,w}^o = \frac{M_L (1 - \bar{v} \rho_o)}{N_A (3\pi \eta_o)} \frac{3\pi \eta_o L}{\Xi}$$

in which ρ_o is the density of water at 20° C, η_o is the viscosity of water at 20° C and \bar{v} is the partial specific volume at 20° C. In view of the requirement of a counterion atmosphere to maintain DNA in its double-stranded form \bar{v} is usually determined in a standard sodium chloride solution and the resulting \bar{v} for NaDNA is substituted for the \bar{v} of DNA. The result is that the factor

$$\frac{M_L (1 - \bar{v} \rho_o)}{N_A (3\pi \eta_o)}$$

is constant for DNA of a given base composition and the dependence of $s_{20,w}^0$ upon the frictional coefficient is described by

$$\frac{3\pi\eta_0 L}{\Xi}$$

Yamakawa and Fujii have calculated the relationship between the factor $3\pi\eta_0 L/\Xi$ and the molecular dimensions L and d as corrections to the rigid rod model in the lower limit and the random coil in the upper limit. Therefore $3\pi\eta_0 L/\Xi$ is described by two equations, one for $L < \sigma$ and the other for $L \geq \sigma$. Sigma is chosen to be 2.278; that is, it is a length corresponding to 2.278 Kuhn statistical lengths. The explicit expressions for $3\pi\eta_0 L/\Xi$ are given in Results.

The principal object of this thesis is to establish the empirical relationship between the $s_{20,w}^0$ and the molecular weight for double-stranded DNA in the size range which covers the conformational transition from rigid rod to wormlike coil behavior and compare the data to the Yamakawa-Fujii theory. In order to do so we have sought a source of homogeneous DNAs in this size range.

Size heterogeneity has always been a complication to those attempting to determine the conformation of the molecular weight of double-stranded DNA in solution. Burgi and Hershey (6) and Studier (7) were among the first investigators to approach these problems by studying the sedimentation velocity of whole and carefully sheared

bacteriophage DNAs. Crothers and Zimm (8) and Gray and Hearst (9) made additional measurements using phage DNAs. They compared their results with the available theories for relating molecular dimensions to the molecular weights and $s_{20,w}^0$ observed. However, bacteriophage and viral DNAs are rather large and though useful for developing wormlike coil models, the data obtained do not reveal much about the behavior of small DNAs.

Recently the conformation of DNA of limited polydispersity has been studied to ascertain if the conformation of small DNAs in solution may be modeled by a rigid rod. Prunell and Bernardi enzymatically degraded DNA and then fractionated native and denatured DNA by exclusion chromatography. This material was then used to establish the relationships between $s_{20,w}^0$, k_{av} , $[\eta]$ and M . Their work covered the molecular weight range of 2.9×10^4 - 2.9×10^5 daltons for native DNA and 2.5×10^4 - 1.4×10^5 daltons for denatured DNA (10). Record, Woodbury and Inman fractionated sonicated double-stranded DNA by exclusion chromatography in order to study the melting behavior of these fragments. They also determined the relationship between $s_{20,w}^0$ and M over a molecular weight range similar to that studied by Prunell and Bernardi (11).

In this thesis restriction fragments were isolated by preparative electrophoresis as an alternative to fractionating heterogeneous

DNA. The DNA isolated in this way is homogeneous in both size and sequence just as undegraded bacteriophage DNA is. However, the isolated restriction fragments range in size from 3.3×10^4 to 1.2×10^6 daltons so that the relationship between $s_{20,w}^0$ and M can be studied over a much lower molecular weight range than with whole bacteriophage DNAs.

DNA restriction fragments are produced from large DNA by the endonucleolytic activity of one or more of a group of nucleases called restriction enzymes. Current work on the structure, function and properties of these interesting nucleases has been reviewed in several recent reviews (12-14). Of particular interest in this work is the group of enzymes designated type two restriction endonucleases by Boyer (13). These restriction endonucleases produce double-stranded breaks within or near certain sequences of bases in the double-stranded DNA. Therefore they produce unique fragments of DNA from larger pieces of unique DNA. For a relatively small, unique DNA, such as a bacteriophage DNA, a small number of fragments which are unique in both size and sequence is produced. The resulting fragments are well resolved by analytical gel electrophoresis. Therefore preparative gel electrophoresis of the restriction digest seemed a logical way in which to recover the individual fragments. Furthermore the continuous elution method developed by Hagen and Young for the preparation of RNA seemed readily

adaptable for the preparative electrophoresis of DNA (15).

The bacteriophage PM2 was selected as a source of DNA because the DNA is small (9,900 basepairs or 6.56×10^6 daltons (16)), the base composition is similar to calf thymus DNA (17) and the DNA can be isolated in 50 mg quantities. Furthermore the bulk of the DNA isolated from the bacteriophage is circular and superhelical. Therefore this DNA contains no single-stranded breaks. Although Hays and Zimm have reported that single-stranded breaks do not affect the sedimentation properties of DNA it seemed important to minimize "nicking" as much as possible (18).

The restriction nuclease chosen to digest the PM2 DNA was endonuclease R HaeIII which was isolated from Haemophilus aegyptius bacteria. The nomenclature used describing the enzymes and restriction fragments is that suggested by Smith and Nathans (19) except that an abbreviation for the source of the DNA precedes the suggested nomenclature for the restriction fragments. Therefore a particular digestion fragment is identified by the following elements in order: (a) an abbreviation for the source of DNA (b) the abbreviation for the enzymatic activity suggested by Smith and Nathans and (c) the letter designation for the fragment. Smith and Nathans have suggested that restriction fragments be lettered alphabetically in order from largest to smallest; where the context is clear the letter is sufficient identification. However several other

restriction digests have been used in this work to provide molecular weight standards. Therefore the complete identification for each of these digests will be used in most cases. For the reader's convenience the abbreviations which will be used are explained below. The abbreviation PM2-HaeIII-A designates the largest fragment from the digestion of PM2 DNA with HaeIII. A digest of simian virus 40 (SV40) DNA with HaeIII is abbreviated SV40-HaeIII. The abbreviation EcoRI identifies a restriction nuclease isolated from Escherichia coli which carry the drug resistance transfer factor RI; the abbreviation for this activity is often abbreviated to RI. A digest of Adenovirus type 2 DNA with RI is therefore denoted Ad2-RI. A mixture of two enzymatic activities can be isolated from Haemophilus influenzae serotype d and so a digest of PM2 DNA with this mixture may be called PM2-Hind. DNA extracted from the bacteriophage lambda and digested with Hind is designated λ -Hind. SV40 DNA digested with both Hind and HaeIII activities is designated SV40-Hind-HaeIII.

There are several properties of endonuclease R HaeIII which make it particularly suited to the requirements of this study. The nuclease has been reported to cleave each strand of a double-stranded DNA between the guanine (G) and cytosine (C) residues of the sequence 5'-GGCC-3' (19). The result is a double-stranded cleavage with no single-stranded character because G and C form

complementary pairs. In contrast both shearing and random nuclease digestion must produce some single-stranded material. If the HaeIII enzyme preparation is completely free of contaminating endo- and exonucleases the PM2-HaeIII digest should be completely double-stranded. Preliminary experiments with the HaeIII preparation revealed it to be remarkably free of other endonuclease activity; large excesses of the enzyme incubated for long time periods with small amounts of DNA revealed no apparent degradation of the double-stranded material. The small size of the restriction site recognized is also particularly useful in this study because more small fragments are produced. The enzyme should cleave DNA which is 50% GC into fragments which are on the average 256 base-pairs (bp) long. If the base composition of PM2 is taken into account the average size is approximately that predicted. The broad range of sizes produced also make the PM2-HaeIII digest particularly useful in this study.

MATERIALS AND METHODS

Endonuclease R-HaeIII and SV40 DNA used in preliminary experiments were the generous gift of Dr. John Newbold, University of North Carolina. A stock culture of Haemophilus aegyptius was obtained from Dr. Marshall H. Edgell and Dr. Clyde W. Hutchison, University of North Carolina. Stocks of PM2 bacteriophage and BAL31, the marine pseudomonad which hosts PM2, were obtained from Dr. Stuart Linn, University of California, Berkeley. Endonuclease R-EcoRI digests of Adenovirus type 2 DNA were the gift of Dr. George Pearson, Oregon State University. SV40 DNA (strain 776) was the generous gift of Dr. Gary Ketner, Johns Hopkins University. Lambda DNA was the gift of Dr. Lyle Brown, Oregon State University.

Permanent Stock Cultures

BAL31 was preserved by growing cells to early midlog phase in BAL broth (Appendix 1), making the suspension 20% glycerol and freezing in liquid nitrogen. After preparing a fresh lysate as described below and removing the cell debris PM2 lysate was preserved by adding glycerol to 7 1/2% and freezing. Freezing immediately reduces the titer by two orders of magnitude but the remaining viable phage are stable indefinitely. For periods of 1-2 months BAL31 plates and PM2 lysates may be stored at 4° C.

Midlog cultures of Haemophilus aegyptius were frozen in liquid nitrogen after an equal volume of glycerol was added aseptically. Because H. aegyptius dies rapidly when not actively dividing the frozen stock must be rapidly thawed and immediately transferred to fresh prewarmed medium or streaked immediately on fresh prewarmed rabbit blood agar plates (Appendix 1).

All cultures were stored at -70°C . PM2 and BAL31 stocks seem stable indefinitely, but Haemophilus aegyptius stocks should be renewed at six month intervals.

Preparation of PM2 Stocks

The procedures of Espejo and Canelo (17) as modified by Le Pecq (20) formed the basis for the procedure outlined below. High titer lysates, 1×10^{11} plaque forming units (pfu/ml), were prepared one to two days in advance of each large scale preparation by innoculating 50 ml of a culture of BAL31 in early log phase with 0.1 ml of low titer ($10^7 - 10^9$ pfu/ml) PM2 stock and incubating overnight at 25°C . Growth medium is BAL broth (Appendix 1) which must be vigorously shaken so that good aeration is maintained throughout the growth period. Titters were assayed as outlined by Le Pecq using BAL top and bottom agars (20) (Appendix 1).

Large Scale Lysates

Large scale lysates were prepared in a 100 liter fermenter (Stainless and Steel Products Co.) by adding the salts and Nutrient Broth (Difco) required to 50 liters of distilled water. The medium was sterilized 15-45 minutes and then cooled to 25° C. The fermenter was then inoculated with 50 ml of an overnight culture of BAL31 diluted with 500 ml of sterile BAL broth. Aeration was maintained at 20 liters/min. with the slowest stirring rate available. After four hours of continuous growth aliquots were withdrawn at 1/2 hour intervals and air bubbles trapped in the aliquot allowed to disperse; the optical density at 550 nm (OD_{550}) was then measured on a Bausch and Lomb 340 Spectrometer. When the OD_{550} reached 0.15 the input port was sterilized and an aliquot of fresh lysate equivalent to 3.5×10^{10} pfu of PM2 lysate was diluted with 500 ml of sterile BAL Broth and added to the contents of the fermenter. As a result of the sterilization procedures the infection is delayed approximately 20 minutes from the initial reading; by 30 minutes the OD_{550} was usually equal to 0.2. Lysis is generally complete 4-6 hours after infection.

The timing of the infection step appears to be particularly important since infections begun when the OD_{550} is 0.15 but not completed until the OD_{550} was over 0.25 resulted in poor titers

($<1 \times 10^{11}$ pfu/ml) even though the input of PM2 was doubled. It should be pointed out that the infection process described here involves at least two lysis-reinfection cycles so that most of the bacteria are not infected until after the second lysis. The critical factor which decides the phage yield therefore is the timing of the second lysis relative to the point in the growth curve at which BAL31 becomes resistant to PM2. The growth temperatures along with the timing of the initial infection can be used effectively to produce consistently high titers. Lowering the growth temperature appears to increase the bacterial generation time without much effect on the phage generation time so that the timing of infection and therefore of the second lysis becomes less crucial. In any event good aeration is important to high yields; this is complicated by the sensitivity of the phage to most antifoams. As a result antifoam was not used in growing the bacteriophage and the fermenter was operated at half of the maximum capacity.

In one case aliquots of the cell suspension taken at four hours cleared after standing a few minutes without aeration while the bulk of the aerated suspension did not clear until six hours post infection. As this lysate yielded the highest recorded titer it would appear that some kind of delayed lysis occurred which permitted the overproduction of PM2 and which might be exploited by the proper timing of infection and manipulation of the growth temperature and aeration.

Large Scale Harvest

To avoid wasting dextran sulfate (used in the concentration step following) titers were taken before harvesting the contents of the fermenter. Because 8-12 hours are required for plaques to develop on the plates, aeration was stopped and cold tap water was circulated through the water jacket effectively halting all growth. Aeration was continued in one experiment to assess the effect that regrowth of the BAL31 had on the titer. Fortunately the titer of PM2 is not affected by overgrowth of the culture with BAL31 in stationary phase so that growth need not be halted as above.

If the titer was better than 1×10^{11} pfu/ml cell debris was removed by passing the lysate through a Super Sharples continuous flow centrifuge and collecting the lysate in a polyethylene garbage can. Alternatively the cell debris was removed and the lysate placed in a cold room so that the concentration step could be begun as soon as the results of the titer were obtained. All subsequent operations were carried out in a cold room (4° C) or on ice.

Concentration of PM2 Lysates

The polyethylene glycol-dextran sulfate method of phase separation as described by Espejo and Canelo (17) was used. However, in place of adding separate solutions of the two polymers or adding a

solution of a mixture of the two, solid polyethylene glycol 6000 was first dissolved in the lysate and then solid sodium dextran sulfate (Pharmacia) was dissolved. Final concentrations of the polymers on a weight to weight basis were 6:1:93 PEG:NaDexSO₄:H₂O. The mixture was stirred periodically for four hours after the addition of the polymers and then allowed to stand for twenty hours. The supernatant was then siphoned into another polyethylene garbage can and the dextran sulfate-rich phase at the bottom collected. The supernatant was then returned to the original container, thoroughly stirred and allowed to settle for an additional forty-eight hours. At the end of that time the supernatant was again siphoned off and the bottom phase collected. The pooled interphases were then thoroughly mixed and the phases re-separated by centrifuging in the Sorvall GSA-3 rotor for ten minutes at 5,000 rpm. The upper phase was removed and discarded; the interface was collected; and the lower phase was pooled, rehomogenized and centrifuged again until it was no longer practical to collect the interphase material. A volume of NTC (Appendix 1) equal to the volume of the pooled interphase material was then added and the mixture homogenized. Next dextran sulfate was removed by the slow addition with very vigorous stirring of one volume of 4 M KCl for every three volumes of phage solution. After all the KCl solution was added, the stirring was stopped and the finely divided potassium dextran sulfate allowed to

settle to the bottom so that the supernatant could be poured off. The supernatant was dialyzed overnight against two changes of NTC buffer. After dialysis 0.359 g of optical grade CsCl/gram of dialyzed phage solution was added to the pooled dialysate and dissolved. The phage-CsCl mixture was then banded to equilibrium by centrifuging for twenty-four hours at 45,000 rpm in the Beckman 50 Ti rotor. The phage band from each tube was collected using a Pasteur pipette.

The bacteriophage may be stored indefinitely in CsCl. However, the DNA in some preparations has become rapidly nicked so that the DNA should be prepared from the phage as soon as possible.

PM2 DNA Isolation

In a typical preparation a suspension of PM2 equivalent to 50 OD₂₆₀/ml is dialyzed against two changes of SCTE (Appendix 1). After dialysis the suspension is made 2% in Sarkosyl (Sigma) by adding one volume of SCTE containing 20% Sarkosyl for each nine volumes of suspension. The mixture is then heated at 60° C for ten minutes, cooled to 37° C and pronase stock solution (Appendix 1) added to a final concentration of 1 mg/ml. The mixture containing pronase is incubated at 37° C for four hours to complete deproteinization. After the incubation 6.7 g of CsCl is combined, in a polyallomer tube for the Spinco 50 Ti rotor, with 7.25 g of a solution

made up of (a) 1.25 ml of digestion mixture (b) 1 ml of ethidium bromide 2.8 mg/ml (c) a balance of 2% Sarkosyl-SCTE. The CsCl is dissolved by sealing the tube with Parafilm and inverting; the tube is then capped, filled completely with mineral oil and sealed. The filled tubes are then centrifuged at 37K for the 36-48 hours required to form the CsCl gradient. The DNA is usually collected by dripping the tube contents from a hole made in the bottom of the tube: the lower band is double-stranded superhelical PM2 DNA; the upper band is relaxed circular or linear PM2 DNA. The ethidium bromide is removed from the DNA by repeated extraction with water-saturated isoamyl alcohol. After all visible color disappears the DNA solutions are extracted six more times and then dialyzed against at least three changes of SSC (Appendix 1) to remove CsCl and isoamyl alcohol. The DNA is routinely stored in SSC at 4° C.

Large Scale Growth of Haemophilus aegyptius

Haemophilus aegyptius causes bacterial conjunctivitis in human beings. The condition is annoying to contract although it is usually easy to treat. Therefore the following precautions are suggested when harvesting the bacteria: (a) wear goggles and a filter mask which covers the nose and mouth (b) wear disposable plastic or rubber gloves when handling the fresh suspension or packed cells.

No special precautions are necessary for the maintenance and transfer of stock cultures.

Haemophilus aegyptius ATCC #11116 is readily cultured in well aerated Brian-Heart Infusion Broth (BHI, Difco) supplemented with 2μ of NAD/ml and $10\mu\text{g}$ of hemin/ml (Appendix 1). The required cells were grown and harvested according to the following protocol: A 50 ml stock culture is maintained by transferring 0.5 ml of growing cells to 50 ml of fresh medium every eight hours. At midnight of the day before the large scale preparation one liter of supplemented BHI is inoculated with 10 ml of the stock culture and incubated at 37°C with vigorous shaking. The following morning the one liter stock is checked for contamination by examination with a phase contrast microscope and a rabbit blood agar plate (Appendix 1) streaked to serve as a further check. The entire one liter volume is emptied into 10 liters of prewarmed medium in a Fermentation Design, Inc. Fermenter. The medium is maintained at 37°C and aerated at 12 liters/min. with Dow Corning Antifoam Y-30 added to control foaming. When the cells have grown to midlog one liter of the suspension is transferred to 10 liters of fresh prewarmed medium which is then maintained at 37°C and aerated as above. The remaining suspension is immediately harvested by passing the uncooled medium through a Sharples continuous flow centrifuge; the freshly inoculated fermenter is harvested when the cells have again

grown to midlog. After each harvest the cells were scraped from the centrifuge bowl, immediately frozen in liquid nitrogen and stored at -70°C . The average yield for 21 liters under these conditions was 28 grams. The above process was repeated until approximately 115 g of cells (wet weight) were accumulated to be carried through the following purification procedure.

Isolation of Endonuclease R HaeIII

The following procedure is a modification of the procedure used by Huang, Newbold and Pagano to prepare "Endonuclease Z", the same activity now called HaeIII (21). Their procedure is a modification of that used by Middleton, Edgell and Hutchison (22) which was in turn a modification of the original Smith and Wilcox procedure for isolating restriction activity from Haemophilus influenzae (23). In the interest of clarity, therefore, the procedure used in this thesis will be described in detail.

The isolated Haemophilus aegyptius cells were thawed and then suspended in 200 ml of SB (Appendix 1). The cells were disrupted by sonicating at full power for five minutes, turning off the power and monitoring the OD_{650} of a 1:200 dilution of the cells, and then resuming sonication after five minutes. As the sonication proceeds the OD_{650} drops to a plateau indicating that all of the cells have been disrupted; the sonication time required for the OD_{650} to

plateau in this case was thirty minutes and would vary depending on the power of the sonicator. To control heating the beaker containing the suspension was placed in a salt water-ice slurry. The sonicated suspension was then centrifuged for two hours at 10,000 rpm in the Sorval GSA rotor to remove the cell debris. The supernatant was then decanted and the optical density of diluted aliquots read at 230, 260, and 280 nm. This procedure provides a crude estimate of the protein and nucleic acid in the solution. A fresh solution of streptomycin sulfate (10%) was then used to precipitate the DNA, which interferes with the enzyme isolation, from the solution. A pilot precipitation in which 0.0, 0.5, 0.1, 0.15, 0.2, 0.25 and 0.3 ml of 10% streptomycin sulfate are added to 1.0 ml aliquots of the supernatant, mixed, left on ice for thirty minutes and centrifuged at 5,000 rpm in the Sorval SS34 rotor was used to determine the minimum proportion of streptomycin sulfate that produced a large increase in OD_{230}/OD_{260} . In the successful preparation this amounted to 0.2 ml/ml of supernatant which corresponded to one ml of streptomycin sulfate/1650 OD_{260} . The streptomycin sulfate was added slowly to the supernatant with moderate stirring in the cold room and the solution allowed to stir overnight. The precipitate was removed the next morning by centrifuging ten minutes at 15,000 rpm in the SS34 rotor and decanting the supernatant. The supernatant was then made 50% saturated in ammonium sulfate by adding 31.3 g of solid ammonium

sulfate/100 ml of supernatant to the solution with stirring in the cold room. Stirring was continued for 15 minutes and the precipitate collected by centrifuging for 15 minutes at 15,000 rpm. The supernatant was decanted and then made 70% in ammonium sulfate by adding 15.9 g of $(\text{NH}_4)_2\text{SO}_4$ /100 ml of the decanted supernatant. The supernatant was decanted and discarded. The pellet is then redissolved in GPB (Appendix 1). The resulting solution was stored on ice in the cold room until the phosphocellulose for the ion exchange chromatography step (Appendix 1) was prepared. The extract was then desalted by exclusion chromatography on a 2.5 x 50 cm G75 Sephadex column previously equilibrated with GPB. The brown salt free extract emerges from the column at the void volume: all fractions containing color and free of ammonium sulfate were pooled and protein determined by the Lowry method (24). A column of freshly prepared phosphocellulose was then packed so that there was one ml of phosphocellulose for each 100 mg of protein. The packing was done in 0.05 M Tris, pH 7.9 and the column then washed with 20 bed-volumes of GPB. The pooled extract was then passed through the column at 10-15 ml per hour. Four bed volumes of GPB following the extract removed the colored material and unbound protein; the bound protein is then eluted stepwise with two bed-volume portions of GPB which were successively 0.1, 0.2, 0.3, 0.5, and 1.0 M in NaCl. Fractions corresponding to 0.5 bed-volume

were collected and assayed for HaeIII activity by incubating 5 μ l of each fraction with 2 μ g of PM2 DNA dissolved in 100 μ l of TBSMgME (Appendix 1). The restriction fragments were detected by electrophoresis in 1.5% agarose-ethidium bromide gels (Appendix 2). Aliquots taken from the fractions containing the bulk of the restriction activity completely digested the PM2 DNA in 1/2 hour at 37^o C. The active fractions were preserved by adding one ml of sterile glycerol to each one ml aliquot of the fractions, mixing and storing at -20^o C.

Analytical Gel Electrophoresis

Acrylamide Gels

The methods of Loening (25) were followed except that the pH of E buffer was 7.2. A detailed description of the procedure used is given in Appendix 2. The percentage of acrylamide was varied over a range of 3.0-6.0% by increasing or decreasing the amount of a stock solution of acrylamide monomer and bis-acrylamide which was added to the other constituents. In some cases the bis-acrylamide:acrylamide ratio was lowered from 1:20 to 1:40 and 4-6% gels were cast. Gels were routinely formed in 0.7 x 30 cm Plexiglas tubes sealed at the bottom with several layers of Parafilm. After at least one hour of polymerization time the Parafilm is replaced

with nylon mesh secured with a rubber band and the gels preelectrophoresed at 80 volts (v) for a minimum of two hours. Samples in 25-100 μ l of buffer made 10% in glycerol are layered onto the gel top and electrophoresed for 4-8 hours at 125 volts. Following electrophoresis the gels are extruded from the tubes with compressed air and stained in 1.0 μ g of ethidium bromide/ml of E buffer. After staining 1-3 hours the DNA may be visualized and photographed by the orange fluorescence of the DNA-ethidium bromide complex under ultraviolet light. Gels were usually photographed through both an ultraviolet haze filter (Tiffen Photar Haze 2-A) and an orange filter (Tiffen Photar Orange) with a Polaroid MP-3 Land camera using type 55 or 107 film.

Agarose Gels

Electrophoresis grade agarose (Biorad or Sigma) was dissolved in E buffer by autoclaving for ten minutes. After autoclaving the solution was mixed and then allowed to solidify. For casting analytical gels this solidified agarose is remelted by autoclaving for ten minutes, and the liquid allowed to cool to 50-60^o C. The warm agarose solution is pipetted into prepared tubes and allowed to polymerize at room temperature for 1/2 hour. To obtain a flat surface to "stack" the sample upon the top of the tube is netted, the tube inverted and the gel seated firmly against the netting; the tightly

stretched Parafilm usually leaves the smooth flat gel surface desired. No preelectrophoresis is needed; the samples are applied as above and electrophoresed for 2-6 hours at 125 v and 5 ma/tube. The gels can then be extruded, stained and photographed as above.

Agarose-Ethidium Bromide Gels

Alternatively 0.5 µg of ethidium bromide/ml of agarose solution may be added when the melted gel reaches 60° C (26); the gels are then cast as described for agarose gels. Running buffer is 0.4 µg of ethidium bromide/ml of E buffer. The principal virtue of this system is the immediate visualization of the results. If glass tubes or a slab apparatus with glass plates are used the progress of the electrophoresis can be continually monitored and the gels can be photographed immediately after removal from the tubes. The electrophoretic mobility of the DNA is reduced in this system however.

Preparative Gel Electrophoresis

The PM2-HaeIII fragments were separated by electrophoresis in acrylamide gels (Appendix 2). The preparative gel apparatus described by Hagen and Young (15), which is currently available from Savant Instruments, Inc., 221 Park Avenue, Hicksville, New York 11801, was used for all preparative electrophoresis. In brief the apparatus consists of a cylindrical gel tube held in a vertical

position by the upper buffer reservoir. An elution chamber fits over the bottom of the tube and the lower part of the tube and the elution chamber are immersed in the lower buffer reservoir. In operation the DNA is electrophoresed continuously toward the elution chamber; buffer is constantly pumped through the elution chamber and sweeps away the DNA as it is eluted from the end of the gel. The effluent is continuously monitored at 254 nm with an Altex Model 153 column monitor equipped with the 100 μ l biochemical flow cell.

Some idea of the difficulties in preparatively resolving the PM2-HaeIII digest can be obtained from the analytical electrophoresis pattern shown in Figure 1 of the Results. For example the bands identified in Figure 1 as A and B lie quite close together and as a result are difficult to resolve from each other. However the smaller fragments such as L, M, N and O are difficult to resolve preparatively because they move more rapidly through the gel than the larger fragments. Therefore several combinations of gel, elution flow rates and DNA loadings were tried and the following guidelines adopted as a result of these experiments: 1) Maintain constant pumping rates of 6.5-7.5 ml/hr and a fraction size of 0.5-2.0 ml. Fast pumping and small fraction sizes provide the best resolution for the small fragments. 2) Vary the length of the gel to promote separation rather than varying the gel percentage. 3) Use the

optimum loading of 250 μ g for 1.7 cm diameter gels. Up to 1.0 mg may be applied, but resolution suffers and the most concentrated bands begin to "stick" to the gel. 4) Pool and concentrate the unresolved fragments from a short low resolution gel and then separate the individual fragments by rerunning under high resolution conditions. The low resolution step may be skipped at the expense of recovering the larger fragments.

A typical preparative electrophoresis run, therefore, begins with 250 μ g of PM2-HaeIII digest in 200 μ l of E buffer applied to the top of a 4 cm 4% acrylamide (40:1 ratio of acrylamide:bis-acrylamide) gel. Electrophoresis is complete in 20 hours; fragments A, B and C are well resolved; the groups of fragments D-H, I-K and L-P are well resolved from each other; and H, K and P may be recovered in a relatively pure state if the fractions are well resolved. For high resolution electrophoresis a 12 x 1.6 cm 3.5% acrylamide gel (20:1) is used. Pooled fragments from several low resolution runs are concentrated on hydroxylapatite (Biorad, DNA grade) and eluted with 0.4 M PB (27) (Appendix 1). The eluate is dialyzed against E buffer and the DNA collected by mixing with three volumes of cold ethanol, precipitating at -20⁰ C overnight and centrifuging at 12,500 rpm in the Sorval SS34 rotor for 0.5 hour. The pellet is redissolved in 200 μ l of 0.1 E buffer, 10% glycerol and layered on top of the gel. Electrophoresis is initiated at 50-75 v

and 15 ma and is continued for 24-48 hours. Yields are 80-90% of the applied OD but may vary depending on the exact loading. The limiting factor seems to be the amount of DNA per peak rather than the size of the DNA in the peak. If the DNA concentration is too high the peak broadens and trails so that both the yield and resolution are reduced.

Sedimentation Analysis

All measurements were made on the Model E ultracentrifuge using scanner optics. Sedimentation velocity measurements were obtained from conventional boundary sedimentation experiments in 12 or 30 mm double-sector cells at DNA concentrations of 5-25 $\mu\text{l/ml}$. Most sedimentation velocity measurements were carried out in BPES (28) (Appendix 1) at 48,000 rpm. In this buffer (ionic strength = 0.201) DNA concentration had no effect on the s values obtained for Fragment H (~ 500 bp) over the full range of concentration. Because concentration effects are more pronounced for large DNAs Fragment A (~ 1740 bp) was sedimented at concentrations of 7.5 and 15 $\mu\text{g/ml}$. No significant effect ($< 1\%$ difference) was found. It was unnecessary to exceed 15 $\mu\text{g/ml}$ because 30 mm double sector cells and the scanner were available. Therefore the remaining velocity measurements were performed at or below 15 $\mu\text{g/ml}$ in 30 mm cells and no extrapolation to zero DNA concentration was made.

To test for the speed dependence of the sedimentation coefficient Fragment D (≈ 850 bp) at a concentration of $5 \mu\text{g/ml}$ was sedimentated at 48,000 rpm and at 34,000 rpm. There was no significant difference between the sedimentation coefficient obtained from these two runs (difference on the order of 1%). Because the speed dependence of the sedimentation coefficient increases as a function of both DNA size and concentration, Fragment A was also tested as above at a concentration of $15 \mu\text{g/ml}$. The two values obtained deviated from each other by less than 1%; they were also the extremes of the deviations observed; in any event the speed dependence for the sedimentation coefficient of 1740 bp DNA at concentrations below $15 \mu\text{g/ml}$ seems negligible.

Sedimentation equilibrium measurements were carried out on native DNA at a sodium ion concentration of 1.002 M (EQB, Appendix 1). The short column technique of Van Holde and Baldwin was adopted to shorten the time required for the DNA to redistribute itself (29). In some experiments the overspeeding technique of Howlett and Nichol was also exploited to shorten the time to equilibrium since the diffusion coefficient is very small for large DNA (30). In one experiment alkaline equilibrium buffer (AEQB, Appendix 1) was used to determine the single-stranded molecular weight. The sodium ion concentration of AEQB is 1.002 M and the partial specific volume (\bar{v}) of single-stranded DNA was assumed to be the

same as that of double-stranded DNA.

In all cases baselines were obtained at the end of the run by increasing the speed to 48,000 rpm to completely sediment the DNA and then reducing the speed to the equilibrium speed for the baseline scans. This procedure presents three difficulties: (a) The meniscus positions have changed, probably due to leakage under the high pressures developed. (b) The baseline at the bottom of the cell is more or less obscured by the DNA which has been sedimented and (c) The DNA becomes more difficult to sediment for the smaller molecular weight fragments.

The scanner was operated at the lowest scanning speed and the chart recorder run at 5 mm/sec. to provide a detailed and expanded record of the concentration gradient. Five such scans were made of each equilibrium and three scans of each baseline. The data were then converted to O.D. units from a least squares line obtained from the calibration stairsteps and the scans averaged point by point. The averaged equilibrium data was then corrected for the baseline by a point by point subtraction of the averaged baseline data. Subsequent calculations were carried out as discussed under Computer Aided Calculations.

The method of Gropper and Boyd (31) was used to determine if the temperature indicated by the run temperature indicator and control (RTIC) system at speed was the true rotor temperature.

Diphenyl ether was substituted for hexadecane and the Clapeyron coefficient reported by Biancheria and Kegeles was assumed (32). The indicated temperature was within 0.1° C of the calculated temperature after the cell came to thermal equilibrium.

Corrections to Standard Conditions

All sedimentation velocity measurements were made at 20° C in order to eliminate the temperature correction in subsequent calculations. Most of the velocity measurements were made in BPES (Appendix 1) which has a sodium ion concentration of 0.195 M and an ionic strength of 0.202. According to Cohen and Eisenberg $(\partial \rho / \partial c_2)_{\mu}^0$ should be substituted for $(1 - \bar{v} \rho)_{20, b}$. The following treatment assumes that they are equivalent. For sodium DNA (NaDNA) in dialysis equilibrium with 0.2 M NaCl, $(\partial \rho / \partial c_2)_{\mu}^0 = 0.457$ (33). According to Svedberg and Pedersen $\eta_{20} / \eta_o = 1.017$, $\Delta \rho = \rho - \rho_o = 0.0083$ and $\rho_o = 0.9982$ for this solution (1). Because the \bar{v} of NaDNA is of interest here \bar{v} can be assumed to be constant. The correction of the s value is therefore easily made:

$$s_{20, w} = (\eta^{20} / \eta_o^{20}) (1 - \bar{v} \rho_o)_{20, w} / (1 - \bar{v} \rho)_{20, b} s_{20}$$

$$s_{20, w} = 1.027 s_{20}$$

A similar correction for sedimentation velocity measurements made in EQB (Appendix 1) is

$$s_{20,w} = 1.143 s_{20}$$

for $(\partial \rho / \partial c_2)^0 = 0.586$, $(\eta^{20} / \eta_o^{20}) = 1.089$, $\Delta \rho = 0.0403$ and $\rho_o = 0.9982$. These values are also from Cohen and Eisenberg (33) and Svedberg and Pedersen (1).

An extrapolation to zero DNA concentration was not made because of the low DNA concentrations used in most experiments. As mentioned above in the section on sedimentation analysis, no significant concentration dependence was found in the concentration range used. Similarly no allowance was made for speed effects since no effect could be detected even for Fragment A (See above). The corrected s values for the separated PM2-HaeIII fragments are therefore reported as $s_{20,w}^0$ values.

Computer Aided Calculations

Analysis of sedimentation velocity and sedimentation equilibrium data was greatly aided by two Fortran programs, *SVEDCOF and *MW, written by Dr. Robert D. Dyson, Oregon State University, for the CDC 3300 computer in the OS-3 timesharing system. The program *SVEDCOF plots the relationship between $\log r$ and t , calculates the least squares fit for the points and calculates the

sedimentation coefficient from the slope. Viscosity and temperature corrections are then applied to correct the sedimentation coefficient. A second version of this program allowed the insertion of the measured values for the distance between the inner to outer reference holes and the distance from the center of the rotor to the outer reference hole rather than the nominal values incorporated into the original version. The program *MW plots $\ln c$ as a function of $r^2 - r_o^2$, calculates a linear least squares fit to the concentration-weighted relationship between $\ln c$ and $r^2 - r_o^2$ and then computes the molecular weight from the slope, the rotor speed, \bar{v} , ρ and the temperature. All plots were performed on a Hewlett Packard 7200A Graphic Plotter when using OS-3 to analyze data.

Extensive use was also made of a Hewlett Packard 9821A programable calculator equipped with the following peripherals; the 9864A digitizer, the 2748 B paper tape reader, a 9864A digitizer, the 2748B paper tape reader, a 9864A plotter and a standard Teletype. A simple program was written to exploit the calculator and digitizer to reduce scans obtained from sedimentation equilibrium experiments to paper tape data compatible with *MW (Appendix 3). A second program calculates and plots both experimental points and the theoretical relationship between the sedimentation coefficient and molecular weight described by Yamakawa and Fujii. Modifications of the basic program permit the output of the coefficients in

the Yamakawa-Fujii equations on the Teletype. Three other programs were designed to plot and fit gel results. These programs for the Hewlett Packard system are also listed and described in detail in Appendix 3. "Optimize Vm" is also discussed in the Results.

RESULTS

PM2-HaeIII Fragments

Figure 1 shows the PM2-HaeIII fragments A-P separated by analytical electrophoresis in 3.5% acrylamide gels (20:1). The DNA is detected by soaking the gel in a 1 $\mu\text{g}/\text{ml}$ solution of ethidium bromide; intercalation of this dye into double-stranded DNA enhances the dye's fluorescence thereby revealing the location of the DNA. Figure 1 also illustrates the resolution of bands D through H by preparative electrophoresis. In this experiment the separated bands were run in individual tubes to determine if the separation is complete. To further verify the identity of the fragments, aliquots of each of the five separated bands were mixed together. From these gels it can be seen that there is no visible sign of cross-contamination and that the fragments have been properly identified.

Figure 2 is a scan of a gel containing the complete PM2-HaeIII digest which has been stained with Toluidine Blue O and scanned at 546 nm using a Gilson gel scanner. The stain is quantitative; increasing the loading of DNA proportionately increases the area under each peak. From this scan it can be seen that peaks A through O represent unique fragments since the relative area under each peak is proportional to the estimated size of each fragment (See Calibration of Molecular Weights by Gel Electrophoresis). Peak P contains about

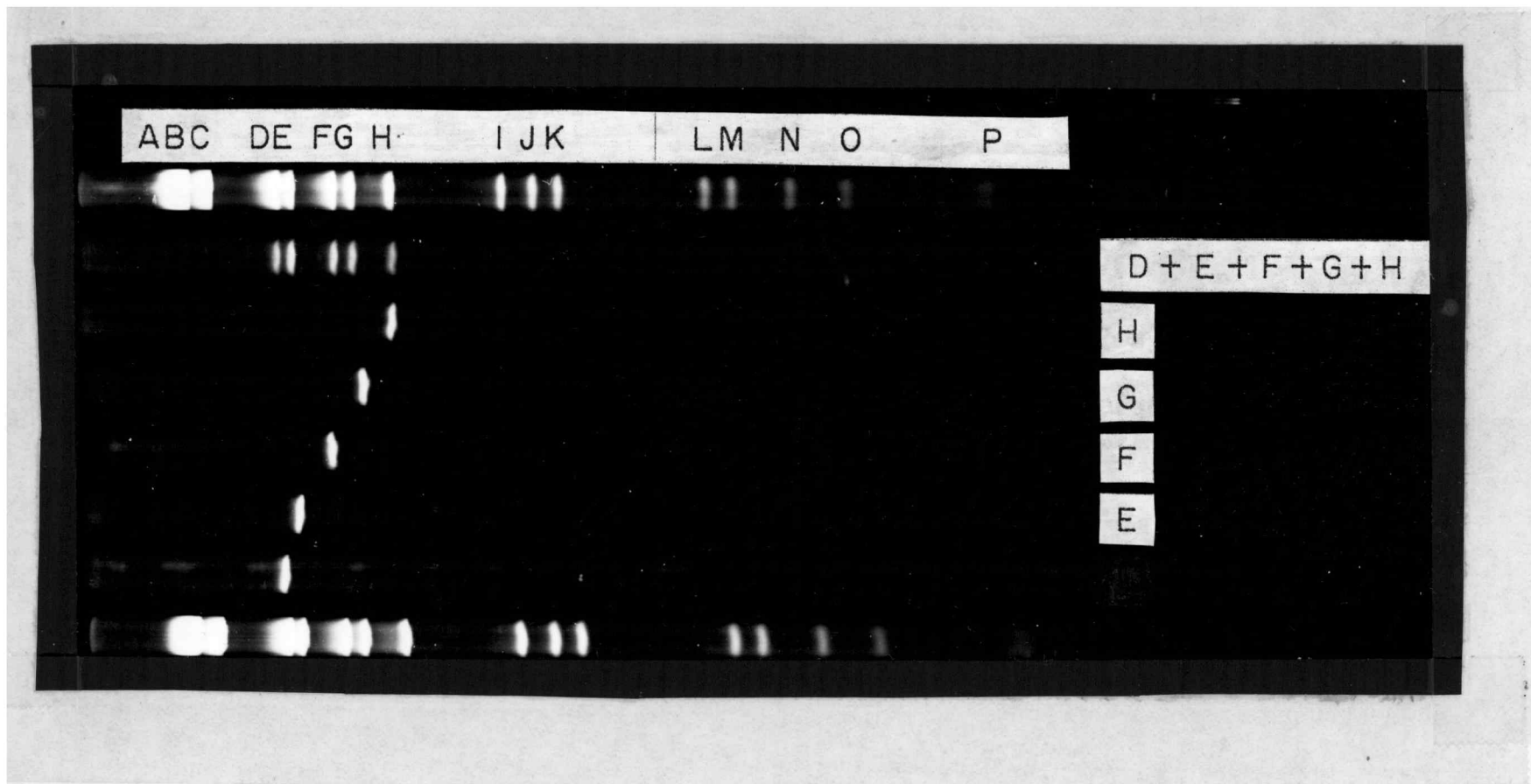


Figure 1. Analytical Electrophoresis Pattern of Whole PM2-HaeIII Digest and the Isolated Fragments D, E, F, G and H.

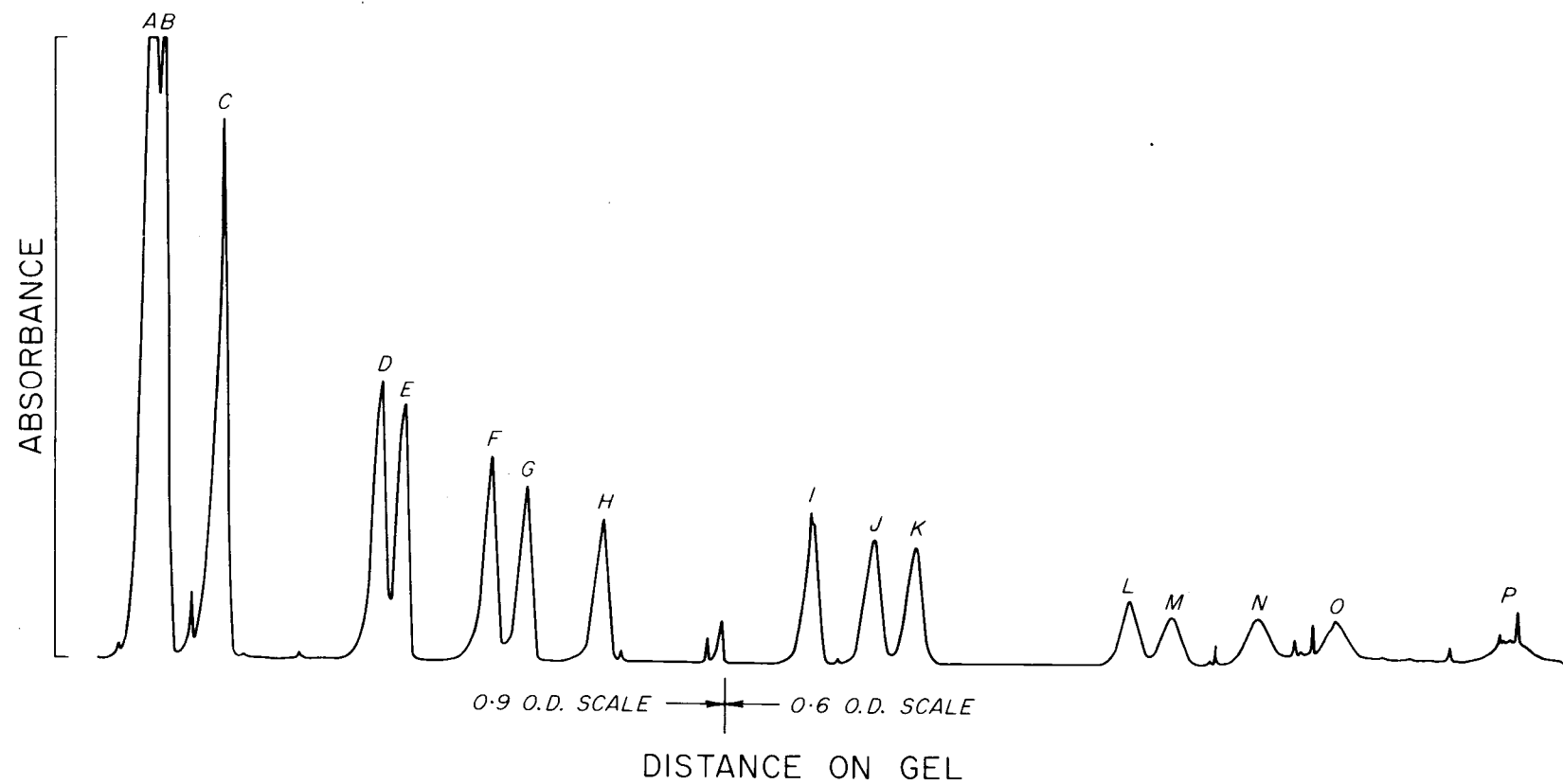


Figure 2. Scan of a Gel Containing PM2-HaeIII Digest Stained with Toluidine Blue O.

twice the area expected and therefore must consist of at least two unique fragments. Electrophoresis of the mixture in 6% acrylamide gels (40:1) resolves P into two distinct bands (not shown). It has not been possible to resolve P into two components by preparative gel electrophoresis although all the other bands may be resolved from each other. Therefore P is the only "fragment" which is not unique in both size and base sequence.

Figure 3 is a scan of a formamide gel containing the complete PM2-HaeIII digest stained with Toluidine Blue. The procedures of Staynov, Pinder and Gratzner (34) as modified by Boedtker, et al. (35) were used in preparing this gel. For the purpose of this thesis it is sufficient to know that the DNA was denatured (i. e. the strands are separated) by boiling in a denaturing solvent before the mixture was applied to the formamide gel. During electrophoresis the formamide prevents the strands from reannealing so that in this system single-stranded DNA is being electrophoresed. Therefore this procedure should detect single-stranded nicks in the fragments if they are present. The result (Figure 3) shows that the PM2-HaeIII digest must be largely unnicked since the same apparent size distribution is seen. The erratic baseline, which is a usual problem with formamide gels, prevents one from detecting interband DNA which would represent nicked strands. Baseline difficulties also make it difficult to precisely quantitate the areas under the peaks.

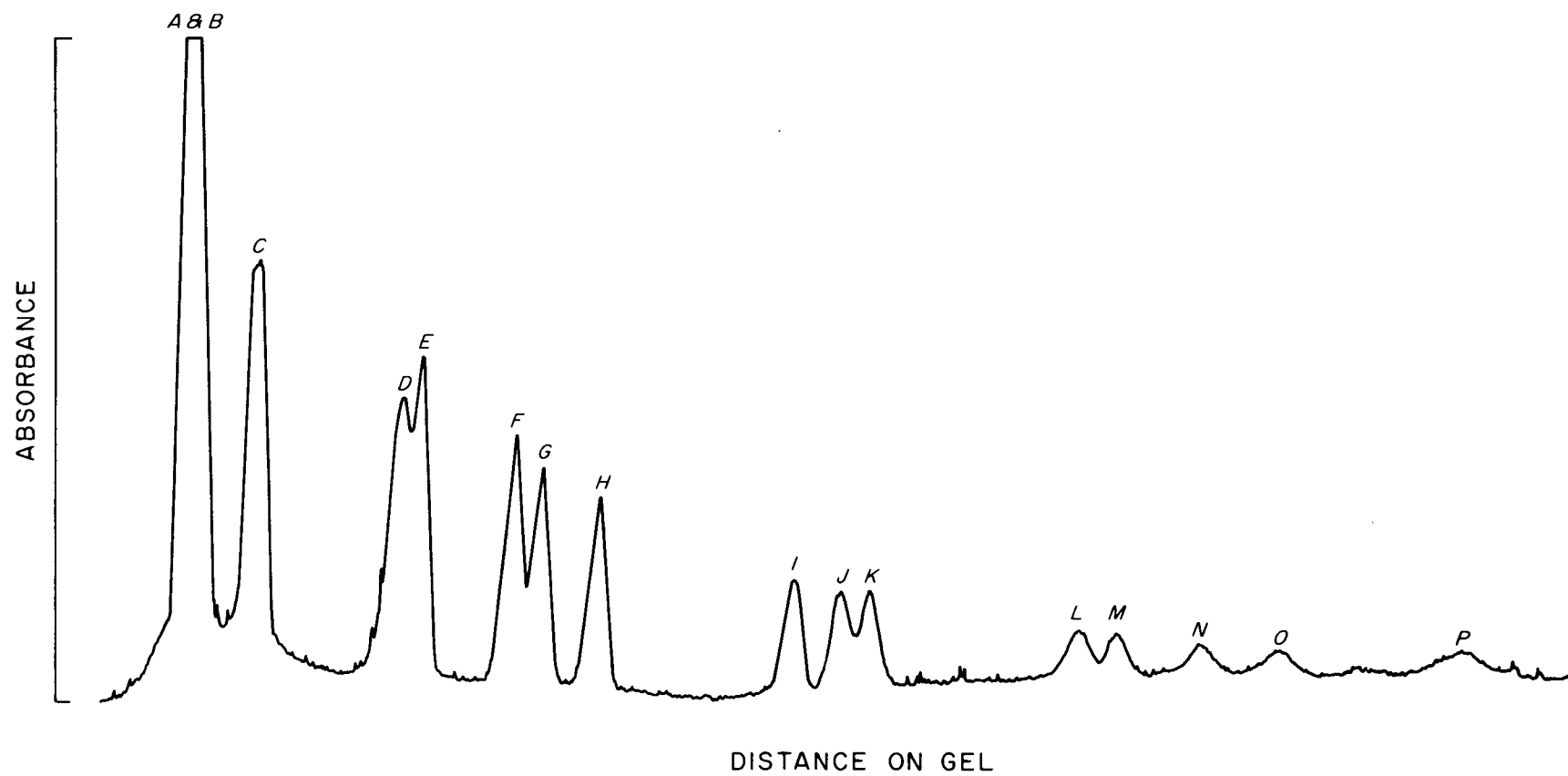


Figure 3. Scan of a PM2-HaeIII Digest Electrophoresed Under Denaturing Conditions.

However the data is good enough to provide an estimate that 90% of the molecules are unnicked.

Sedimentation Equilibrium Studies

Table 1 lists the fragments for which the molecular weights were determined by sedimentation equilibrium. This method was originally intended to provide the principal independent measure of molecular weight over the full size range. However a marked upward concavity in the plot of $\ln c$ vs $r^2 - r_0^2$ was noted in many experiments (Figure 4). In some experiments the curvature was nearly absent (Figure 5) but even in these cases the same sample could be run again only to produce a curved $\ln c$ vs $r^2 - r_0^2$ plot. Since most experiments gave curved plots and since no satisfactory way was found to correct the data or the experimental conditions, the sedimentation equilibrium method was abandoned in favor of molecular weights from gel calibrations (See Calibration of Molecular Weights by Gel Electrophoresis). Sedimentation equilibrium in an alkaline equilibrium buffer promises to provide more satisfactory data (See Figure 6 and Table 1), but this method needs to be examined in more detail. The remainder of this section of the thesis is an explanation of two attempts to correct the data and a discussion of the probable causes for the curvature in the $\ln c$ vs $r^2 - r_0^2$ plots.

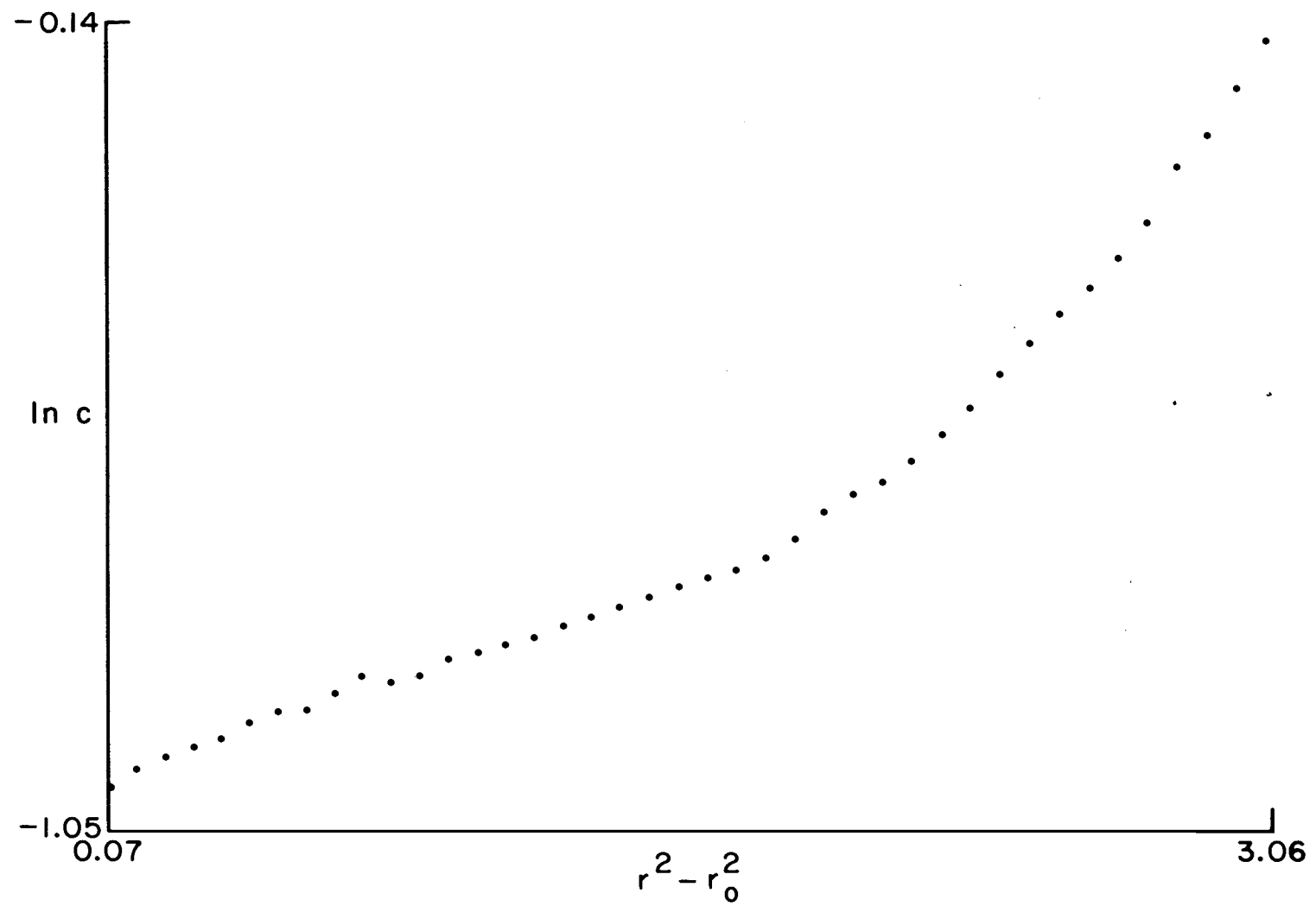


Figure 4. Upward Curvature in the Plot of $\ln c$ vs $r^2 - r_0^2$ for Sedimentation Equilibrium Data.

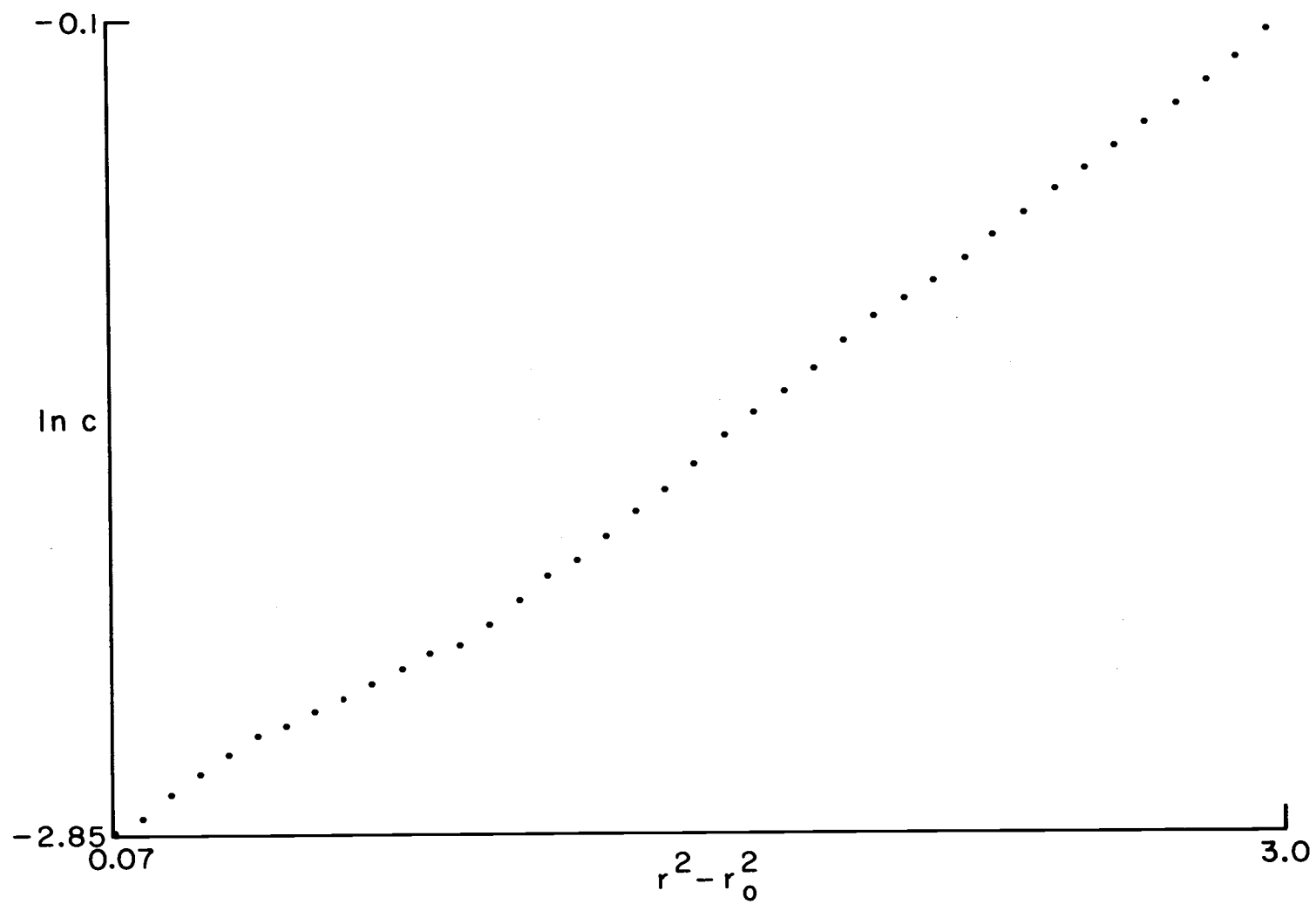


Figure 5. Normal Plot of $\ln c$ vs $r^2 - r_0^2$ for Sedimentation Equilibrium Data.

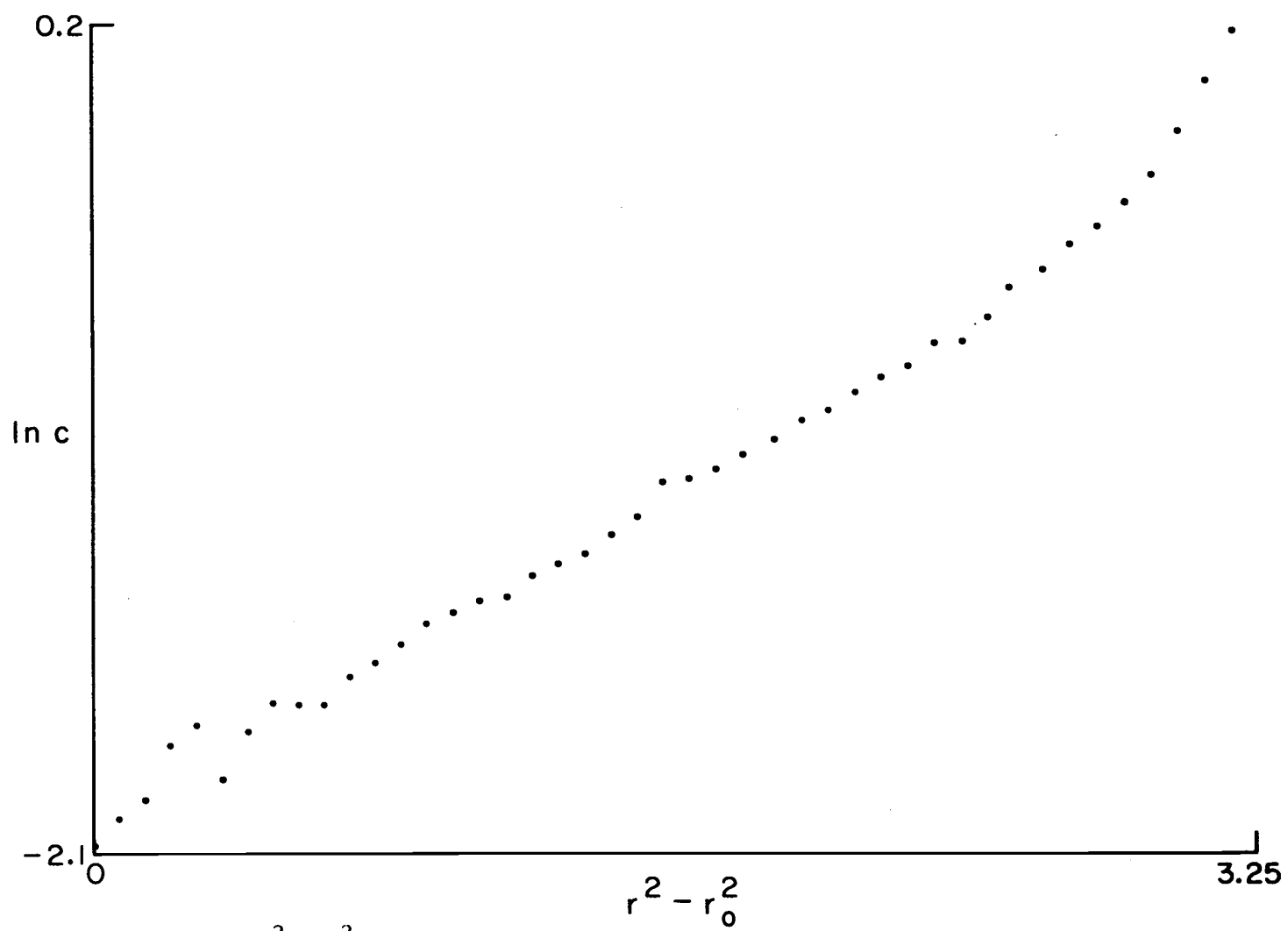


Figure 6. Plot of $\ln c$ vs $r^2 - r_0^2$ for a Sedimentation Equilibrium Experiment with Alkali Denatured DNA.

Table 1. Molecular Weights of PM2-HaeIII Fragments Determined by Sedimentation Equilibrium Measurements.

Fragment and Run Number	Condition	Molecular Weight ^a		
		After Weighted Least Squares	After CZERO	Iterating to Constant c_o^b
H(2327)	Denatured	497	N. C. ^c	N. C.
L(2051)	Native	136	127	134
M(2054)	Native	116	N. C.	N. C.
N(2060)	Native	97.8	115	119
N(2063)	Native	101.	94.8	105

^a Molecular weights are in bp. 1 bp = 663 daltons.

^b c_o is the apparent concentration at the meniscus.

^c The data does not converge to a unique solution.

One explanation for the observed curvature is the systematic overestimation of the concentration at each point due to ultraviolet absorbing substances in the sample solution which do not redistribute appreciably under the run conditions. Although the baseline runs revealed little nonsedimenting material the difficulties in doing satisfactory baselines led us to suspect the scanner optics of the Model E ultracentrifuge as well. Therefore several numerical methods were applied in an attempt to find some satisfactory way to correct equilibrium data displaying such curvature. One method, CZERO, is an option of the program *MW. CZERO adds the same constant to each data point and seeks the best least squares fit to the data by varying the sign and magnitude of the constant. The other method adjusts the concentration at each of the points in the same way. However the additive constant is the difference between the meniscus concentration predicted by the least squares fit to the data and the apparent concentration at the meniscus (c_o). The data is alternatively fit and adjusted until the predicted and apparent concentrations agree to the desired accuracy. Both procedures work well on smooth synthetic data, but the noise in real data often prevents both iterative methods from converging to a unique solution. Furthermore, the second method is far too dependent on the relationship of the meniscus concentration to the rest of the data since an inconsistently low value would lower the apparent molecular

weight and an inconsistently high value raise it. Finally these procedures are no solution if the curvature arises for other reasons. However the molecular weights predicted by CZERO and by iterating to constant c_0 are included in Table 1 for comparison with the molecular weights obtained from the usual procedure.

An attempt was made to determine if the scanner was recording absorbance properly by centrifuging nucleotide solutions of known absorbance. The recorder values were not substantially different from the known values and so errors in recording the absorbance can be ruled out for absorbances greater than 0.1 absorbance unit.

Because baseline and recorder errors do not seem to explain the observed curvature one is forced to look for other causes. One possibility that should not be overlooked is an association reaction occurring as the result of salt bridges formed between the highly charged DNA molecules. Fortunately association is easily detected by considering the apparent molecular weights at different positions in the solution column. If the molecules of solute are associating the apparent molecular weight determined from the slope of the $\ln c$ vs $r^2 - r_0^2$ plot near the bottom of the cell will be greater than the molecular weight for nonassociating material. Since there are good estimates for the molecular weights of unassociated fragments from gel data it is easy to test this hypothesis. Upon examination the data do not indicate an association between native double-stranded DNA

molecules since the molecular weights observed at the bottom of the centrifuge cell are somewhat lower than the estimated sizes. The data could indicate the dissociation of the DNA into separate single-strands but the double helix is so stable at pH 7.6 under these conditions of salt and temperature that this explanation of the data is absurd.

Size heterogeneity will also cause an upward curvature in $\ln c$ vs r^2 plots of equilibrium data. The observed curvature is far more serious than that usually observed for heterogeneous samples; sedimentation equilibrium is notoriously insensitive to heterogeneity. Furthermore both sedimentation velocity experiments and gel electrophoresis of the separated fragments (Figure 1) reveal no heterogeneity. Therefore heterogeneity does not seem to be a likely explanation.

The remaining and most probable explanation for the observed curvature in $\ln c$ vs r^2 plots is that the DNA has not come to equilibrium within the solution column. The reasons for this failure are probably complex since the usual reason, that the experiment was not continued long enough does not explain the direction of curvature. In this case convection, precession, vibration or some combination of the three is probably disturbing the equilibrium distribution of the DNA. Convection and precession are known to be more serious problems at the low speeds required for these experiments. Precession can be and was minimized by using the heavier AN-J rotor. Convection and vibration are not so easy to prevent. Unfortunately the use of overspeeding technique may also contribute to disturbing

the equilibrium distribution when the speed is changed to the final equilibrium speed. This cannot be the whole explanation since runs carried out entirely at one speed also display the characteristic upward curvature. The low diffusion coefficient for double-stranded DNA contributes to the problem because the return to the equilibrium distribution is slow, allowing time for additional disturbance to occur.

Because it seems so difficult to achieve a stable equilibrium in sedimentation equilibrium experiments on double-stranded DNA, the equilibrium method for obtaining molecular weights from denatured DNA should be considered. Denatured DNA is half the size of native DNA and is less rodlike in solution. Higher equilibrium speeds may therefore be used and the effects of convective, precessional and vibrational disturbances will be correspondingly less disruptive. Furthermore the return to equilibrium will be more rapid because the denatured strands are less extended. There are, however, unique problems with alkaline sedimentation equilibrium experiments on DNA; the high pH slowly degrades the DNA and the solutions are highly corrosive. In addition the strands may tend to renature so that association becomes a problem. Finally the gains made with respect to decreased size of the fragments and their increased diffusion coefficient may not offset the disturbances to the equilibrium condition that plagued the sedimentation equilibrium experiments with the double-stranded fragments. For the purpose of this thesis therefore the molecular weight for each of the fragments was obtained from analytical gel electrophoresis.

Calibration of Molecular Weights by Gel Electrophoresis

Although originally intended to provide preliminary estimates of the molecular weights of each of the fragments, analytical gel electrophoresis of the PM2-HaeIII digest became increasingly important as the difficulties in obtaining meaningful sedimentation equilibrium data became apparent. Of course there are unique problems associated with determining molecular weights from gel electrophoresis as well; the three most prominent problems are: (a) Correcting for base compositional effects. (b) Obtaining appropriate size standards and (c) Relating the observed electrophoretic mobility to the molecular weight.

Effects of base composition on the electrophoretic mobility of native DNA have been previously reported. Zeiger, et al. observed that for DNAs of roughly equivalent size the electrophoretic mobility increased as a function of the relative amount of guanine and cytosine in the DNA (36). However, their experiments were carried out with very large DNAs and so their observations may not apply to smaller DNAs. Maniatis, Jeffrey and van de Sande have reported deviations from the expected mobilities for several restriction fragments ranging in size from 600 to 150 basepairs in length (37). They concluded that denaturing gels gave more reliable results than nondenaturing gels. However base compositions were not reported

for these fragments and so one cannot determine if the anomalies they observed were due to base compositional effects. In any event the molecular weights obtained from the anomalous electrophoretic mobilities deviated less than 10% from accepted sizes for these fragments. Presuming that the observed deviations are due to some base compositional effect, the possible error introduced by neglecting base compositional effects would be on the order of 10%. Since Maniatis, et al. found only a few fragments with anomalous behavior out of many that were studied it seems reasonable to neglect the error which may result from a base compositional effect.

Restriction digests for which the sizes of the fragments have already been determined are probably the most convenient and useful size standards. In a growing number of cases restriction fragments have been or will be sequenced because of the biological importance of the DNA from which they are derived. Since the molecular weights obtained by comparison with sequenced DNAs are tied to a precisely known standard, a calibration done with a digest of DNA which will eventually be sequenced is a real advantage. Fortunately the PM2-HaeIII fragments have been compared with restriction digests of two DNAs which have already been well characterized and which will be sequenced because they are derived from two cancer viruses.

Figure 7 and Table 2 summarize the calibration of the PM2-HaeIII fragments against a HaeIII digest of SV-40 DNA (obtained from Dr. John Newbold). The digests were applied separately to two 3.5% acrylamide gels (20:1) and electrophoresed together. In order to relate the molecular weights of the SV-40 fragments to their mobilities the logarithm of the molecular weight was assumed to be a linear function of the mobility except at high molecular weights. This relationship between the molecular weight and the mobility has been suggested by many investigators. Maniatis, Jeffrey and van de Sande have reported a linear relationship in both denaturing and nondenaturing polyacrylamide gels for DNA (37). Helling, Goodman and Boyer have observed a similar relationship for the electrophoresis of large DNAs in agarose gels (38). Therefore a straight line was hand drawn to best fit the SV40-HaeIII fragments in the linear region and the upward curvature at the high molecular weight end of the scale was sketched in later. The molecular weights for the PM2-HaeIII fragments were then read from the graph as a function of fragment mobility. The sizes for the SV40-HaeIII fragments are from a personal communication with Dr. John Newbold, University of North Carolina (39); very similar results have recently been published by Lebowitz, Siegel and Sklar (40).

The deviations from linearity observed for high molecular weight fragments in acrylamide gels makes it difficult to fix the

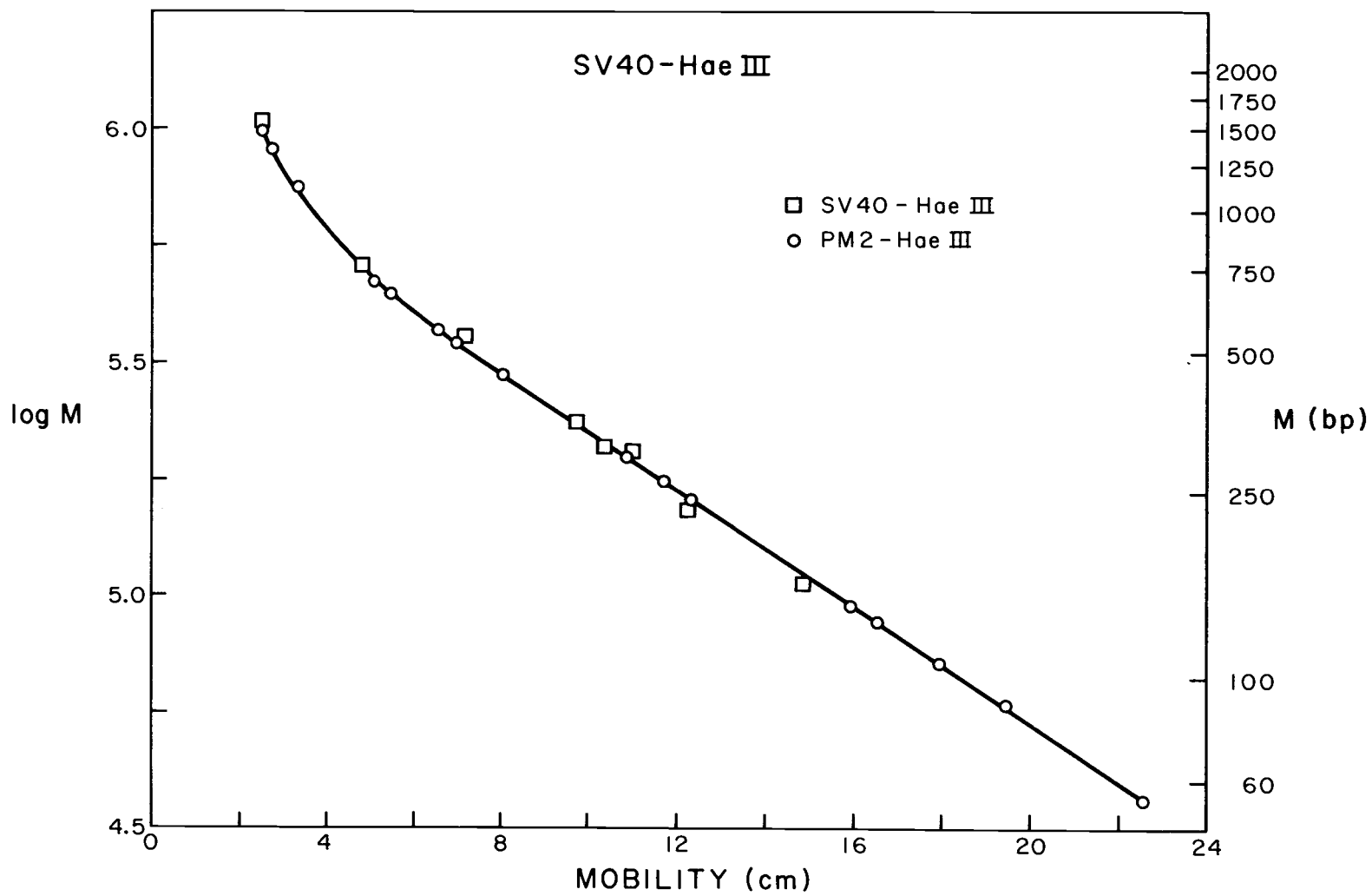


Figure 7. Calibration of the PM2-HaeIII Digest with SV40-HaeIII Fragments.

Table 2. Calibration of PM2-HaeIII Fragments by Comparison With SV40-HaeIII Fragments.

Fragment	SV-40- <u>Hae</u> III Standard Sizes ^a (bp ^b)	Estimated PM2- <u>Hae</u> III Sizes (bp)
A	1550	1500
B	765	1367
C	540	1130
D	355	708
E	315	670
F	615 ^c	560
G	230	525
H	160	448
I	4530 ^d (total)	299
J		265
K		242
L		143
M		132
N		108
O		88
P		55
		8240 (total)

^a The sizes of the SV40-HaeIII fragments were obtained from Dr. John Newbold, University of North Carolina (39). Similar sizes have been reported by Lebowitz, Siegel and Sklar (40).

^b 1 bp = 663 daltons.

^c The "fragment" SV-40-HaeIII -F contains two unresolved fragments F₁ and F₂.

^d The relative sizes of the SV-40-HaeIII fragments are based on a size of 5000 bp for whole SV-40 DNA. There are estimated to be 8 additional fragments of 50 bp or less.

sizes of the large restriction fragments. Therefore the PM2-HaeIII digest was coelectrophoresed with an EcoRI digest of Adenovirus type 2 DNA in 1.5% agarose-ethidium bromide gels. In this experiment the two digests were mixed together and applied to the same gel so as to minimize the differences between individual gels. In this system the linear region appears to extend from 2500 bp to 250 bp. The results of this calibration are summarized in Table 3; the Ad2-RI fragments have been thoroughly characterized by Pettersson, et al. (41). The agreement between the SV40-HaeIII calibrated sizes and the AD2-RI calibrated sizes is quite good up to 560 bp. As was expected the Ad2-RI calibration suggests that the sizes of fragments A through E were underestimated in the SV40-HaeIII calibration.

An independent calibration of the PM2-HaeIII sizes is summarized in Table 4. These values (PM2-Hind Calibration) were obtained in a telephone conversation with Dr. Peter Phillipsen, Stanford University (42). The sizes were obtained by coelectrophoresing PM2-Hind together with PM2-HaeIII fragments in a 4% acrylamide (40:1) slab gel. The sizes of the PM2-Hind fragments were determined by electron microscopy and therefore provided a set of size standards for the PM2-HaeIII digest. The electrophoresis pattern for the PM2-Hind digest has been reported by Streeck, Phillipsen and Zachau (43).

Table 3. Calibration of PM2-HaeIII Fragments by Comparison With Ad2-RI Fragments.

Fragment	Ad2-RI Standard Sizes ^a (bp ^b)	Estimated PM2- <u>Hae</u> III Sizes	
		From Ad2-RI Calibration	From SV40- <u>Hae</u> III Calibration
A	20500	1660	1500
B	4072	1585	1367
C	3469	1334	1130
D	2564	750	708
E	2112	717	670
F	1659	563	560
G	34376 (total)	519	525
H		451	448
I		291	299
J		260	265
K		247	242
L		----	143
M		----	132
N		----	108
O		----	88
P		----	55
		8377 (total ^c)	8240 (total)

^a The Ad2-RI sizes are from Petterson et al. (41).

^b 1 bp = 663 daltons.

^c Fragments L-P were in the non-linear portion of the plot of log M vs mobility for the PM2-HaeIII fragments.

Table 4. Phillipsen's Calibration of PM2-HaeIII Fragments By Comparison With PM2-Hind Fragments.

Fragment	PM2- <u>Hind</u> Calibration ^b	PM2- <u>Hae</u> III Sizes ^a		Combined Calibration ^c
		SV40- <u>Hae</u> III Calibration	Ad2-RI Calibration	
A	2000	1500	1660	1660
B	1750	1367	1585	1585
C	1350	1130	1334	1334
D	910	708	750	750
E	716	670	717	720
F	620	560	563	562
G	560	525	519	522
H	480	448	451	450
I	300	299	291	296
J	265	265	260	262
K	240	242	247	244
L	145	143	---	143
M	135	132	---	132
N	110	108	---	108
O	95	88	---	88
P	--	55	---	55
Total	9676	8240	8377	8911

^a Sizes are in bp. 1 bp = 663 daltons.

^b The calibration of the PM2-HaeIII digest against PM2-Hind fragments was carried out by Dr. Peter Phillipsen, Stanford University (42). Fragment P was not included in this calibration.

^c The results of the SV40-HaeIII and the Ad2-RI calibrations were combined to provide size estimates over the full range of molecular weight.

The results of the SV40-HaeIII and Ad2-RI calibrations are included in Table 4 for comparison with the Phillipsen calibration. A set of PM2-HaeIII sizes which represents a combination of the SV40-HaeIII and Ad2-RI calibrations is also included. This set of PM2-HaeIII sizes represents the best estimate obtained in this laboratory. The agreement between the Phillipsen results and the combined calibration is very good below 500 bp; the deviations above 500 bp may be created in part by the different ways in which the molecular weights for the restriction fragments used as standards were obtained. The sizes of the PM2-HaeIII fragments obtained by combining the SV40-HaeIII and the Ad2-RI calibrations will be used in this thesis with the understanding that the molecular weights above 500 bp may be somewhat larger than reported.

It should be emphasized here that all the calibrations discussed in this thesis have been relative calibrations not absolute calibrations. The sizes for each of the fragments in the SV40-HaeIII and the Ad2-RI digests were determined from the fraction of radioactivity contained in each fragment after digestion of DNA which was uniformly labeled with phosphorus 32. The sizes of the Ad2-RI fragments were also measured in the electron microscope using whole PM2 DNA as a size standard. The PM2-Hind fragments were also measured relative to whole PM2 DNA. Therefore these sizes are all dependent on an assumption about the size of the DNA used as a relative

standard. This is probably the reason that the sizes of the PM2-HaeIII fragments reported here do not add up to the molecular weight of 9,900 bp which has been reported for whole PM2 DNA (16). The Phillipsen sizes add up to a total closer to the reported size of whole PM2 DNA because the sizes were calculated with reference to Phillipsen's size estimate for PM2 DNA. Since it is more difficult to determine the absolute size of a large piece of DNA than it is to determine the absolute size of a small piece of DNA the uncertainty in the sizes will probably be resolved when SV40 DNA is completely sequenced. As long as the principal disagreement is in the relative size of the reference DNA the reported sizes can be corrected by a multiplicative factor. If the electrophoretic behavior of DNA is not adequately described as a linear relationship between the logarithm of the molecular weight and the mobility, the corrections may not be so simple.

Up to this point the calibration has depended on the assumption that the logarithm of the molecular weight is a linear function of the mobility over a certain size range. If DNA containing a wide range of sizes is electrophoresed the relationship between log and the mobility is clearly not linear; the shape of the resulting curve is sigmoidal. Therefore a curve fitting procedure based on fitting the data to a sigmoidal form was developed as a better method for inter-relating the data. The method applies a least squares linear fit to

the data in a somewhat different form; $\log M$ is the dependent variable while $\log \left(\frac{V_m - V}{V} \right)$ is the independent variable. V_m is a hypothetical maximum mobility in the gel while V is the mobility of a particular band. The magnitude of V_m is dependent on the gel percentage when different percentage gels are run together so that the shape of the electrophoresing molecules must be considered; otherwise V_m could be interpreted as the free mobility for a hypothetical double-stranded DNA monomer. If V_m were known it could be inserted directly and a simple fit obtained. However V_m is not readily obtained a priori and so the following procedure was adopted.

The Hewlett Packard calculator was programmed to obtain a least squares fit to the data beginning with a preliminary V_m . The preliminary V_m is then incremented and the fit is again calculated. The sum of the squares of the deviations in $\log M$ for the initial and test V_m are compared and the V_m with the lowest sum of squares is retained for the next test. The program is designed to change the sign and size of the increment so that V_m may be determined to any accuracy. The program terminates when V_m has been determined to the desired accuracy; the calculator then prints out V_m , the slope, the intercept, the sum of the deviations and the sum of the squares of the deviations for the data fitted. This program is called "Optimize V_m " and is fully described in Appendix 3.

The fit resulting from "Optimize Vm" is, as one might expect, strongly dependent on the input data; Vm is largely determined by the molecular weights chosen for the smaller restriction fragments. However, there is some evidence which confirms that the PM2-HaeIII sizes reported here are correct.

If the mobility of a fragment of DNA is determined relative to a dye marker in a series of gels of different concentrations the relative mobility of the DNA fragment may be plotted as a function of gel percentage. Therefore one ought to be able to extrapolate to zero percentage and determine the "free" mobility of the DNA. Ferguson has proposed that this be done by plotting the logarithm of the relative mobility vs the gel percentage (44). Such a plot for all of the PM2-HaeIII fragments electrophoresed in 3-6% acrylamide (20:1) gels is shown in Figure 8. All of the fragments except A, B and C give approximately the same relative "free" mobility relative to bromphenol blue. Since the data are the same as that fitted and plotted in Figure 9 and since the relative Vm for each of these gels is listed in Table 5, the relative Vm and relative "free" mobility may be compared. In every gel concentration the Vm relative to the bromphenol blue dye marker used in this experiment is very close to the relative "free" mobility which is predicted by the Ferguson plot. Therefore it appears that "Optimize Vm" is a way of locating the position of the Ferguson "free" mobility. Furthermore the result

implies that the molecular weights chosen for the PM2-HaeIII fragments must be close to the absolute values since the relative V_m determined from them is the same as the relative "free" mobility which was determined from the Ferguson plot without reference to the molecular weights.

Therefore "Optimize V_m " was applied to data for several different gel concentrations in each of the gel systems used in this work. The results are displayed graphically in Figures 9, 10, and 11 for 20:1 acrylamide, agarose-ethidium bromide and 40:1 acrylamide gels respectively. Table 5 lists the V_m , slope, intercept and V_m relative to bromphenol blue for the line fitted in each gel percentage. The fits in all cases were done for all of the PM2-HaeIII fragments which could be distinguished; in the agarose-ethidium bromide gel system some of the smaller fragments cannot be detected. The agarose-ethidium bromide gels also contained Ad2-RI fragments, but they were not included in the fit. Each point represents an individual restriction fragment; the molecular weight of each PM2 fragment is from the set obtained by combining the SV40-HaeIII and the Ad2-RI calibrations (Table 4) and the mobility is the distance of each band from the top of the gel. The agreement between the sigmoidal fit and the points is generally quite good. The notable exceptions are the Ad2-RI fragments in agarose-ethidium bromide gels. These deviations become larger as the gel percentage is

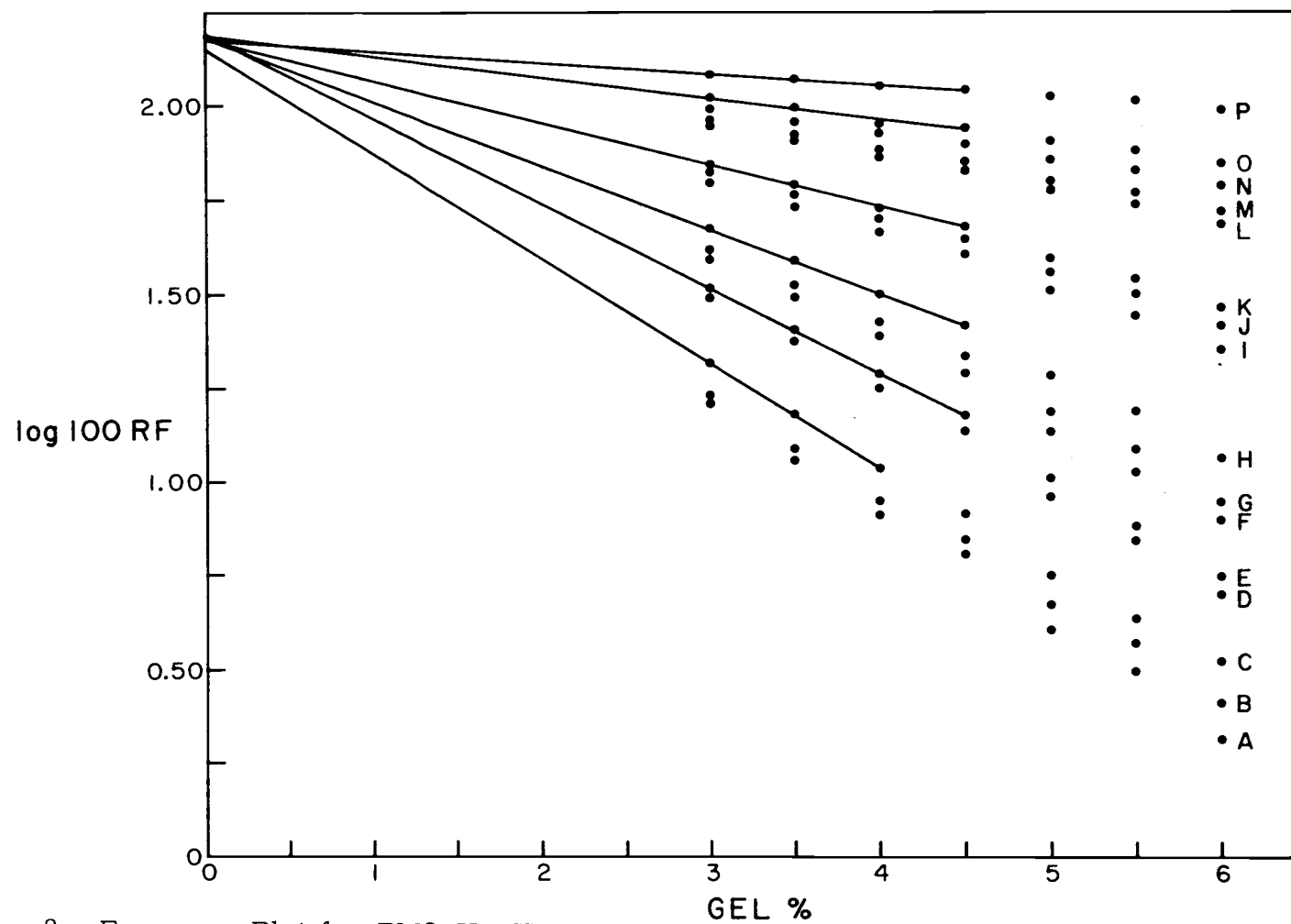


Figure 8. Ferguson Plot for PM2-HaeIII Fragments Electrophoresed in 3 to 6% Acrylamide (20:1) Gels.

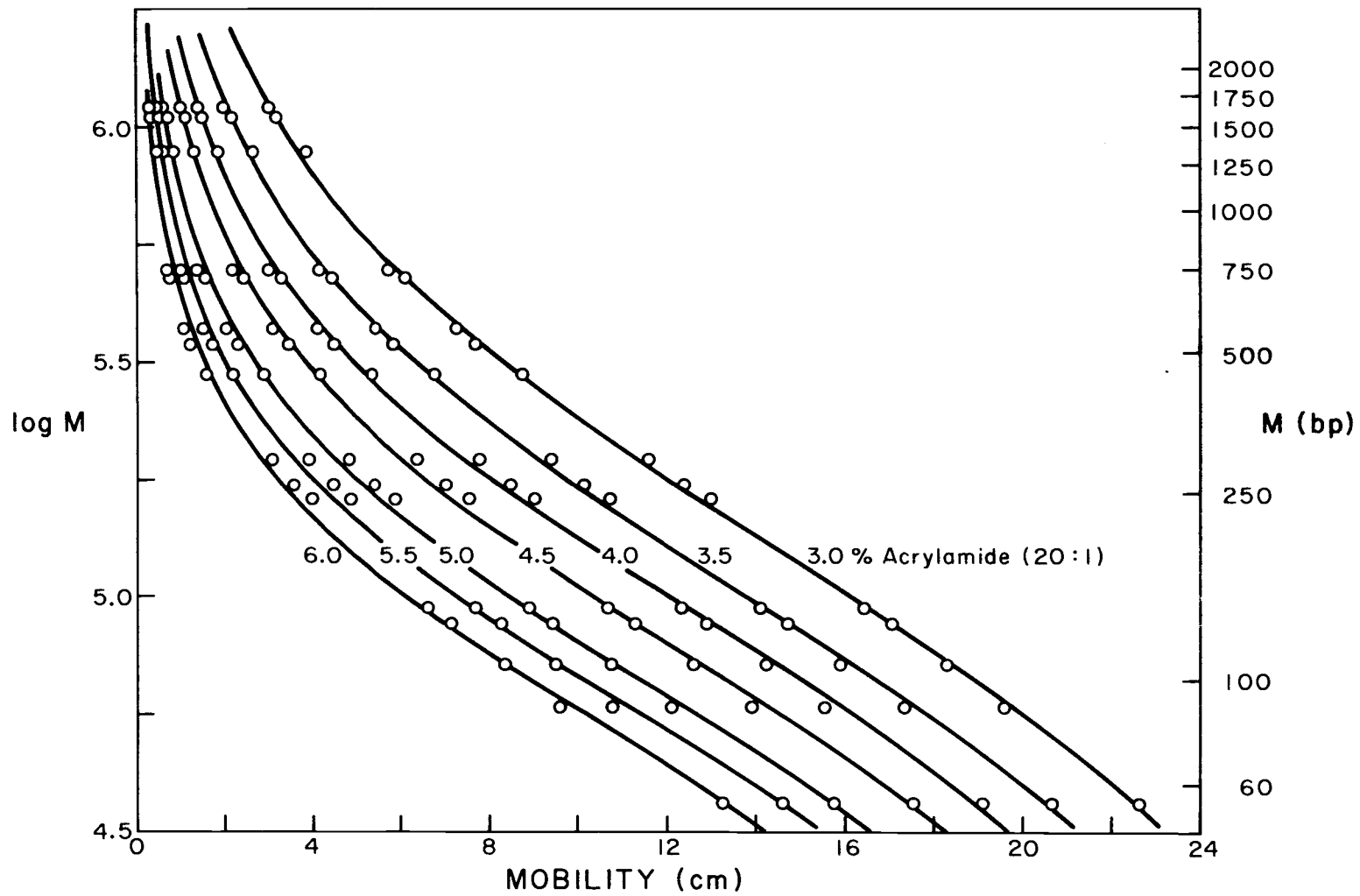


Figure 9. Sigmoidal Fit for PM2-HaeIII Fragments Electrophoresed in 3 to 6% Acrylamide (20:1) Gels. The equation for each line is given in Table 5.

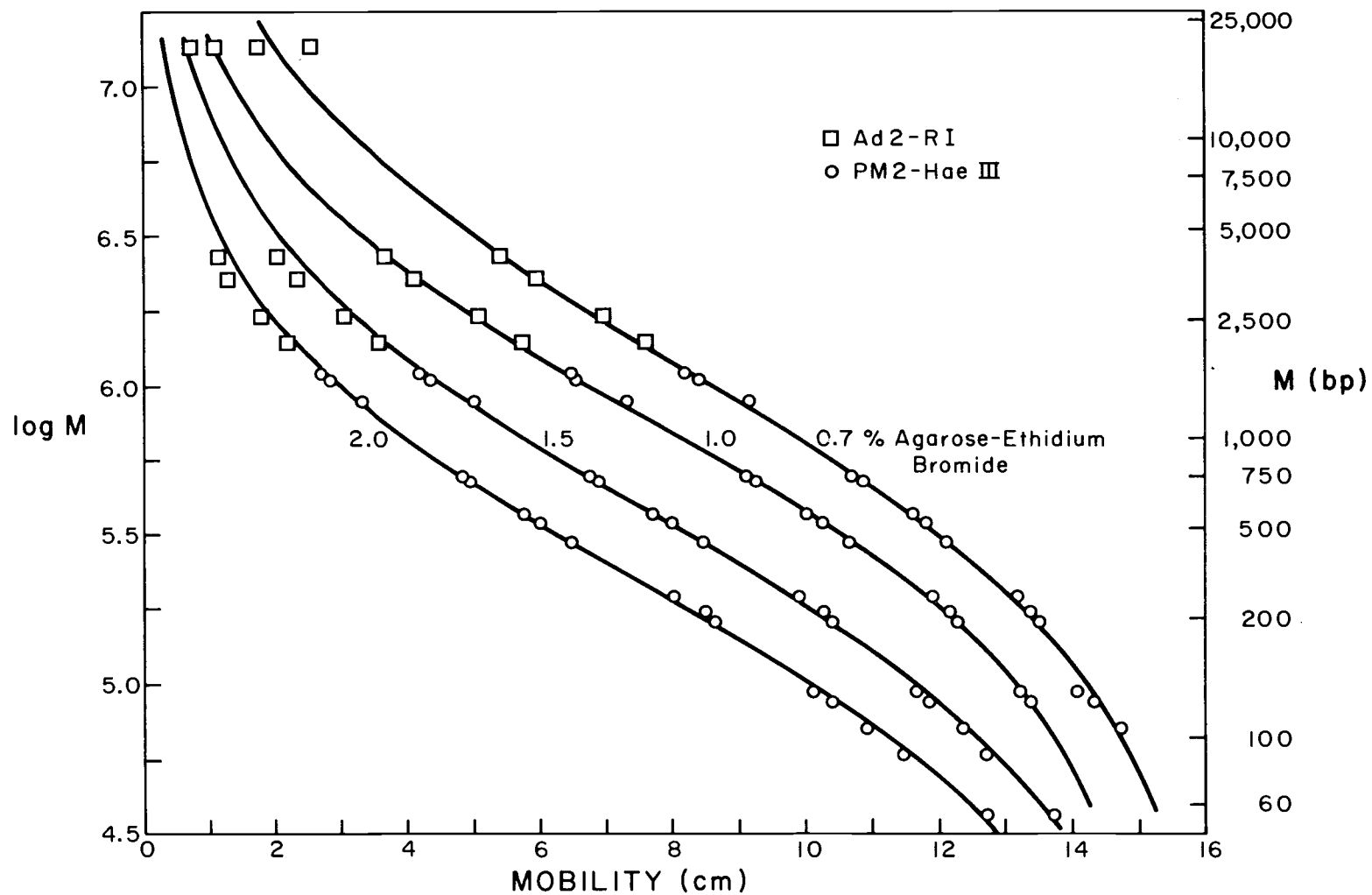


Figure 10. Sigmoidal Fit for PM2-HaeIII Fragments Electrophoresed in 0.7 to 2.0% Agarose-Ethidium Bromide Gels. The equation for each line is given in Table 5.

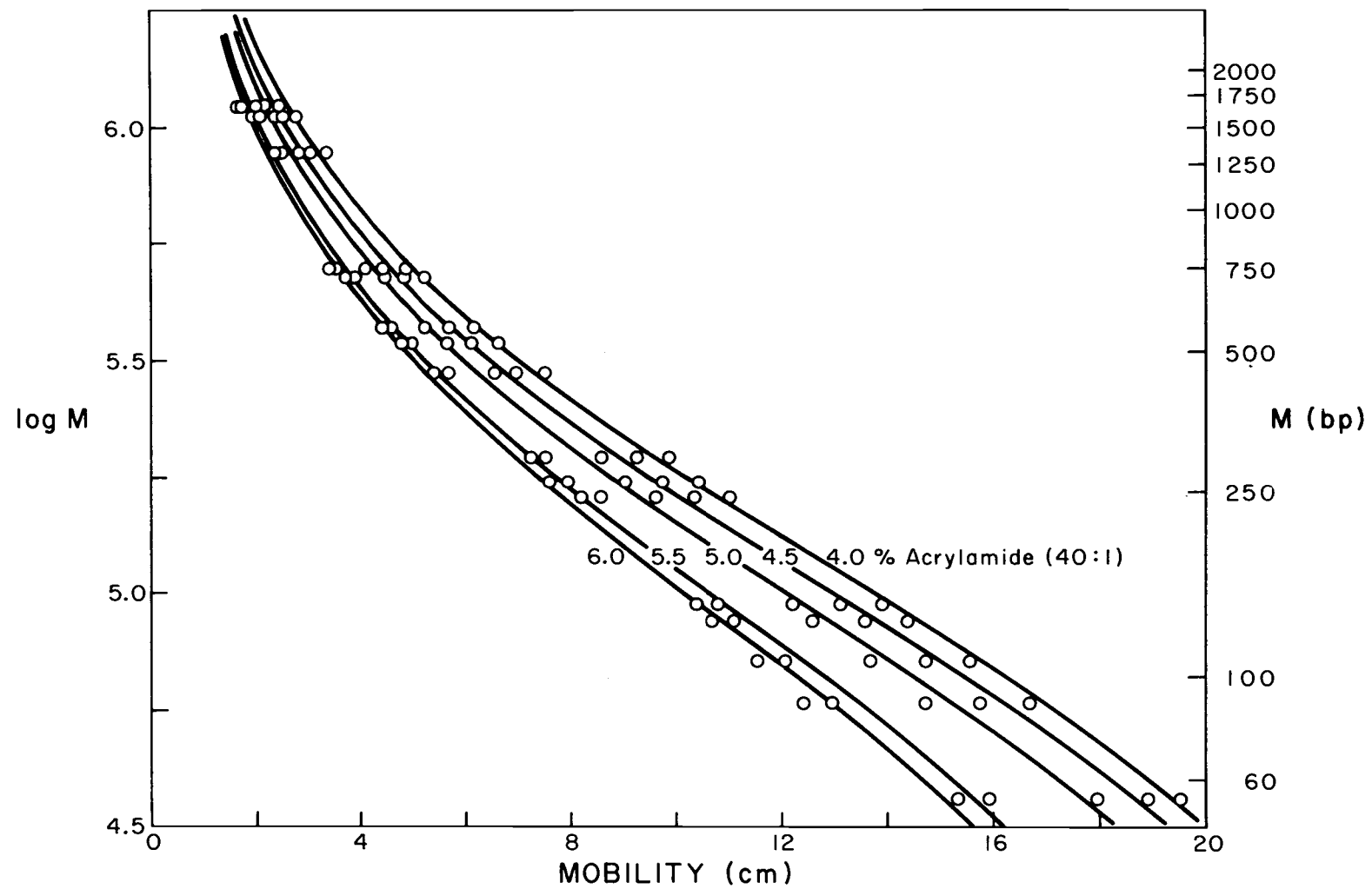


Figure 11. Sigmoidal Fit for PM2-HaeIII Fragments Electrophoresed in 4 to 6% Acrylamide (40:1) Gels. The equation for each line is given in Table 5.

Table 5. The V_m , Slope, Intercept and Relative V_m For The Sigmoidal Fits Shown in Figures 9, 10, 11^a.

Gel System ^b and Electrophoresis Time	Gel Percentage	V_m (cm)	Slope (m)	Intercept (b)	Relative V_m^c
20:1 Acrylamide	3.0	29.14	1.0120	5.0970	1.566
<u>bis</u> acrylamide	3.5	27.45	0.9479	5.0060	1.568
7.2 hrs.	4.0	25.77	0.8802	4.9500	1.525
"	4.5	24.68	0.8425	4.8820	1.552
"	5.0	22.92	0.7731	4.8220	1.533
"	5.5	22.36	0.7418	4.7639	1.587
"	6.0	20.56	0.6934	4.7428	1.512
1.5% Agarose-	0.7	16.19	1.2570	6.0700	n.d. ^d
Ethidium	1.0	15.19	1.1070	5.8950	"
bromide 5.5 hrs.	1.5	15.53	1.1700	5.5580	"
"	2.0	15.08	1.0960	5.3350	"
40:1 Acrylamide	4.0	25.68	1.0370	5.0620	1.492
<u>bis</u> acrylamide	4.5	25.33	1.0340	5.0210	1.499
7.2 hrs.	5.0	24.80	1.0570	4.9750	1.517
"	5.5	22.00	1.0520	4.9700	1.456
"	6.0	21.40	1.0610	4.9570	1.436

^a The functional form for the fit is $\log M = m \log \left(\frac{V_m - V}{V} \right) + b$.

The molecular weight is given in daltons and V is the mobility in centimeters.

^b All gels in a system were electrophoresed together at 125 v and ~ 5 ma. Each gel contained the same amount of DNA.

^c Relative to bromphenol blue

^d not done

increased. The variations are not nearly so large for the PM2-HaeIII fragments.

Of particular interest are the gel systems in which the initial calibrations were carried out. Table 6 lists the PM2-HaeIII sizes obtained from Peter Phillipsen and from the combined SV40-HaeIII and Ad2-RI calibrations for comparison with the sizes calculated from the sigmoidal fit for 3.5% acrylamide (20:1). 1.5% agarose-ethidium bromide and 4.0% acrylamide (40:1) gels. The data are the same as that plotted in Figures 9, 10 and 11. The numerical results indicate that the sigmoidal fit to the set of PM2-HaeIII fragments consistently predicts the size of any particular fragment. However, the molecular weight of PM2 DNA obtained by adding the sizes of the individual restriction fragments is significantly lower than the reported molecular weight. Therefore the calibration experiment was repeated in a 3.0% acrylamide (20:1) slab gel with five restriction digests for standards.

Figure 12 graphically displays the results of the calibration of the PM2-HaeIII digest by comparison with four other restriction digests in the 3.0% acrylamide slab gel. The sigmoid fit includes equally weighted data from SV40-HaeIII, SV40-HindIII, SV40-Hind-HaeIII, λ -HindIII and PM2-HaeIII digests. The molecular weights of the PM2-HaeIII fragments are from an independent calibration carried out by Noll (45). For identification the PM2-HaeIII data with

Table 6. Sizes of PM2-HaeIII Fragments Calculated From The Sigmoidal Fit in Several Gel Systems^a.

Fragment	PM2-HaeIII Sizes ^b				
	3.5% Acrylamide (20:1)	1.5% Agarose- Ethidium bromide	4.0% Acrylamide (40:1)	Combined Calibration	Phillipen Calibration
A	1703	1739	1799	1660	2000
B	1582	1643	1554	1585	1750
C	1273	1302	1247	1334	1350
D	784	741	782	750	910
E	725	712	711	720	716
F	577	556	572	562	620
G	527	508	519	522	560
H	440	443	435	450	480
I	284	282	284	296	300
J	254	249	258	262	265
K	233	238	234	244	240
L	145	151	147	143	145
M	134	139	136	132	135
N	113	112	111	108	110
O	92	94	92	88	95
P	53	52	53	55	--
Total	8919	8961	8934	8911	9676

^a The data presented in Figures 9, 10 and 11 were used. The molecular weights were determined from the mobilities and the fitted line for each of the gels listed here.

^b Sizes are in bp. 1 bp = 663 daltons.

the Noll molecular weights are plotted as filled circles. The molecular weights for the SV40-HaeIII, SV40-Hind and the SV40-Hind-HaeIII restriction fragments are those reported by Yang, Van de Voorde and Fiers assuming the size of SV40 DNA to be 5,000 bp (46). SV40-Hind-H has been sequenced by Fiers, et al. (47). Although originally reported to be 277 bp plus a 4 base single-stranded end, the size was recently revised to be 266 bp plus the 4 base "tail" (48). The mobility and molecular weight of this sequenced fragment is indicated in Figure 12. The sizes of the λ -Hind fragments are from Maniatis, Jeffrey and Van de Sande (37). The straight line in Figure 12 is a least squares linear fit to the data for which the mobility ranges between 4.5 cm and 16 cm.

Table 7 lists the molecular weights of all the fragments used in the calibration graphed in Figure 12. In addition the PM2-HaeIII sizes calculated from both the sigmoidal and the linear fits are listed. The equations for each curve are also given. Both fits predict a size of 263 bp for SV40-Hind-H which is in very good agreement with the sequenced size. The PM2 DNA size predicted by the sigmoid fit is also in better agreement with the reported molecular weight for PM2 DNA. The linear fit gives substantially the same sizes over the range of mobility for which the log M vs mobility plot seems linear but the sigmoidal fit performs better in both the high and low molecular weight range. Therefore the

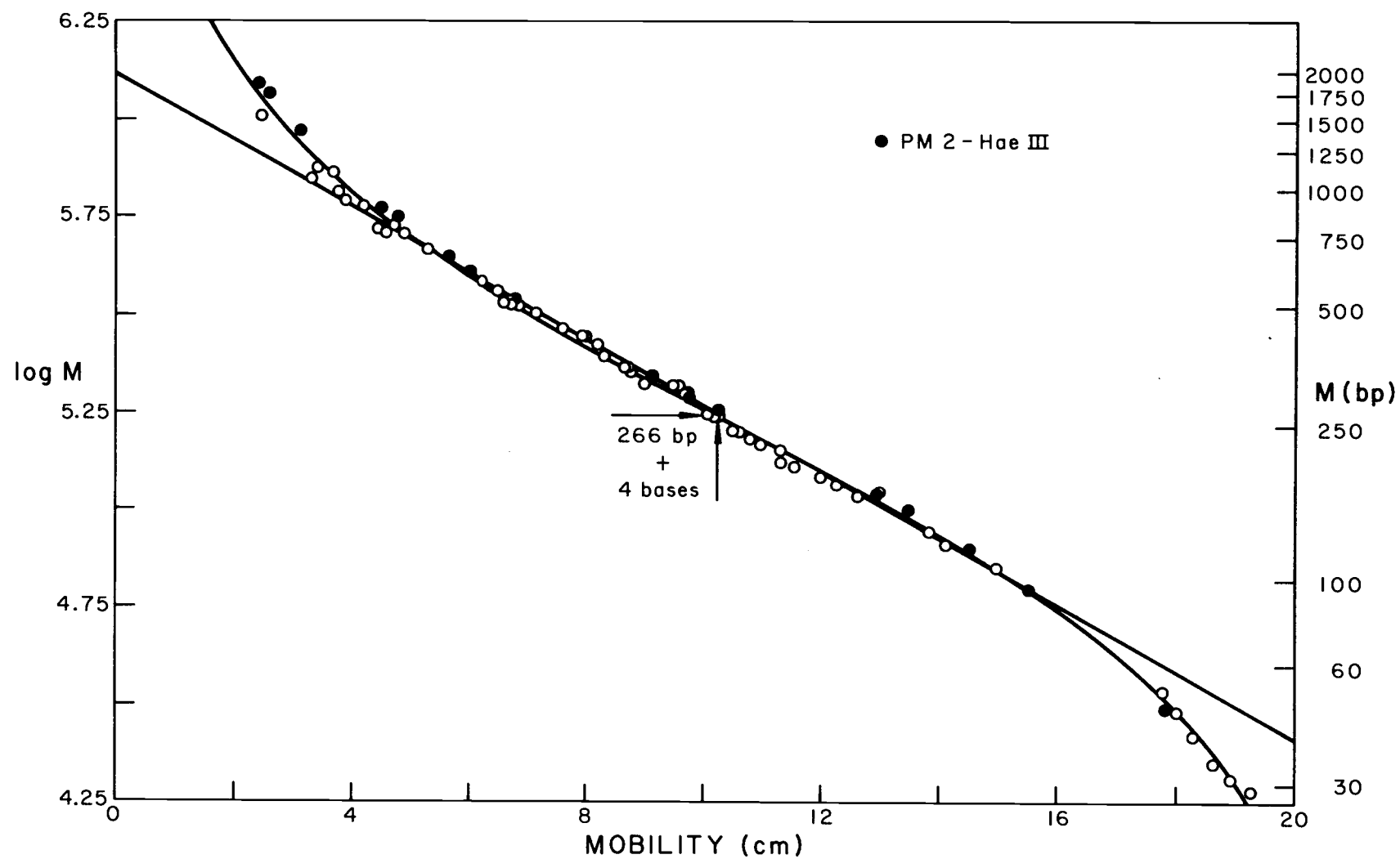


Figure 12. Calibration of the PM2-HaeIII Digest by Coelectrophoresis with 4 Other Restriction Digests in a 3% Acrylamide (20:1) Slab Gel. The molecular weights of the fragments and the equations for the linear and sigmoidal fit are given in Table 7. The filled circles are PM2-HaeIII fragments with molecular weights from Noll (45).

Table 7. Sizes of PM2-HaeIII Fragments from Sigmoidal and Linear Fits to the Data for Five Restriction Digests Coelectrophoresed in a 3.0% Acrylamide (20:1) Slab Gel.

Fragment	Standard Sizes ^a				Predicted PM2-HaeIII Sizes		
	SV40-HaeIII ^b	SV40-Hind ^b	SV40-Hind-HaeIII ^b	λ Hind ^c	PM2-HaeIII ^d	Sigmoidal ^e	Linear ^f
A	1535	1057	770	1125	1860	1735	1236
B	787	768	420	1090	1760	1606	1193
C	512	508	350	980	1410	1310	1075
D	350	505	314	930	890	854	817
E	335	425	305	900	845	794	773
F	315	420	265	800	672	642	650
G	305	350	260	700	615	592	606
H	305	260	240	580	525	498	516
I	215	240	215	550	333	322	330
J	164	223	184	520	295	288	292
K		195	176	500	272	263	265
L			164	480	167	160	155
M			133	440	152	145	141
N			123	400	120	117	114
O			108	375	95	94	94
P			52	340	47	50	60
Q			46	320	10,058	9,470	8,317
R			40	230			
S			34	200			
T			31				
U			29				

a. Sizes are in bp. 1 bp = 663 daltons.

b. Sizes reported by Yang, Van de Voorde and Fiers for SV40 DNA of 5,000 bp (46).

c. Sizes reported by Maniatis, Jeffrey and Van de Sande (37).

d. Sizes reported by Noll (45)

e. Calculated from the mobility, V , and the V_m from the equation $\log M = m \log \left(\frac{V_m - V}{V} \right) + b$.
 V_m is 21.02 cm, m is 0.94412 and b is 5.2208.

M is in daltons.

f. Calculated from the mobility, V , and the equation $\log M = mV + b$. V is in cm and M is in daltons. The slope, m , is -0.08526 and b is 6.1181.

PM2-HaeIII sizes predicted by the sigmoidal fit will be used in the examination of the relationship between the $s_{20,w}^0$ and M which follows.

Sedimentation Velocity Results

The average $s_{20,w}^0$ for each of the PM2-HaeIII fragments is given in Table 8. In addition the individual $s_{20,w}^0$ values which make up the average for each fragment are listed. The molecular weight of each fragment as determined by the sigmoidal fit to the five sets of restriction fragments coelectrophoresed in a 3.0% acrylamide (20:1) slab is also included. This table summarizes the empirical relationship between the $s_{20,w}^0$ and molecular weight over the transition from rigid rod to stiff coil behavior for double-stranded DNA molecules. The data in Table 8 will be used in all the results and discussion which follow.

The Yamakawa-Fujii theory is the most sophisticated theory dealing with the transition from rigid rod to stiff coil behavior for polymers with a cylindrical cross section (5). Therefore, it is appropriate to this thesis to make some comparisons between the empirical relationship obtained here and the theory. Preliminary to that comparison it was useful to reformulate the equations presented in their paper as follows:

Table 8. Molecular Weight and Average $s_{20,w}^0$ for PM2-HaeIII Fragments.

Fragment	Mw(bp)	Average $s_{20,w}^0$	Individual $s_{20,w}^0$
A	1735	10.778	10.81, 10.78, 10.75, 10.82, 10.73, 10.74, 10.79, 10.78
B	1606	10.672	10.66, 10.66, 10.63, 10.84, 10.76, 10.56, 10.63, 10.63
C	1310	9.985	9.97, 9.96, 9.99, 10.06, 10.05, 10.09, 9.87, 9.90
D	854	8.72	8.75, 8.69
E	794	8.59	8.52, 8.65
F	642	8.03	7.97, 8.09
G	592	7.89	7.87, 7.88, 7.93
H	498	7.615	7.63, 7.60, 7.63, 7.61
I	322	6.70	6.70
J	288	6.37	6.37
K	263	6.24	6.24
L	160	5.41	5.38, 5.44
M	145	5.20	5.20
N	117	4.92	4.92
O	94	4.58	4.58
P	50	3.51	3.58, 3.44

The Yamakawa-Fujii theory expresses the coefficient, \overline{E} , in terms of L and d where L is the contour length and d is the diameter; these dimensions are in units of the Kuhn statistical length (λ^{-1}).

For $L > \sigma$ ($\sigma = 2.278$)

$$\frac{3\pi\eta_o L}{\overline{E}} = A_1 L^{1/2} + A_2 + A_3 L^{-1/2} + A_4 L^{-1} + A_5 L^{-3/2} \quad (1)$$

$$A_1 = 4/3 (6/\pi)^{1/2} = 1.843$$

$$A_2 = -(1 - 0.01412 d^2 + 0.00592 d^4) \ln d - 1.0561 - 0.1667 d \\ - 0.1900 d^2 - 0.0224 d^3 + 0.0190 d^4$$

$$A_3 = 0.1382 + 0.6910 d^2$$

$$A_4 = -(0.04167 d^2 + 0.00567 d^4) \ln d - 0.3301 + 0.5 d \\ - 0.5854 d^2 - 0.0094 d^3 - 0.0421 d^4$$

$$A_5 = -0.0300 + 0.1209 d^2 + 0.0259 d^4$$

These expressions apply when the length L is longer than 2.278

Kuhn statistical lengths; for DNA this would correspond to molecular weights greater than 870 basepairs for $M_L = 195$ daltons/ \AA and $\lambda^{-1} = 1300 \text{\AA}$.

For polymers like DNA, with a uniform mass per unit length (M_L) the contour length is $L = M/M_L \lambda^{-1}$ and the equation is easily recast in terms of the molecular weight M ; the result is

$$\frac{3\pi\eta_o L}{\overline{E}} = A_1 (M_L \lambda^{-1})^{-1/2} M^{1/2} + A_2 + A_3 (M_L \lambda^{-1})^{1/2} M^{-1/2} \\ + A_4 M_L \lambda^{-1} M^{-1} + A_5 (M_L \lambda^{-1})^{3/2} M^{-3/2}$$

A set of new coefficients may then be defined so that

$$\frac{3\pi\eta_o L}{\Xi} = B_1 M^{1/2} + B_2 + B_3 M^{-1/2} + B_4 M^{-1} + B_5 M^{-3/2} \quad (2)$$

The A_i and the B_i are listed for several values of d and λ^{-1} which are appropriate to the dimensions of double-stranded DNA in Tables 9 and 10.

The Yamakawa-Fujii theory takes a somewhat different form for short DNA.

For $L \leq \sigma$

$$\frac{3\pi\eta_o L}{\Xi} = C_1 \ln (L/d) + C_2 + C_3 L + C_4 L^2 + C_5 L^3 \quad (3)$$

The coefficients are described by the following equations:

$$C_1 = 1 - 0.01412 d^2 + 0.00592 d^4$$

$$C_2 = 0.3863 - 0.1667 d + 0.0016 d^2 - 0.0224 d^3 - 0.0007 d^4$$

$$C_3 = 0.1667 + 0.0222 d^2 + 0.0017 d^4$$

$$C_4 = 0.01883 - 0.00789 d^2 - 0.00038 d^4$$

$$C_5 = -0.002039 + 0.000805 d^2 + 0.000017 d^4$$

Again the equation is simply recast in terms of molecular weight as the equation

$$\frac{3\pi\eta_o L}{\Xi} = D_1 \ln M + D_2 + D_3 M + D_4 M^2 + D_5 M^3 \quad (4)$$

Table 9. Coefficients of Yamakawa-Fujii Equation 1 for Several Combinations of the Helix Diameter and the Kuhn Statistical Length.^a

$d'(\text{\AA})^b$	$\lambda^{-1}(\text{\AA})$	A_1	A_2	$10A_3$	$10A_4$	$10A_5$
23	1233	1.8426	3.3354	1.3839	-3.2188	-2.9966
23	1225	1.8426	3.2561	1.3838	-3.2235	-2.9968
23	1253	1.8426	3.2763	1.3838	-3.2221	-2.9969
23	1275	1.8426	3.2962	1.3837	-3.2236	-2.9970
23	1333	1.8426	3.1157	1.3836	-3.2251	-2.9971
23	1325	1.8426	3.1348	1.3836	-3.2265	-2.9972
23	1353	1.8426	3.1535	1.3835	-3.2278	-2.9973
23	1375	1.8426	3.1719	1.3835	-3.2291	-2.9974
23	1433	1.8426	3.1930	1.3834	-3.2304	-2.9975
25	1233	1.8426	2.8115	1.3850	-3.1987	-2.9943
25	1225	1.8426	2.8322	1.3849	-3.2007	-2.9953
25	1253	1.8426	2.8525	1.3848	-3.2027	-2.9952
25	1275	1.8426	2.8724	1.3847	-3.2046	-2.9954
25	1333	1.8426	2.8918	1.3846	-3.2064	-2.9955
25	1325	1.8426	2.9113	1.3845	-3.2082	-2.9957
25	1353	1.8426	2.9297	1.3844	-3.2098	-2.9959
25	1375	1.8426	2.9481	1.3843	-3.2115	-2.9960
25	1433	1.8426	2.9662	1.3842	-3.2130	-2.9961
33	1233	1.8426	2.6285	1.3863	-3.1787	-2.9924
33	1225	1.8426	2.6492	1.3861	-3.1811	-2.9927
33	1253	1.8426	2.6695	1.3860	-3.1835	-2.9930
33	1275	1.8426	2.6893	1.3858	-3.1857	-2.9933
33	1333	1.8426	2.7088	1.3857	-3.1879	-2.9936
33	1325	1.8426	2.7283	1.3855	-3.1900	-2.9938
33	1353	1.8426	2.7467	1.3854	-3.1923	-2.9943
33	1375	1.8426	2.7652	1.3853	-3.1939	-2.9942
33	1433	1.8426	2.7832	1.3852	-3.1958	-2.9944

^a The mass per unit length, M_L , was held constant at 195 daltons/ \AA .

^b Within the Yamakawa-Fujii Theory the diameter, d , is expressed in Kuhn statistical length units. Therefore $d = d'/\lambda^{-1}$.

Table 10. Coefficients of the Modified Yamakawa-Fujii Equation 2 for Several
Combinations of the Helix Diameter and the Kuhn Statistical Length. ^a

$d'(\text{\AA})^b$	$\lambda^{-1}(\text{\AA})$	$B_1 \times 10^3$	B_2	$B_3 \times 10^{-1}$	$B_4 \times 10^{-4}$	$B_5 \times 10^{-6}$
20	1200	3.8392	3.0354	6.6945	-7.5322	-3.3923
20	1225	3.7721	3.0561	6.7635	-7.6929	-3.4987
20	1250	3.7322	3.0763	6.8318	-7.8538	-3.6065
20	1275	3.6954	3.0962	6.8994	-8.0146	-3.7154
20	1300	3.6597	3.1157	6.9664	-8.1755	-3.8254
20	1325	3.6251	3.1348	7.0328	-8.3364	-3.9364
20	1350	3.5913	3.1535	7.0985	-8.4973	-4.0485
20	1375	3.5585	3.1719	7.1637	-8.6581	-4.1616
20	1400	3.5266	3.1900	7.2282	-8.8190	-4.2757
25	1200	3.8392	2.8115	6.6997	-7.4849	-3.3899
25	1225	3.7721	2.8322	6.7686	-7.6457	-3.4966
25	1250	3.7322	2.8525	6.8367	-7.8066	-3.6044
25	1275	3.6954	2.8724	6.9042	-7.9674	-3.7133
25	1300	3.6597	2.8918	6.9711	-8.1282	-3.8233
25	1325	3.6251	2.9110	7.0373	-8.2891	-3.9344
25	1350	3.5913	2.9297	7.1029	-8.4499	-4.0464
25	1375	3.5585	2.9481	7.1679	-8.6108	-4.1596
25	1400	3.5266	2.9662	7.2324	-8.7716	-4.2737
30	1200	3.8392	2.6285	6.7061	-7.4382	-3.3373
30	1225	3.7731	2.6492	6.7748	-7.5989	-3.4940
30	1250	3.7322	2.6695	6.8427	-7.7597	-3.6019
30	1275	3.6954	2.6893	6.9100	-7.9205	-3.7108
30	1300	3.6597	2.7088	6.9767	-8.0813	-3.8208
30	1325	3.6251	2.7280	7.0428	-8.2421	-3.9319
30	1350	3.5913	2.7467	7.1083	-8.4029	-4.0440
30	1375	3.5585	2.7652	7.1731	-8.5637	-4.1571
30	1400	3.5266	2.7832	7.2374	-8.7246	-4.2713

^aThe mass per unit length, M_L , was held constant at 195 daltons/ \AA .

^bWithin the Yamakawa-Fujii Theory the diameter, d , is expressed in Kuhn statistical length units. Therefore $d = d'/\lambda^{-1}$.

in which the new coefficients are defined by the following equations:

$$D_1 = C_1$$

$$D_2 = C_2 - C_1 (\ln (dM_L \lambda^{-1}))$$

$$D_3 = C_3 (M_L \lambda^{-1})^{-1}$$

$$D_4 = C_4 (M_L \lambda^{-1})^{-2}$$

$$D_5 = C_5 (M_L \lambda^{-1})^{-3}$$

The first two terms to the right in equation (4) describe the behavior of a rigid rod model for DNA polymers. The C_i and the D_i are listed in Tables 11 and 12 for the same values of d and λ^{-1} previously chosen.

Since the sedimentation coefficient may be expressed as

$$s_{20,w}^0 = \frac{M_L (1 - \bar{v} \rho_o)}{N_A (3\pi\eta_o)} \frac{3\pi\eta_o L}{\Xi}$$

the effect of the factors $M_L (1 - \bar{v} \rho_o) / N_A (3\pi\eta_o)$ and $3\pi\eta_o L / \Xi$ on the functional relationship between $s_{20,w}^0$ and the molecular weight may be examined separately. In Figure 13 the effect of varying $M_L (1 - \bar{v} \rho_o) / N_A (3\pi\eta_o)$ is illustrated. For this example M_L is 195 daltons/ \AA , λ^{-1} is 1300 \AA and the diameter is 25 \AA ; π and N_A assume their usual values. For the lower curve $\bar{v} \rho_o$ is 0.556 and η_o is 0.01 poise; $M_L (1 - \bar{v} \rho_o) / N_A (3\pi\eta_o)$ is therefore 1.525×10^{-13}

Table 11. Coefficients of Yamakawa-Fujii Equation 3 for Several Combinations of the Helix Diameter and the Kuhn Statistical Length.^a

$d'(\text{\AA})^b$	$\lambda^{-1}(\text{\AA})$	C_1	$10C_2$	$10C_3$	$100C_4$	$1000C_5$
20	1200	1.0000	3.8352	1.6671	1.8828	-2.0388
20	1225	1.0000	3.8358	1.6671	1.8828	-2.0388
20	1250	1.0000	3.8363	1.6671	1.8828	-2.0388
20	1275	1.0000	3.8369	1.6671	1.8828	-2.0388
20	1300	1.0000	3.8374	1.6671	1.8828	-2.0388
20	1325	1.0000	3.8378	1.6671	1.8828	-2.0388
20	1350	1.0000	3.8383	1.6670	1.8828	-2.0388
20	1375	1.0000	3.8388	1.6670	1.8828	-2.0388
20	1400	1.0000	3.8392	1.6670	1.8828	-2.0388
25	1200	1.0000	3.8283	1.6671	1.8827	-2.0387
25	1225	1.0000	3.8290	1.6671	1.8827	-2.0387
25	1250	1.0000	3.8297	1.6671	1.8827	-2.0387
25	1275	1.0000	3.8303	1.6671	1.8827	-2.0387
25	1300	1.0000	3.8309	1.6671	1.8827	-2.0387
25	1325	1.0000	3.8316	1.6671	1.8827	-2.0387
25	1350	1.0000	3.8321	1.6671	1.8827	-2.0387
25	1375	1.0000	3.8327	1.6671	1.8827	-2.0387
25	1400	1.0000	3.8332	1.6671	1.8827	-2.0387
30	1200	1.0000	3.8213	1.6671	1.8825	-2.0385
30	1225	1.0000	3.8222	1.6671	1.8825	-2.0385
30	1250	1.0000	3.8230	1.6671	1.8825	-2.0385
30	1275	1.0000	3.8238	1.6671	1.8826	-2.0385
30	1300	1.0000	3.8245	1.6671	1.8826	-2.0385
30	1325	1.0000	3.8253	1.6671	1.8826	-2.0385
30	1350	1.0000	3.8260	1.6671	1.8826	-2.0385
30	1375	1.0000	3.8266	1.6671	1.8826	-2.0385
30	1400	1.0000	3.8273	1.6671	1.8826	-2.0385

^aThe mass per unit length, M_L , was held constant at 195 daltons/ \AA .

^bWithin the Yamakawa-Fujii Theory the diameter, d , is expressed in Kuhn statistical length units. Therefore $d = d'/\lambda^{-1}$.

Table 12. Coefficients of the Modified Yamakawa-Fujii Equation 4 for Several Combinations of the Helix Diameter and the Kuhn Statistical Length.^a

$d'(\text{\AA})^b$	$\lambda^{-1}(\text{\AA})$	D_1	D_2	$D_3 \times 10^7$	$D_4 \times 10^{13}$	$D_5 \times 10^{19}$
23	1200	1.0000	-7.8352	7.1242	3.4385	-1.5912
20	1225	1.0000	-7.8851	6.9788	3.2996	-1.4958
23	1250	1.0000	-7.8851	6.8392	3.1689	-1.4078
23	1275	1.0000	-7.8850	6.7051	3.0459	-1.3266
23	1300	1.0000	-7.8850	6.5761	2.9299	-1.2515
23	1325	1.0000	-7.8849	6.4521	2.8204	-1.1820
23	1350	1.0000	-7.8849	6.3326	2.7169	-1.1176
23	1375	1.0000	-7.8848	6.2174	2.6193	-1.0577
23	1400	1.0000	-7.8848	6.1064	2.5263	-1.0021
25	1200	1.0000	-8.1090	7.1243	3.4383	-1.5911
25	1225	1.0000	-8.1089	6.9789	3.2994	-1.4957
25	1250	1.0000	-8.1089	6.8393	3.1688	-1.4077
25	1275	1.0000	-8.1088	6.7052	3.0457	-1.3265
25	1300	1.0000	-8.1087	6.5763	2.9297	-1.2515
25	1325	1.0000	-8.1087	6.4522	2.8202	-1.1820
25	1350	1.0000	-8.1086	6.3327	2.7168	-1.1175
25	1375	1.0000	-8.1086	6.2175	2.6189	-1.0577
25	1400	1.0000	-8.1085	6.1065	2.5262	-1.0023
30	1200	1.0000	-8.2920	7.1245	3.4380	-1.5910
30	1225	1.0000	-8.2919	6.9791	3.2991	-1.4956
30	1250	1.0000	-8.2918	6.8395	3.1685	-1.4076
30	1275	1.0000	-8.2918	6.7054	3.0455	-1.3264
30	1300	1.0000	-8.2917	6.5764	2.9295	-1.2514
30	1325	1.0000	-8.2916	6.4523	2.8202	-1.1819
30	1350	1.0000	-8.2915	6.3328	2.7166	-1.1174
30	1375	1.0000	-8.2915	6.2176	2.6187	-1.0575
30	1400	1.0000	-8.2914	6.1066	2.5260	-1.0020

^a The mass per unit length, M_L , was held constant at 195 daltons/ \AA .

^b Within the Yamakawa-Fujii Theory the diameter, d , is expressed in Kuhn statistical length units. Therefore $d = d'/\lambda^{-1}$.

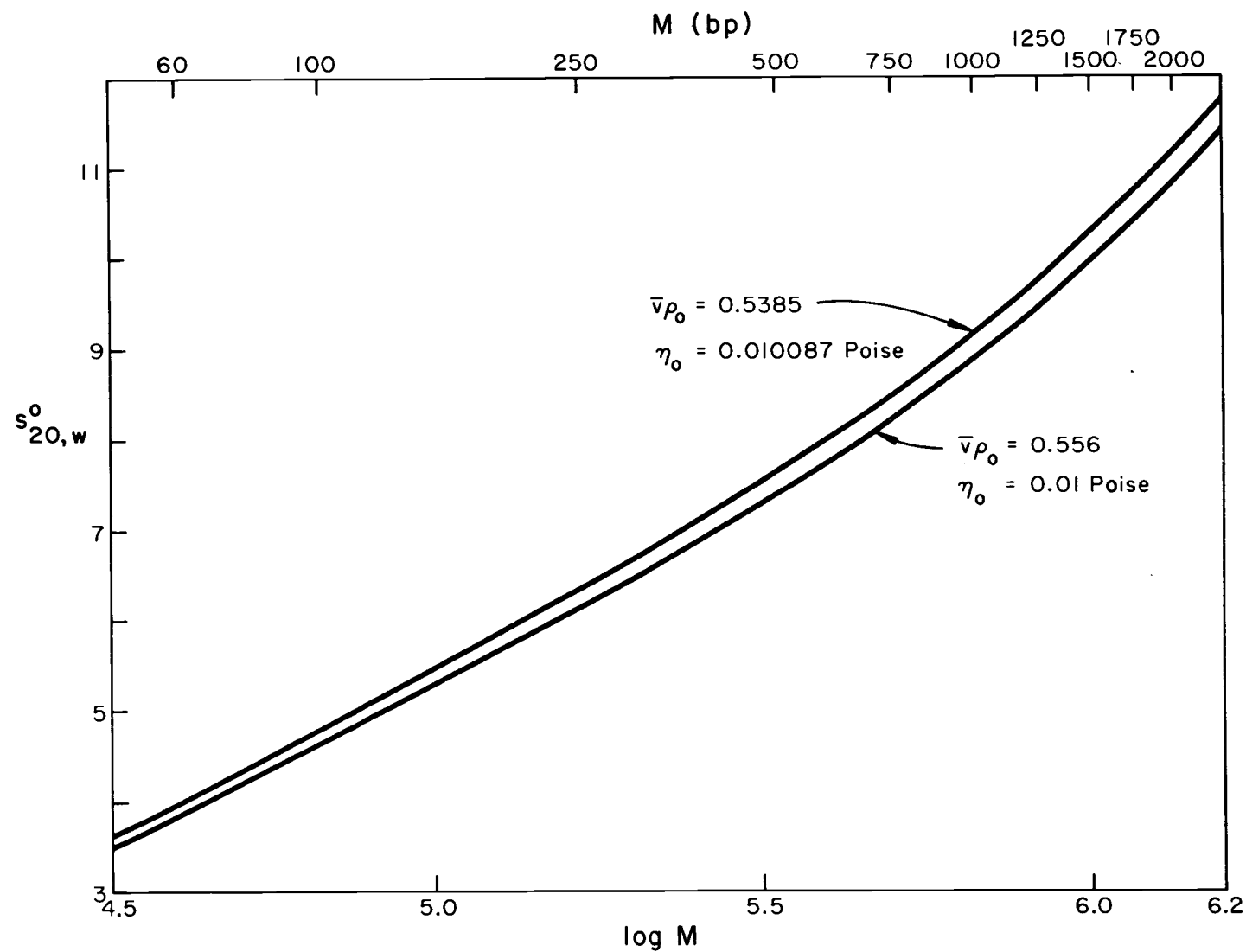


Figure 13. Effect of $\bar{v}\rho$ and η_0 on the Shape of the Yamakawa-Fujii Theoretical Curve.

sec. Since the $s_{20,w}^0$ value is usually measured in units of the Svedberg (S) which is 1×10^{-13} seconds, $M_L(1 - \bar{v}\rho_o)/N_A(3\pi\eta_o)$ is equal to 1.525 S; this is the value chosen by Yamakawa and Fujii. For the upper curve $M_L(1 - \bar{v}\rho_o)/N_A(3\pi\eta_o)$ is 1.572 S. The upper curve differs only in that $\bar{v}\rho_o$ corresponds with the careful measurements of $(\partial\rho/\partial C_2)_\mu^0$ made by Cohen and Eisenberg (33) for native DNA in 0.2 M NaCl (See Corrections to Standard Conditions). The value of η_o is taken from Svedberg and Pedersen (1).

Figure 14 illustrates the effect of varying the diameter and the Kuhn statistical length λ^{-1} while holding $M_L(1 - \bar{v}\rho_o)/N_A(3\pi\eta_o)$ constant at 1.525 S. Varying the diameter has nearly the same effect as varying $M_L(1 - \bar{v}\rho_o)/N_A(3\pi\eta_o)$ in that the shape of the curve is unchanged but the curve is shifted to higher or lower $s_{20,w}^0$. Changing λ^{-1} principally affects the shape of the curve; increasing λ^{-1} flattens the curve while decreasing λ^{-1} increases the curvature. Increasing λ^{-1} also increases the molecular weight at which the deviation from rigid rod behavior becomes significant.

In Figure 15 the straight line describes the hypothetical hydrodynamic behavior of a rigid rod with a diameter of 27 \AA and a mass per unit length of 195 daltons/\AA , appropriate dimensions for a rod of DNA. The factor $M_L(1 - \bar{v}\rho_o)/N_A(3\pi\eta_o)$ equal to 1.572 S and the first two terms of equation 4 for $3\pi\eta_o L/\Xi$ were used to obtain the slope and the intercept from the Yamakawa-Fujii theory. The curved

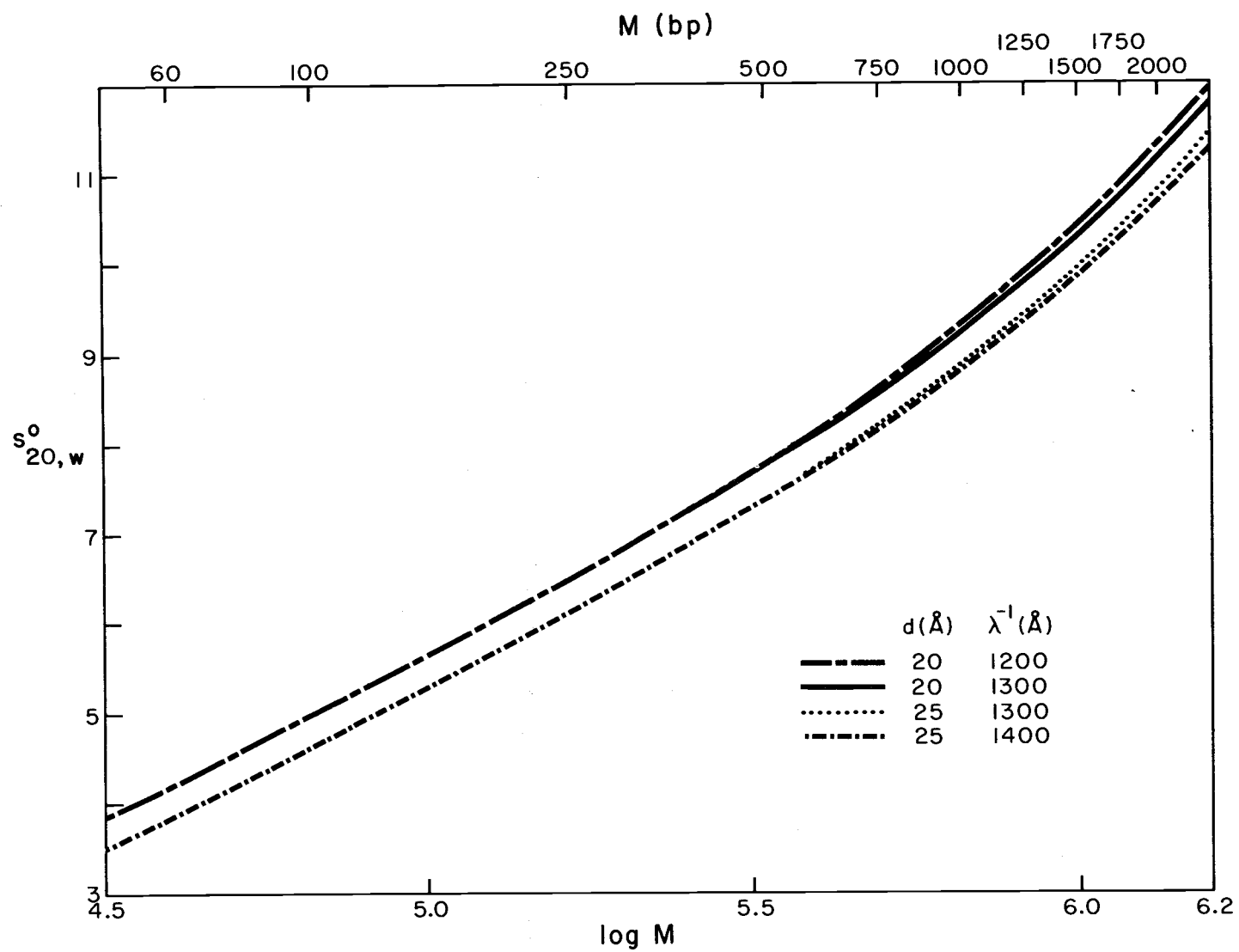


Figure 14. Effect of d and λ^{-1} on the Shape of the Yamakawa-Fujii Theoretical Curve.

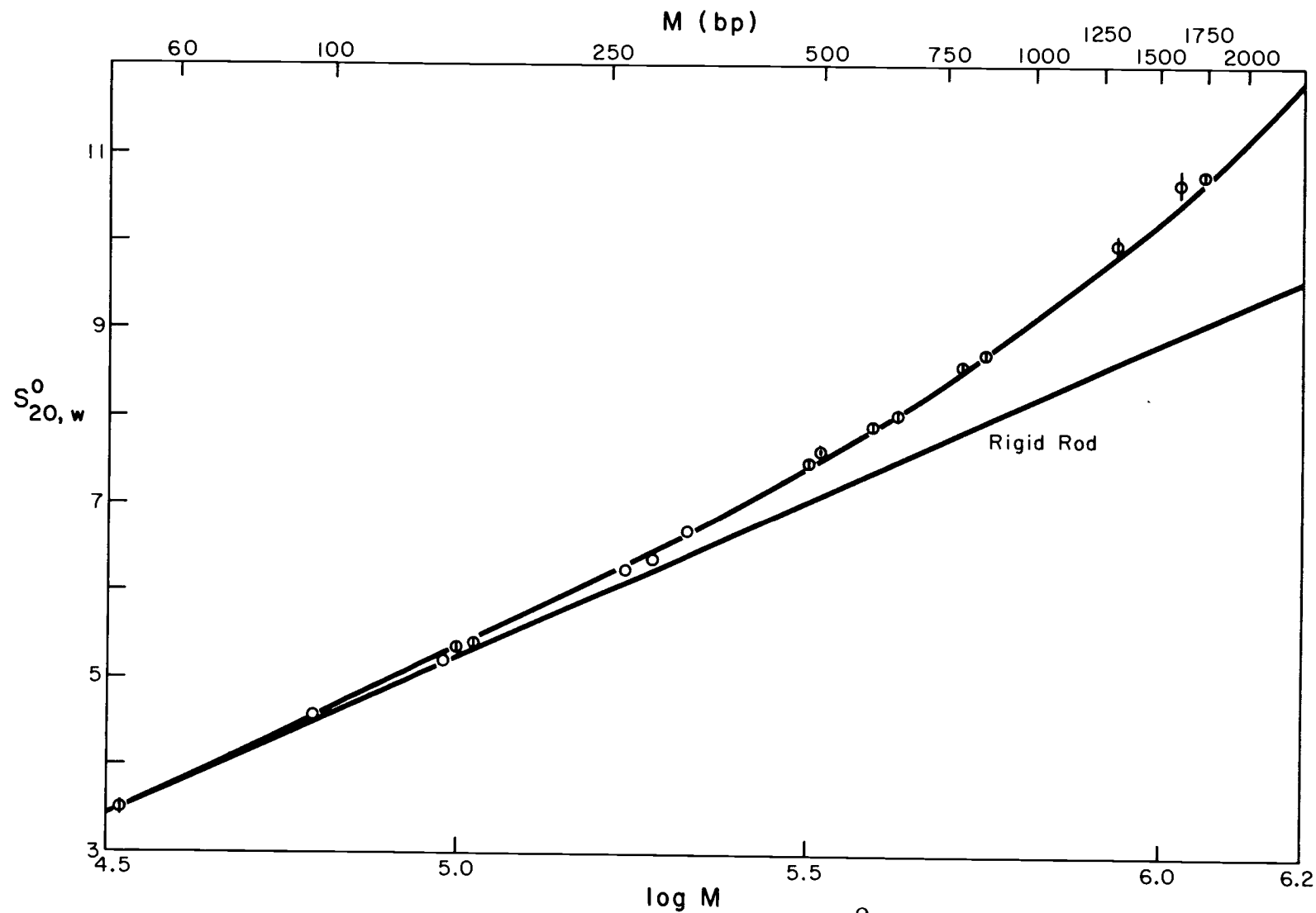


Figure 15. Comparison of the Empirical Relationship Between $s_{20,w}^0$ and M_w with the Predictions of the Yamakawa-Fujii Theory. The vertical bar represents the range of deviations from the mean $s_{20,w}^0$ for each fragment.

line is the theoretical relationship from the full Yamakawa-Fujii theory for the transition from rigid rod to wormlike coil. The molecular dimensions are a diameter of 27 \AA and a mass per unit length of 195 daltons/\AA . The Kuhn statistical length was chosen to be 1200 \AA and $M_L(1 - \bar{v}\rho_o)/N_A(3\pi\eta_o)$ is 1.572 S . Therefore the difference between the curved line and the straight line is the deviation from the hydrodynamic behavior of a hypothetical rigid rod predicted by the Yamakawa-Fujii theory for a flexible polymer of the same dimensions. The points are the experimental results obtained in this thesis for the relationship between $s_{20,w}^o$ and molecular weight for each of the PM2-HaeIII restriction fragments. The vertical bar represents the range of deviations from the mean which were observed for the individual $s_{20,w}^o$ values determined from each fragment. The circles are centered on the mean $s_{20,w}^o$ which was determined for each fragment. The molecular weights were those obtained from the sigmoidal fit to the five sets of restriction fragments coelectrophoresed in the 3.0% acrylamide (20:1) slab gel (Figure 12 and Table 7). These data are also summarized in Table 8.

DISCUSSION

The fragments from the digestion of PM2 DNA with the restriction enzyme endonuclease R HaeIII have proved to be very useful in this study of the conformation of DNA in solution. It has been shown that the fragments produced by digesting unnicked PM2 DNA are largely unnicked. Furthermore 15 of the 16 restriction bands reported here for the PM2-HaeIII digest contain DNA which is unique in both sequence and size. Therefore they should be useful in other experiments in which sequence heterogeneity as well as size heterogeneity is an important consideration. The separated fragments would be very useful in thermal denaturation and renaturation studies for this reason alone.

The PM2-HaeIII restriction fragments were readily separated by continuous elution preparative electrophoresis. This procedure might be simplified somewhat by separating the large restriction fragments from the small restriction fragments by gel chromatography prior to high resolution preparative electrophoresis. Alternatives to continuous elution preparative electrophoresis should be explored since this method becomes rather tedious if large quantities of DNA are required. Other methods for extracting DNA from gels have been reported by Young and Young (49) and Thuring, Sanders and Borst (50).

The difficulties in obtaining good molecular weights from the isolated PM2-HaeIII fragments by the short column sedimentation equilibrium technique are largely technical ones which are complicated by the hydrodynamic properties of double-stranded DNA. The main difficulty seems to be a disturbance of the equilibrium distribution of the DNA by convection, rotor precession, vibration or some combination of these factors. The low diffusion coefficient of double-stranded DNA only allows the system to respond sluggishly to any disturbance thereby increasing the probability that it will be disturbed again before reaching equilibrium. This difficulty can in part be resolved by carrying out the sedimentation equilibrium experiments in alkaline equilibrium buffer since denaturing the DNA effectively reduces the molecular weight by one half as well as increasing the diffusion coefficient because of the more compact random coil conformation for denatured DNA.

Fortunately the molecular weights of the PM2-HaeIII fragments can be obtained from their electrophoretic mobility in comparison with other restriction digests for which the sizes of the fragments are known. The results of a preliminary calibration of the PM2-HaeIII fragments against SV40-HaeIII fragments and Ad2-RI fragments are consistent with the sizes obtained independently by Peter Phillipsen below 500 bp (Table 4). However, the size of PM2 DNA which is obtained by adding up the sizes of the HaeIII fragments is

significantly smaller than the reported molecular weight for PM2 DNA. This discrepancy may in part be the result of a calibration in which the standard digests do not cover the full range of sizes represented in the PM2-HaeIII digest. Therefore it became apparent that the calibration would be greatly improved by coelectrophoresing the PM2-HaeIII digest with many different restriction digests for which the sizes of the fragments have been reported and which cover the same molecular weight range. This was done by coelectrophoresing SV40-Hind, SV40-HaeIII, SV40-Hind-HaeIII, λ -Hind and PM2-HaeIII in parallel tracks in a 3.0% acrylamide (20:1) slab gel. The mobility of each of the fragments could then be measured and combined with the respective molecular weight to make a comprehensive calibration curve (Figure 12). The questions which remain are (a) the effect of base composition on electrophoretic mobility and (b) the relationship between mobility and molecular weight.

Since the effect of base composition on the mobility has not been studied systematically for DNA molecules in this size range and since the base composition of each of the PM2-HaeIII fragments studied here has not been determined, the effect of base composition is an open question. Any base compositional effect will be neglected here because it should only contribute randomly to the overall error for the set of the PM2-HaeIII fragments. Furthermore the known errors due to base composition when they do occur, are less than

10% of the presumed sizes.

The relationship between the mobility and the molecular weight for double-stranded DNA is also unclear. Many previous workers have found that the logarithm of the molecular weight is approximately a linear function of the mobility. If DNA fragments with a wide range of molecular weights are electrophoresed, however, the relationship between $\log M$ and the mobility is a sigmoidal function. Therefore a linear fit to coordinates which linearize sigmoidal functions would be preferred. Such a fitting procedure was developed in the Results section of this thesis. The success of this fitting procedure is illustrated in Figures 9, 10 and 11. Since the molecular weights of the fragments fitted were estimated by the approximation that the logarithm of the molecular weight is a linear function of the mobility, the real strength of the sigmoidal function appears in those regions in the gel where the plots of $\log M$ vs mobility are very curved. Furthermore the sigmoidal fit works well even for the high molecular weight fragments in high percentage acrylamide gels where the "linear range" has been shifted to low molecular weights. The fact that the procedure works so well in three different gel systems and for several different gel percentages reinforces a strong preference for the sigmoidal fit. Therefore "Optimize VM" was applied to the data shown in Figure 12 to provide the best sigmoidal fit. The result (Table 7) is significantly different

sizes for the PM2-HaeIII fragments over most of the molecular weight range. However, there are several marked improvements. One improvement is that the total of the fragments adds up to a very reasonable size for PM2 DNA. The other is that the predicted size of the SV40-Hind-H fragment is 263 bp. This is in very good agreement with the 266 bp plus 4 nucleotide size which has been determined by sequence analysis (47, 48). The previous PM2-HaeIII calibrations would underestimate the size of SV40-Hind-H by 25-35 bp. The linear fit over the mobility range of 4.5-16 cm predicts the same size for the SV40-Hind-H fragment and throughout this mobility range is in close agreement with the sigmoidal fit (Figure 12 and Table 7). The PM2-HaeIII fragment sizes predicted by the sigmoidal fit were used in relating $s_{20,w}^0$ to molecular weight because the fit is in good agreement with all the calibration data. Furthermore the data from sedimentation equilibrium experiments is in good agreement with the sigmoidal fit. Finally the estimated error in M for any of the fragments is $\sim 3\%$ based on the sigmoidal fit and the reported sizes of SV40-Hind-H and PM2 DNA.

The $s_{20,w}^0$ of each of the fragments is just as well established as the molecular weight. The maximum deviation from the mean $s_{20,w}^0$ of any individual sedimentation coefficient determined for any single fragment was 1.6%. The difference between the mean and the individual values was usually less than 1%. Because a 1% error in

$s_{20,w}^0$ represents a 3% error in M the measurements of $s_{20,w}^0$ and M presented here have been determined to about the same precision. Since no special precautions were taken beyond controlling the run temperature at 20° C and operating the Model E ultracentrifuge at the same speed with the same rotor for most runs the precision of the measurements is very gratifying. The accuracy of these measurements depends in part on whether the fragments have been well resolved and are therefore truly homogeneous. With the exception of "fragment" P, reelectrophoresis of the fragments revealed them to be homogeneous within the limits of the technique. "Fragment" P is a single band under most conditions of electrophoresis although it can be resolved by analytical electrophoresis in high percentage gels into two bands. These two fragments were not separated by preparative gel electrophoresis and so it should be remembered that the results for "fragment" P are for this mixture.

The data presented in Table 8 and Figure 15 represent the empirical relationship between the $s_{20,w}^0$ and the molecular weight. The $s_{20,w}^0$ seems to be a smooth monotonically increasing function of the molecular weight. In the low molecular weight range the hydrodynamic behavior of the double-stranded DNA is well modeled by a rigid rod (See Figure 15). Data in this size range should provide the most information about the diameter and the $\bar{v}\rho$ of DNA

in solution. When the Yamakawa-Fujii theoretical relationship is applied in this range the combination of $\bar{v} \rho_0$ equal to 0.5385 and a diameter of 27 \AA for hydrated double-helical DNA fit the data very well. This information provides a useful point of departure for examining the region of most interest, the transition from rigid rod to stiff coil behavior. The shape of the transition will depend on the mode in which the DNA actually bends; the Yamakawa-Fujii theory is based on the premise that the bending is a uniform function of the length and that the function is independent of the underlying base sequence. For large DNAs this approximation works very well because any differences caused by sequence heterogeneity will average out. In the transition region the situation should be quite different especially with DNA which is homogeneous in both size and sequence. If the bending function is a function of the underlying sequence the Kuhn statistical length for a DNA of unique sequence may be changed enough to be detected experimentally as a change in the sedimentation coefficient. DNA which is 1 to 4 Kuhn statistical lengths long (average) should be an ideal test material since it is large enough to bend but not so long as to contain enough sequence variety to produce an average bending function. Recently Crick and Klug have proposed that DNA may "kink" under certain circumstances (51). If these postulated kinks occur preferentially in certain kinds of sequences and if kinking is a property of DNA in solution

there should be an effect on the hydrodynamic properties of the DNA. Unfortunately an added complication enters the discussion at this point: if kinks are produced only transitorily on a time scale much faster than the measurement kinking may not be apparent. Sedimentation velocity measurements are made on a very long time scale compared to events at the molecular level and so this effect could be missed. The results can also be obscured by differences in \bar{v} for each of the fragments. As demonstrated in the Results, the theoretical relationship is shifted to higher or lower $s_{20,w}^0$ by a change in \bar{v} , ρ_0 , η_0 , d or combinations of these parameters. Therefore in order to be entirely correct the base composition and hence the \bar{v} of each fragment must be known. The base composition of each of the fragments has not been determined in the work completed: determining \bar{v} itself is complicated principally by the amount of DNA required to make a conventional \bar{v} measurement. The \bar{v} for each fragment could be obtained from sedimentation equilibrium measurements if the molecular weight of each fragment were known. The difficulties in carrying out sedimentation equilibrium experiments on the restriction fragments have been previously discussed. Therefore deviations from any theoretical curve may be interpreted as differences in \bar{v} as well as changes in conformation.

Over the full size range the results presented here are not in good agreement with the choice of a 25 \AA diameter and a 1300 \AA

Kuhn statistical length made by Yamakawa and Fujii when they formulated their theory (5). However a diameter of 27 \AA , a Kuhn statistical length of 1200 \AA and the $\bar{v}\rho$ of 0.5385 derived from Cohen and Eisenberg's work (33) taken together with the Yamakawa-Fujii theory fit the data quite well. These values are not far from those chosen by Yamakawa and Fujii. It will be interesting, however, to compare other theories for the wormlike coil with the data presented here.

The results presented here would be improved if the base composition of each fragment were determined so that an estimate of $\bar{v}\rho$ could be made for each. Alternatively additional data from other restriction fragments in this size range would minimize the variation due to base composition. In addition $s_{20,w}^0$ data from fragments with approximately the same molecular weights would provide a test of differences in conformation due to base sequence.

In any event isolated restriction fragments should be very useful in further studies of DNA conformation. They would be particularly useful in studies of the rotational diffusion coefficient which is more sensitive to shape than the translational diffusion coefficient. Interpretation of experimental measurements of the rotational diffusion coefficient has been complicated by the need to separate the effects of heterogeneity from the conformational effects. Homogeneous material would be ideal. The temperature and ionic

strength dependence of the Kuhn statistical length would also provide useful information about the thermodynamic stability of the DNA double helix. Restriction fragments would also be very useful in experiments which look at more rapidly occurring events on the molecular time scale. Such experiments would also clarify the mechanism by which DNA bends. Finally the isolated fragments would be very useful for determining the size and sequence dependence of the dissociation and reassociation reactions for DNA as well as elucidating the mechanisms of dissociation and reassociation.

CONCLUSIONS

When DNA fragments with a wide range of sizes are electrophoresed, the relationship between $\log M$ and the mobility is sigmoidal. A procedure to produce the best sigmoidal fit to the relationship was developed in the Results section of this thesis. It offers a significant improvement over the assumption that $\log M$ is a linear function of the mobility. The sizes of PM2-HaeIII fragments have been determined from the sigmoidal fit to five restriction digests electrophoresed together in a slab gel. The $s_{20,w}^0$ for each of the PM2-HaeIII fragments was determined after the fragments were separated by preparative gel electrophoresis. These results (Table 7 and Figure 14) represent the empirical relationship between $s_{20,w}^0$ and M in the region of transition from rigid rod to wormlike coil behavior. The $s_{20,w}^0$ is a smooth, monotonically increasing function of the molecular weight. In the low molecular weight range the hydrodynamic behavior of the double-stranded DNA is well modeled by a rigid rod (Figure 14). The rigid rod limit of the Yamakawa-Fujii theory (5) together with a helix diameter of 27 \AA and a $\bar{v} \rho_0$ of 0.5385 derived from the work of Cohen and Eisenberg (33) fit the data very well in this region. In the sense that the Cohen and Eisenberg value appears to be the most carefully measured in the literature, and that the 27 \AA diameter is physically reasonable for hydrated DNA one may conclude that the sedimentation coefficient

can be predicted a priori in this region. In the region of transition from rodlike to stiff coil behavior the data may be fit by the Yamakawa-Fujii relationship with the same values of $\bar{v} \rho_0$ and d and a Kuhn statistical length of 1200 Å. The data would be improved if the base composition and $\bar{v} \rho_0$ were known for each fragment. Comparison of the data with other models for the wormlike coil will also be interesting. The results indicate that there is a unique Kuhn statistical length and therefore the mode of bending is independent of sequence. This conclusion should be confirmed by a more sensitive measure of conformation such as the rotational diffusion coefficient. In addition the relationship between ionic strength, temperature and the Kuhn statistical length for several of the fragments should answer this question as well as provide information about the thermodynamic stability of double-stranded DNA.

The isolated PM2-HaeIII restriction fragments have proven to be very useful for these studies. Their combination of unique size and sequence should be exploited in other studies of the physical properties of double-stranded DNA. An added advantage is that PM2 DNA can be isolated in very large quantities compared to other small DNAs. Therefore important contributions to our knowledge of the structure and properties of double-stranded DNA would be made if this work was extended to studies of the rotational diffusion

coefficient, the temperature and ionic strength dependence of the Kuhn statistical length and experiments which look at fast events on the molecular time scale. Finally these fragments would be very useful for studies of the dissociation and reassociation reactions for double-stranded DNA.

BIBLIOGRAPHY

1. Svedberg, T. and K. O. Pedersen. The Ultracentrifuge. London, Oxford University Press. 1940.
2. Kuhn, W. "Über die Gestalt fadenförmiger Moleküle in Lösung. Kolloid Zeitschrift, 1934, 68:2-15.
3. Kratky, O. and G. Porod. "Röntgenuntersuchung Gelöster Fadenmoleküle. Recueil des Travaux Chimiques des Pays-Bas, 1949, 68:1106-1122.
4. Hearst, J. E. and W. H. Stockmayer. Sedimentation Constants of Broken Chains and Wormlike Coils. Journal of Chemical Physics, 1962, 37:1425-1122.
5. Yamakawa, H. and M. Fujii. Translational Friction Coefficient of Wormlike Chains. Macromolecules, 1973, 6:407-415.
6. Burgi, E. and A. D. Hershey. Sedimentation Rate as a Measure of Molecular Weight of DNA. Biophysical Journal, 1963, 3:309-321.
7. Studier, F. Sedimentation-Studies of the Size and Shape of DNA. Journal of Molecular Biology, 1965, 11:373-390.
8. Crothers, D. M. and B. H. Zimm. Viscosity and Sedimentation of the DNA from Bacteriophages T2 and T7 and the Relationship to Molecular Weight. Journal of Molecular Biology, 1965, 12:525-536.
9. Gray, H. B. Jr. and J. E. Hearst. Flexibility of Native DNA from the Sedimentation Behavior as a Function of Molecular Weight and Temperature. Journal of Molecular Biology, 1968, 35:111-129.
10. Prunnell, A. and G. Bernardi. Fractionation of Native and Denatured Deoxyribonucleic Acid on Agarose Columns. Journal of Biological Chemistry, 1973, 248:3433-3440.
11. Record, M. T. Jr., C. P. Woodbury and R. B. Inman. Characterization of Rodlike DNA Fragments. Biopolymers, 1975, 14:393-408.

12. Arber, W. and S. Linn. DNA Modification and Restriction. Annual Reviews of Biochemistry, 1969, 38:467-500.
13. Boyer, H. W. DNA Restriction and Modification Mechanisms in Bacteria. Annual Reviews of Microbiology, 1971, 25:153-176.
14. Meselson, M., R. Yuan and J. Heywood. Restriction and Modification of DNA. Annual Reviews of Biochemistry, 1972, 41:447-466.
15. Hagen, F. S. and E. T. Young. Preparative Polyacrylamide Gel Electrophoresis of Ribonucleic Acid. Identification of Multiple Molecular Species of Bacteriophage T7 Lysozyme Messenger Ribonucleic Acid. Biochemistry, 1974, 13:3394-3400.
16. Kriegstein, H. J. and D. S. Hogness. Mechanisms of DNA Replication in Drosophila Chromosomes: Structure of Replication Forks and Evidence for Bidirectionality. Proceedings of the National Academy of Science, U.S.A., 1974, 71:135-139.
17. Espejo, R. T. and E. S. Canelo. Properties of Bacteriophage PM2: A Lipid-Containing Bacterial Virus. Virology, 1968, 34:738-747.
18. Hays, J. B. and B. H. Zimm. Flexibility and Stiffness in Nicked DNA. Journal of Molecular Biology, 1970, 48:297-317.
19. Smith, H. O. and D. Nathans. A Suggested Nomenclature for Bacterial Host Modification and Restriction Systems and Their Enzymes. Journal of Molecular Biology, 1973, 81:419-423.
20. Le Pecq, J. -B. Use of Ethidium Bromide for Separation and Determination of Nucleic Acids of Various Conformational Forms and Measurement of Their Associated Enzymes. In Methods of Biochemical Analysis, Vol. 20, D. Glick (ed.) New York, Interscience Publishers, John Wiley & Sons, 1971, p. 41-86.
21. Huang, E. S., J. E. Newbold and J. S. Pagano. Analysis of Simian Virus 40 DNA with the Restriction Enzyme of Haemophilus aegyptius, Endonuclease Z. Journal of Virology, 1973, 11:508-514.

22. Middleton, J. H., M. H. Edgell and C. A. Hutchison III. Specific Fragmentation of ϕ X 174 Deoxyribonucleic Acid Produced by a Restriction Enzyme from Haemophilus aegyptius, Endonuclease Z. *Journal of Virology*, 1972, 10:42-50.
23. Smith, H. O. and K. W. Wilcox. A Restriction Enzyme from Hemophilus influenzae. I. Purification and General Properties. *Journal of Molecular Biology*, 1970, 51:379-391.
24. Lowry, O. H., N. J. Rosenbrough, A. L. Farr, and R. J. Randall. Protein Measurement with the Folin Phenol Reagent. *Journal of Biological Chemistry*, 1951, 193:265-275.
25. Loening, U. E. The Fractionation of High-Molecular Weight Ribonucleic Acid by Polyacrylamide-Gel Electrophoresis. *Biochemical Journal*, 1967, 102:251-257.
26. Sharp, P. A., B. Sugden and J. Sambrook. Detection of Two Restriction Endonuclease Activities in Haemophilus parainfluenzae Using Analytical Agarose-Ethidium Bromide Electrophoresis. *Biochemistry*, 1973, 12:3055-3063.
27. Britten, R. J., D. E. Graham and B. R. Neufeld. Analysis of Repeating DNA Sequences by Reassociation. In Methods in Enzymology, Vol. 29, L. Grossman and K. Moldave (eds.) New York, Academic Press, 1974, p. 363-418.
28. Reinert, K. E., J. Strassburger and H. Triebel. Molecular Weights and Hydrodynamic Properties for Homogeneous Native DNA Derived from Diffusion, Sedimentation, and Viscosity Measurements on Polydisperse Samples. *Biopolymers*, 1970, 10:285-307.
29. Van Holde, K. E. and R. L. Baldwin. Rapid Attainment of Sedimentation Equilibrium. *Journal of Physical Chemistry*, 1958, 62:734-743.
30. Howlett, G. J. and L. W. Nichol. An Examination of the Overspeeding Technique in Relation to Sedimentation Equilibrium. *Journal of Physical Chemistry*, 1972, 76:2740-2743.
31. Gropper, L. and W. Boyd. Temperature Measurement and Control of Analytical Rotors in the Ultracentrifuge. *Analytical Biochemistry*, 1965, 11:238-245.

32. Biancheria, A. and G. Kegeles. Thermodynamic Measurements of Ultracentrifuge Rotor Temperatures. *Journal of the American Chemical Society*, 1954, 76:3737-3741.
33. Cohen, G. and H. Eisenberg. Deoxyribonucleate Solutions: Sedimentation in a Density Gradient, Partial Specific Volumes, Density and Refractive Index Increments, and Preferential Interactions. *Biopolymers* 6:1077-1100.
34. Staynov, D. A., J. C. Pinder, and W. B. Gratzer. Molecular Weight Determination of Nucleic Acids by Gel Electrophoresis in Non-aqueous Solution. *Nature New Biology (London)*, 1972, 235:108-110.
35. Boedtker, H., R. B. Crkvenjakov, K. F. Dewey and K. Lanks. Some Properties of High Molecular Weight Ribonucleic Acid Isolated from Chick Embryo Polysomes. *Biochemistry*, 1973, 12:4356-4360.
36. Zeiger, R. S., R. Salomon, C. W. Dingman and A. C. Peacock. Role of Base Composition in the Electrophoresis of Microbial and Crab DNA in Polyacrylamide Gels. *Nature New Biology (London)*, 1972, 238:65-68.
37. Maniatis, T., A. Jeffrey and H. van de Sande. Chain Length Determination of Small Double- and Single-Stranded DNA Molecules by Polyacrylamide Gel Electrophoresis. *Biochemistry*, 1975, 14:3787-3793.
38. Helling, R. B., H. M. Goodman and H. W. Boyer. Analysis of Endonuclease R·EcoRI Fragments of DNA from Lambdoid Bacteriophages and Other Viruses by Agarose-Gel Electrophoresis. *Journal of Virology*, 1974, 14:1235-1244.
39. Newbold, J. W. Professor, The University of North Carolina, Department of Bacteriology and Immunology, Chapel Hill, North Carolina. Letter of June 22, 1974.
40. Lebowitz, P., W. Siegel and J. Sklar. Hemophilus aegyptius Restriction Endonuclease Cleavage Map of the Simian Virus 40 Genome and its Colinear Relation with the Hemophilus influenza Cleavage Map of SV40. *Journal of Molecular Biology*, 1974, 88:105-123.

41. Pettersson, U., C. Mulder, H. Delius and P. A. Sharp. Cleavage of Adenovirus Type 2 DNA into Six Unique Fragments by Endonuclease R·RI. *Proceedings of the National Academy of Science, U.S.A.*, 1973, 70:200-204.
42. Phillipsen, P. Research Associate, Stanford University, Department of Biochemistry, Palo Alto, California. Telephone Conversation of June 5, 1975.
43. Streeck, R. E., P. Phillipsen and H. G. Zachau. Cleavage of Small Bacteriophage and Plasmid DNAs by Restriction Endonucleases. *European Journal of Biochemistry*, 1974 45:489-499.
44. Ferguson, K. A. Starch-Gel Electrophoresis-Application to the Classification of Pituitary Proteins and Polypeptides. *Metabolism, Clinical and Experimental*, 1964, 13:985-1002.
45. Noll, M. Differences and Similarities in Chromatin Structure of Neurospora Crassa and Higher Eukaryotes, *Cell*, In Press, 1976.
46. Yang, R. C-A., A. Van de Voorde, and W. Fiers. Cleavage Map of the Simian-Virus-40 Genome by the Restriction Endonuclease III of Haemophilus aegyptius. *European Journal of Biochemistry*, 1976, 61:101-117.
47. Fiers, W., R. Rogiers, E. Soeda, A. Van de Voorde, H. VanHeuverswyn, J. Van Herreweghe, G. Volckaert, and R. Yang. Nucleotide Sequence Analysis of SV40 DNA. In Organization and Expression of the Viral Genome. *Proceedings of the Tenth FEBS Meeting*, Vol. 39, F. Chapeville and M. Grunberg-Manago (eds.). Amsterdam, the Netherlands, North-Holland Publishing Company, 1975, p. 17-33.
48. Fiers, W. Director, Laboratorium voor Moleculaire Biologie, University of Ghent, B9000 Ghent, Belgium. Letter of June 4, 1976.
49. Young, Y. P. L. and R. J. Young. A Method for Recovery of Nucleic Acids from Polyacrylamide Gels. *Analytical Biochemistry*, 1974, 58:286-293.

50. Thuring, R. W. J., J. P. M. Sanders and P. Borst. A Freeze-Squeeze Method for Recovering Long DNA from Agarose Gels. *Analytical Biochemistry*, 1975, 66:213-220.
51. Crick, F. H. C. and A. Klug. Kinky helix. *Nature (London)*, 1975, 255:530-533.

APPENDICES

APPENDIX I

MEDIA, STANDARD SOLUTIONS AND SPECIAL PROCEDURES

PM2 DNA PreparationAMS (Synthetic Sea Water)

12.0 g $\text{MgSO}_4 \cdot 7\text{H}_2\text{O}$

26.0 g NaCl

3.5 ml of 20% KCl

10 ml 1.0 M CaCl_2

Add distilled water to make 1 liter.

BAL Broth

Dissolve 8 g Bacto Nutrient Broth in 1 liter of AMS.

Dispense into containers and autoclave for 30 minutes to sterilize.

BAL Agar

Dissolve 18 g of Bacto Nutrient Agar in 1 liter of AMS.

Sterilize by autoclaving for 30 minutes. Cool to $50-60^\circ\text{C}$ and

pour 20-25 ml into sterile disposable plastic Petri dishes.

Allow to harden and refrigerate.

BAL Top Agar

Dissolve 5 g of Bacto Agar in 1 liter of AMS by autoclaving.

Dissolve 8 g/l of Bacto Tryptone in the melted agar and then dispense 2.5 ml aliquots into tubes and cap. Sterilize the filled tubes by autoclaving for 15 minutes. Refrigerate until use. Melt the agar in boiling water and cool to 45° C before titering.

NTC (Virus Diluent)

58.45 g NaCl

10.0 ml 1.0 M CaCl

2.5 g Tris HCl

0.48 g Tris base

Add distilled water to make 1 liter.

For titering PM2 dispense into large tubes, cap and autoclave for 30 minutes.

SC TE

0.1 M NaCl

0.1 M Tris, pH 8.0

0.01 M Na₂EDTA

Pronase Stock

10 mg/ml pronase dissolved in

0.1 M NaCl

0.1 M Tris, pH 8.0

0.01 M Na₂EDTA

0.1% Sarkosyl

Heat to 80° C for 2 minutes, then incubate at 37° C for 3 hrs. Store frozen at -20° C.

SSC

0.15 M NaCl

0.015 M Na₃Citrate

Endonuclease R ~~Hae~~ III PreparationRabbit Blood Agar Plates

Prepare Bacto Blood Agar base according to the directions on the label. Sterilize and cool to 45° C. Add aseptically 3.5% sterile defibrinated rabbit blood. Mix and pour into sterile disposable Petri dishes.

Supplemented Brain Heart Infusion Broth

Prepare Brain Heart Infusion Broth (Difco) according to the instructions on the label. Autoclave for 15-30 minutes. Cool. Before innoculating the sterile broth add filter-sterilized NAD solution and hemin solution to final concentrations of 2 & 10 $\mu\text{g/ml}$ respectively. An NAD stock is easily prepared by dissolving NAD in distilled water and filtering through a 0.2 μ Millipore filter. The hemin solution should be prepared as follows:

Hemin Stock (1 mg/ml)

Dissolve 4 ml of triethanolamine in 96 ml of distilled water and then add 0.1 g hematin and 0.1 g L-histidine. Heat with periodic mixing in a 50-60 $^{\circ}$ C water bath until most of the hematin is dissolved. Sterilize by filtering through a 0.22 μ Millipore filter. Store at 4 $^{\circ}$ C.

SB (Sonication Buffer)

Autoclave 0.025 M Tris, pH 7.9

Add dithiothreitol to 1 mM.

GPB

Autoclave a solution of:

0.01 M NaH_2PO_4 - Na_2HPO_4 , pH 7.2

0.001 M Na_2EDTA

Add sterile glycerol and β -mercaptoethanol to final concentrations of

1 mM β -mercaptoethanol

1 mM Na_2EDTA

Phosphocellulose

1. Stir 25 g of phosphocellulose (Whatman, P-11) into 800 ml of 0.1 N HCl, 48% ethanol and stir for 30 minutes.
2. Collect and wash the resin with 800 ml portions of distilled water. Repeat the wash until the pH of the wash water is near neutrality.
3. Collect the washed resin, resuspend in 800 ml of 0.1 N NaOH and stir for 30 minutes.
4. Collect and resuspend in 800 ml portions of 1 mM EDTA. Stir for 30 minutes and then collect and wash the resin with successive 800 ml portions of 1 mM EDTA until the wash water approaches neutral pH.
5. Resuspend the collected resin in 2 volumes of 0.5 M Tris pH 7.9 and stir for 15 minutes. At the end of the time check the pH and titrate to pH 7.9 with HCl.
6. Stir at room temperature for 4-5 hours and then retitrate to pH 7.9. Store at 4⁰ C and use within a week of preparation.

TBS MgME (HaeIII Assay Buffer)

Autoclave TBS which is a solution of:

0.05 M Tris, pH 7.4 at 25° C

0.15 M NaCl

1. Before digestion dissolve ethanol-precipitated DNA in TBS.
2. Before beginning the digestion add 0.1 ml of 0.5 M β -mercaptoethanol and 0.1 ml of 0.13 M MgCl_2 for each ml of TBS.
3. Initiate the reaction by adding 0.050 ml or less of the enzyme preparation. Incubate at 37° C.

Large Scale HaeIII Digestion

1. Dissolve DNA to a concentration of 1 mg/ml in TBS.
2. Add 0.1 ml of 0.5 M β -mercaptoethanol and 0.2 ml of 0.13 M MgCl_2 for each ml of TBS.
3. Initiate the reaction by adding 0.025 ml of the enzyme preparation for each ml of TBS. Incubate at 37° C.
4. Add two additional 0.025 ml portions of enzyme at two hour intervals. Digestion should be complete in six hrs. Digestion time and/or amount of enzyme added may have to be adjusted to complete the digestion.
5. Stop the reaction by adding EDTA to a concentration of 0.05 M.

Centrifugation BuffersBPES

0.006 M Na_2HPO_4

0.002 M NaH_2PO_4

0.001 M Na_2EDTA

0.179 M NaCl

$[\text{Na}^+] = 0.195 \text{ M}$ Ionic Strength = 0.202

EQB (Equilibrium Buffer)

1.0 M NaCl

0.01 M Tris

0.001 M Na_2EDTA

$[\text{Na}^+] = 1.002$ Adjust pH to 7.6 with HCl

AEQB (Alkaline Equilibrium Buffer)

0.9 M NaCl

0.1 M NaOH

0.001 M Na_2EDTA

$[\text{Na}^+] = 1.002$

MiscellaneousPB (Phosphate Buffer for Hydroxylapatite Chromatography)

0.2 M NaH_2PO_4

0.2 M Na_2HPO_4

After preparing the solution pass it through a column made up of the hydrogen form of Chelex-100 (Biorad) to remove trace metals. Three or four milliliters of this resin are enough to treat one liter of buffer.

APPENDIX II

POLYACRYLAMIDE GEL ELECTROPHORESIS

Stock Solutions3 E

0.12 M Tris

0.06 M sodium acetate

0.003 M Na₂EDTA

Adjust to pH 7.2 at 25⁰ C with glacial acetic acid (~6.4 ml/l).

3 E + TEMED

2.5 ml of N, N, N', N' -tetramethylethylenediamine (TEMED)

3 E to make one liter

20% Acrylamide (20:1)

20 g acrylamide monomer

1 g N,N-methylene-bis-acrylamide

Dissolve and dilute to 100 ml with distilled water.

1% (NH₄)₂S₂O₈ (w/v)

Make fresh weekly.

Gel Preparation

The percentage of polyacrylamide gels may be varied by adjusting the proportions of water and acrylamide stock solution. For the purposes of illustration the preparation of a 3.5% gel is outlined below.

For each 10 ml of 3.5% gel combine:

4.5 ml of distilled water

3.3 ml of 3 E + TEMED

1.75 ml 20% acrylamide stock

Mix thoroughly. Then add:

0.5 ml 1% $(\text{NH}_4)_2\text{S}_2\text{O}_8$

Mix again.

Pipette into 30 X 0.64 cm Plexiglas tubes which have been cleaned, dried and sealed at the bottom with two layers of stretched Parafilm. As soon as all gels have been poured, carefully overlayer the acrylamide in each tube with 100 μl of water. Allow to polymerize a minimum of 1 hour.

Prior to electrophoresis the Parafilm is removed and replaced with nylon netting secured with a rubber band. The Parafilm can be left in place and punctured repeatedly with a fine wire to allow electrical contact but the danger of extruding the gel into the lower reservoir and draining the upper reservoir is much greater.

Electrophoresis

Running buffer (E buffer) is one part 3 E diluted with two parts of distilled water. Acrylamide gels should be preelectrophoresed for at least two hours at 80 volts (v). A longer preelectrophoresis may be desirable if the gels are to be scanned at 265 nm. If the gels are preelectrophoresed for extended times the buffer should be changed before applying the samples. This will not be necessary if the buffer is recirculated.

Samples are layered directly on top of the gel after making the solution 10% in glycerol. A sample volume of 25 μ l is the most practical compromise between the need for a thin lamella of sample and ease of sample handling. Up to 200 μ l can be applied but with this volume the bands formed by the smaller fragments become very diffuse because of poor stacking at the beginning of the run and diffusion during the run.

Electrophoresis is carried out at room temperature at 125 v for 30 cm tubes. The current per tube (0.64 x 30 cm) is \sim 5 ma; if the current increases as the electrophoresis proceeds the current may be too high. Excessive current causes the gels to overheat; the voltage therefore should be adjusted so that the current remains approximately constant.

Electrophoresis is usually continued for 5-8 hours without recirculating the buffer. The electrophoresis can probably be continued for up to 10 hours without changing the buffer or circulating it; the practical limit on the time is the pH shift resulting from electrolysis of the buffer and therefore varies with the size of the buffer reservoir.

Visualization of DNA Bands

After electrophoresis the gels are extruded with compressed air into 50-100 ml of E buffer which contains 1 μ g ethidium bromide/ml. The gels are soaked for 1-4 hours and then removed and arranged on a grooved plate. The DNA is then located by shining ultraviolet light on the gels; the ethidium bromide intercalated into DNA fluoresces a bright orange. The fluorescence may be photographed using a combination of an ultraviolet filter (Photar Haze H2-A) and an orange filter (Photar Orange). A Polaroid MP-3 Land camera loaded with Type 55 or 107 film is used routinely to photograph the gels.

Toluidine blue or Stains All may also be used to locate and quantitate the bands. However ethidium bromide provides the most sensitive way to locate the DNA bands, though it has not proved to provide a quantitative measure of the amount of DNA present.

40:1 Acrylamide : bis-Acrylamide Gels

The 20:1 acrylamide : bis-acrylamide gel system described above was used routinely for both analytical and preparative gel work. In some cases a ratio of acrylamide to bis-acrylamide of 40:1 was substituted because the resolution of both high and low molecular weight DNAs appeared to be improved in this system. In all other respects the gels were prepared according to the procedures established for 20:1 gels except that 20 g of acrylamide and one half gram of bis-acrylamide are used for each 100 ml of 20% stock solution.

Preparative Electrophoresis

Preparative electrophoresis of the PM2-HaeIII restriction fragments was performed using the apparatus described by Hagen and Young (15). In this apparatus the DNA is continuously eluted by a continuous flow of buffer through a chamber attached to the bottom of the gel tube; as the DNA is electrophoresed into the chamber the buffer sweeps it away. Therefore the PM2-HaeIII fragments can in principle be isolated from smallest to largest in one step. However, there are several difficulties which prevent it.

The first difficulty is retaining resolution over the entire size range (50-2000 bp). Resolution is promoted by increasing the gel concentration and the gel length. Since the smallest fragments are

the most difficult to resolve, the larger fragments are overresolved on long, high percentage gels. Furthermore the bands formed by the larger fragments are electrophoresed out of the gel very slowly so that the peak is broad and diffuse. In some cases it may not be practical to try to recover the DNA. Slowing the flow rate of the elution buffer only allows the DNA to electrophorese across the chamber to be lost before it is swept out; presumably the DNA is held tightly by the electric field against the dialysis membrane which forms the bottom of the chamber.

A second difficulty was also observed while carrying out experiments to determine optimal loadings and flow rates. The problem was that larger DNAs were not eluted as soon or in as high a concentration as one might predict that they would be. At first this appeared to be a problem of over-resolution, since one might expect the yield of the larger DNAs to suffer because of the long electrophoresis and the slow elution. However it also occurs with the smaller fragments. For example fragments D through P were pooled, concentrated and reelectrophoresed under conditions which had previously given both good resolution and recovery of all of the fragments except A, B and C. The reelectrophoresis resulted in poor recoveries of D, E, F and G. Therefore the recovery problem is a question of the amount or concentration of the DNA which is applied to the gel and not simply a matter of the size of the applied DNA. Resolution and limits on the

DNA loading therefore prevent a one step separation of all the PM2-HaeIII fragments.

Our solution to these difficulties was to resolve the mixture by crudely separating groups of the fragments and then separating the groups into individual fragments. For the crude separation a 4% acrylamide (40:1) gel 4 cm in length was used, while a 3.5% acrylamide (20:1) gel 6-12 cm long was used for resolving the individual fragments. Agarose gels could be used for the crude separation but optimum loadings are lower in agarose gels.

The gels are cast in cylindrical borosilicate glass gel tubes 1.7 cm in diameter which has been sealed with three layers of Parafilm. The gel is overlaid with 500 μ l of isoamyl or isobutyl alcohol instead of water; these alcohols attack plastic and therefore should not be used to overlayer analytical gels in Plexiglas tubes.

The apparatus is assembled and preelectrophoresis is carried out overnight at a current of 15-20 milliamperes (ma). E buffer is circulated through the elution chamber at a flow rate of 6.5-7.5 ml/hr during preelectrophoresis. The buffer in the upper and lower reservoirs was not circulated in most experiments but the buffer was changed every 24-48 hours of continuous electrophoresis. The gels can be used for several separations if all of the DNA from a previous run has been eluted. After three to four runs the resolution deteriorates sufficiently to require a new gel.

After preelectrophoresis the sample is applied in 200 μ l of 10 fold diluted E buffer which has been made 10% in glycerol. Electrophoresis is then continued at 15-20 ma and buffer pumped through the elution chamber at 6.5-7.5 ml/hr. All of the fragments are eluted from the short 4% gel in 20 hours, and so a new sample may be applied and separated every 24 hours. The short gel only resolves fragments A, B and C from each other. However the groups of fragments D-H, I-K and L-P are resolved from each other so that the pooled fractions can be concentrated and the individual fragments can be resolved in the longer 20:1 gel. Concentration of the DNA in E buffer is done by hydroxylapatite chromatography at room temperature as described by Britten, Graham and Neufeld (27). Further concentration of the material eluted from hydroxylapatite is accomplished by dialysing against E buffer and precipitating the DNA with 3 volumes of ethanol. The concentrated DNA is applied in the same volume of solution as previously and electrophoresed at the same current. However, the voltage will be higher due to the longer gel. If desired the eluted material may again be concentrated by hydroxylapatite chromatography and ethanol precipitation. Smaller isolated restriction fragments do not precipitate well because of their size and low concentration, but the recovery is somewhat improved by using 5 volumes of absolute ethanol in the precipitation.

APPENDIX III

PROGRAMS FOR THE HEWLETT PACKARD 9821A CALCULATOR

The programs which follow were written for the Hewlett Packard 9821A Calculator. Several of the programs require the following peripherals; the 9864A digitizer, the 2748B paper tape reader, the 9862A plotter and a standard Teletype interfaced to the calculator. The following selection codes were assigned to the respective peripherals: Code 1 to the tape reader; code 2 to the Teletype and code 3 to the digitizer. In addition the following Read Only Memory (ROM) modules are required; 1) Peripheral Control II (Model 11224A); 2) Mathematics (Model 11221A); 3) Peripheral Control I (Model 11220A). The ROMs are installed in numerical order from left to right.

"Digitize Equilibrium Data"

The program "Digitize Equilibrium Data" utilizes the 9864A digitizer to reduce the scanner output for the Model E ultracentrifuge to optical density as a function of position within the centrifuge cell. The output is recorded on paper tape via the Teletype. The resulting tape is perfectly compatible with the program *Mw for the CDC 3300 computer in the OS-3 timesharing system.

This program requires the slope and intercept for the linear relationship between the optical density in the centrifuge cell and calibration stairsteps. The calibration stairsteps relate pen displacement to optical density. The position of the meniscus and the outer reference hole at 1.00 OD are also required.

The sequence of operations is as follows: 1) Align the scan within the coordinate system of the digitizer. The y coordinate is proportional to optical density and the x coordinate is the relative position within the cell. 2) Enter the slope (m) and intercept (b) for the relationship $OD = my + b$. 3) Enter the position of the meniscus and the outer reference hole. The zero point is the inner reference hole. The measurements may be in cm or mm, but they both must be in the same units. 4) Sample the meniscus position at $y = 0$ with the digitizer in the single sample mode. 5) Sample the outer reference hole at $y = (1.00 - b)/m$. The Teletype will print 0, x at the outer reference. 6) Sample the data from the meniscus to the bottom of the cell with the digitizer in the single sample mode. After each point is sampled the Teletype will print the coordinates x, OD for that point. 7) Finish the tape by typing 0, CR, LF on the Teletype. 8) Return to the beginning of the program for new data.

"Fit and Plot in 3 Coordinate Systems"

The program "Fit and Plot in 3 Coordinate Systems" is used to carry out a least squares fit for gel data in any one of three coordinate systems. The data and the line for the linear fit may then be plotted in the coordinate system for which the fit was made. The input data is paper tape with the format M 1, Mob 1, M 2, Mob 2, etc. M = 0 terminates loading. The molecular weight (M) may be in daltons or basepairs for any data set and the mobility (Mob) is usually in centimeters. Any linear scale for the mobility can be used. The optional coordinate systems are as follows: 1) LOGMW vs MOB in which the logarithm of the molecular weight in daltons is plotted as a function of the mobility. 2) MW vs 1/MOB in which the molecular weight in daltons is plotted as a function of the reciprocal of the mobility. 3) LMW vs LDU/U in which the logarithm of the molecular weight in daltons is plotted as a function of the quantity $\log (U_m - U) / U$. U is the electrophoretic mobility and U_m is the same as the V_m in the text. As stated before, V_m is the hypothetical maximum mobility in the gel.

The sequence of operations is as follows. 1) Enter the minimum and maximum x and y coordinates for the plot. The units must be those of the coordinates of the plot, i. e. the minimum y coordinate is the logarithm of the minimum molecular weight in daltons if

the plot is for a coordinate system in which $y = \log MW$. "NUMBER OF POINTS" is the number of points into which the range from the minimum x to the maximum x will be divided. The calculator plots a line by calculating the y for successive x coordinates in the range. Therefore "NUMBER OF POINTS" determines the distance between successive x coordinates. 2) Select and enter the desired interval between the tic marks which will be drawn on the axes. 3) Select the coordinate system. 4) Draw axes if desired. 5) Input tape data. If the LMW vs LDU/U system has been chosen enter U_m . 6) Plot the data. 7) Plot individual points if desired. 8) Fit the data in the chosen coordinate system. The fit routine allows the exclusion of individual points from the fit. 9) Output the slope and intercept of the fit. U_m is output if applicable. The coordinate system for the fit is also printed. 10) Plot the least squares line if desired. 11) Input new data or return to the fit if desired.

"Plot Slope-Intercept Data in 3 Coordinate Systems"

The program "Plot Slope-Intercept Data in 3 Coordinate Systems" is used primarily to plot a line in any of the coordinate systems described under "Fit and Plot in 3 Coordinate Systems" from the slope and intercept of the linear fit in any other coordinate system. Data on paper tape and individual points may also be plotted. The sequence of operations is as follows. 1) Enter the

information listed in steps 1, 2, and 3 of "Fit and Plot". This establishes the axes. 2) Select the coordinate system in which the plot is to be made. 3) Draw axes if desired. 4) Plot data from paper tape. If the system LMW vs LDU/U has been chosen U_m must be entered. Remember that U_m and V_m are interchangeable. 5) Plot individual points if desired. 6) Enter the slope and intercept for the linear fit. 7) Select the coordinate system in which the fit was carried out. Enter U_m if the coordinate system is LMW vs LDU/U. 8) Plot the line. 9) Return to step 6 or go to the beginning of the program for new data.

"Optimize V_m "

The program "Optimize V_m " minimizes the sum of the squares of the deviations for the linear fit to data in the LMW vs LDU/U coordinate system by systematically changing the value of V_m . In this program as in the others V_m and U_m are interchangeable. The program prints out the optimum V_m , the slope and intercept of the line and the sum of the deviations and of the squares of the deviations in log M. The sequence of operations is as follows. 1) Input tape data. 2) Enter a preliminary U_m . The number entered must be larger than any of the mobilities given in the data set. 3) Initiate the iteration by pressing run program. 4) The result will be printed out when the iteration is complete. The iteration is terminated by an

internal check on the size of the increment by which V_m is changed (Program line 20). Therefore V_m may be determined to any desired accuracy. In the program presented here the program terminates when V_m has been determined to 2 decimal places.

"Y-F Equations"

The program "Y-F Equations" calculates the coefficients for the two Yamakawa-Fujii equations and plots the relationship between the $s_{20,w}^0$ and the molecular weight predicted by the theory. The program also allows the operator to plot individual points. The coordinate system for the plot is the $s_{20,w}^0$ in Svedbergs (S) as a function of the logarithm of the molecular weight in daltons; the individual points are also plotted in these coordinates although the input data may contain molecular weights in either daltons or base-pairs.

The program offers several options which allow for the direct manipulation of all the parameters included in the Yamakawa-Fujii equations. The helix diameter and the Kuhn statistical length in \AA are input individually along with the mass per unit length in daltons/ \AA . The factor $M_L(1 - \bar{v}\rho_o)/N_A(3\pi\eta_o)$ can be input directly or individual values of \bar{v} , ρ_o and η_o may be input individually and the factor calculated from these parameters. The molecular weight corresponding to σ is calculated from the Kuhn statistical length and the

mass per unit length; the change from Yamakawa-Fujii equation 4 to equation 2 is made automatically at this molecular weight.

The sequence of operations is as follows. 1) Set the constants desired for the Yamakawa-Fujii equation. 2) Set the minimum and maximum x and y and the number of points. The tic marks are preset at 1 Svedberg and $\log M = 0.5$. 3) Plot the Yamakawa-Fujii equation. This is done automatically after "YMAX" is entered. 4) Draw axes if desired. 5) Plot individual points. A multiplicative correction to the $s_{20,w}^0$ may be applied to all of the sedimentation coefficients; the units of the $s_{20,w}^0$ to be entered is the Svedberg. Molecular weights may be in daltons or basepairs.

Program "Digitize Equilibrium Data"

0:	9:
DSP "ALIGN SCAN"	DSP "MEASURE SCA
;CFG 0;STP F	N";STP F
1:	10:
IF FLG 0=1;GTO 7	ENT "MENISCUS";R
F	3,"OR";R4;DSP "S
2:	ET TO 0";STP F
RED 3,X,YF	11:
3:	DSP "SAMPLE ORY"
IF Y>.1;DSP Y;	;STP F
GTO 1F	12:
4:	RED 3,R5,R6;FMT
IF Y<-.1;DSP Y;	FXD 1.0,FXD 5.0;
GTO 1F	WRT 2,0,R4F
5:	13:
IF Y=0;WRT 3;	DSP "READ DATA";
DSP Y;WRT 3;DSP	STP F
Y;GTO 1F	14:
6:	RED 3,X,Y;((R4-R
WRT 3;DSP Y;GTO	3)/R5)X+R3+A;(R2
1F	/R6)YR0+R1+B
7:	15:
DSP "STAIRSTEPS"	FMT FXD 4.0,FXD
;STP F	6.3;WRT 2,A,B;
8:	GTO -1F
ENT "SLOPE",R0,"	16:
INTERCEPT",R1;(1	END F
-R1)/R0+R2F	Z1127
	R1134

Program "Fit and Plot in 3 Coordinate Systems"

```

0:
ENT "XMIN?",R0,"
XMAX?",R1,"NO. 0
F POINTS?",R2F
1:
ENT "YMIN?",R12,
"YMAX",R13F
2:
ENT "X TIC",R14,
"Y TIC",R15F
3:
FXD 2:PRT "XMIN"
,"XMAX",R0,R1;
SPC F
4:
PRT "YMIN","YMAX
",R12,R13;SPC F
5:
PRT "X TIC","YTI
C",R14,R15;SPC 3
F
6:
ENT "LOG MW VS M
OB=1",R18,"LMW V
S LDU/U=2",R18,"
MW VS 1/MOB=3",R
18F

```

```

7:
PEN ;CFG 13;ENT
"AXES? YES=1",Z;
IF FLG 13#0;GTO
+2F
8:
SCL R0,R1,R12,R1
3;AXE R0,R12,R14
,R15F
9:
CFG 13;ENT "TAPE
? NO=1",Z;IF
FLG 13=0;GTO 13F
10:
0+R16;IF R18=2;
ENT "UM",R19F
11:
RED 1,Y,X;Y+R(26
+3R16);IF Y=0;
GTO +2F
12:
X+R(27+3R16);1+R
16+R16;GTO -1F
13:
CFG 13;ENT "PLOT
TAPE? NO=1",Z;
IF FLG 13=0;GTO
21F
14:
GSB "DBP"F

```

```

15:
GSB "ERASE"F
16:
CFG 13;ENT "PLOT
? NO=1",Z;IF
FLG 13=0;GTO 21F
17:
GSB "SELECT"F
18:
IF FLG 13=1;GTO
+2F
19:
PLT X,Y;PEN ;
GTO -2F
20:
CFG 13;ENT "ERAS
EMORE=1",Z;IF
FLG 13=0;GTO 15F
21:
PEN ;CFG 13;ENT
"HANDPLT PTS? Y=
1",Z;IF FLG 13#0
;GTO +4F
22:
GSB "DBP"F
23:
GSB "HENT"F
24:
PLT X,Y;PEN ;IF
FLG 13=0;GTO -1F

```

```

25:
CFG 13;ENT "LSQR
S? NO=1",Z;IF
FLG 13=0;GTO 9F
26:
GSB "DBP"F
27:
0+R3+R4+R5+R6+R7
+R8+R10+R11F
28:
GSB "ERASE"F
29:
GSB "SELECT"F
30:
IF FLG 13=1;GTO
+2F
31:
R5+Y+R5;R8+YY+R8
;R4+X+R4;R6+XY+R
6;R7+XX+R7;R3+1+
R3;GTO -2F
32:
CFG 13;ENT "NEW
DATA? YES=1",Z;
IF FLG 13=0;0+R1
6;GTO 9F

```

Program "Fit and Plot in 3 Coordinate Systems" (Cont.)

33:	40:	51:	62:
CFG 13;ENT "LIST	PLT X;Y;IF (X+Z+	IF R18=2;(R19-X)	1+R(25+3(Z-1));
M&B? NO=1";Z;	X)R1;GTO -1F	/X+X;LOG X+X;	GTO -1F
IF FLG 13=0;GTO	41:	RET F	63:
+4F	PEN ;CFG 13;ENT	52:	"HENT" F
34:	"MORE LSQRS? Y=1	"F" F	64:
END 0;PRT "N=";R	";Z;IF FLG 13=0;	53:	CFG 13;IF R9=2;
3;PRT "Y=MX+B" F	0+R16;GTO 9F	R10X+R11+Y;RET F	ENT "MW IN D";Y;
35:	42:	54:	GTO +2F
(R4R5-R3R6)/(R4R	GTO 27F	"DBP" F	65:
4-R3R7)+R10;FLT	43:	55:	ENT "MW IN BP";Y
5;PRT "M=";R10F	"MW" F	ENT "D=2 OR BP=0	F
36:	44:	"R9;RET F	66:
(R4R6-R7R5)/(R4R	IF R9=0;GTO +3F	56:	IF FLG 13=1;RET
4-R3R7)+R11;FLT	45:	"CLR1" F	F
5;PRT "B=";R11;	IF R18<2;LOG Y+Y	57:	67:
GSB "LABEL" F	;RET F	0+R(25+3R17);IF	ENT "MOBILITY";X
37:	46:	R17<R16;1+R17+R1	;GSB "MW" F
CFG 13;ENT "PLTL	RET F	7;GTO -0F	68:
SQLINE? NO=1";Z;	47:	58:	GSB "MOB" F
IF FLG 13=0;GTO	663Y+Y;GTO -2F	0+R17;RET F	69:
+4F	48:	59:	RET F
38:	"MOB" F	"ERASE" F	70:
SCL R0;R1;R12;R1	49:	60:	"SELECT" F
3;R0+X;(R1-R0)/R	IF R18=1;RET F	GSB "CLR1" F	71:
2+2F	50:	61:	R(25+3R17)+Z;IF
39:	IF R18=3;1/X+X;	ENT "ERASE-END W	Z=1;1+R17+R17;
GSB "F" F	RET F	ITH 0";Z;IF Z=0;	GTO -0F
		0+R17;RET F	

Program "Fit and Plot in 3 Coordinate Systems" (Cont.)

```

72:      CFG 13;R(26+3R17
      )+Y;IF Y=0;SFG 1
      3;0+R17;RET +
73:      R(27+3R17)+X;1+R
      17+R17;GSB "MW"+
74:      GSB "MOB"+
75:      RET +
76:      "LABEL"+
77:      IF R18=3;-R10/R1
      1+R20;PRT "UM=",
      R20+
78:      SPC ;PRT "FOR X=
      ";IF R18=1;PRT "
      MOBILITY
      "+
79:      IF R18=2;PRT "
      (UM-U)/U";
      PRT "UM=",R19+
80:      IF R18=3;PRT "
      1/MOBILITY"+
81:      PRT "FOR Y=";IF
      R18=2;PRT "
      LOG MW";SPC 8
      ;RET +
82:      PRT "          MW"
      ;SPC 8;RET +
83:      END +
      Σ19092
      R900

```

Program "Plot Slope-Intercept Data in 3 Coordinate Systems"

```

0: SFG 14;ENT "XMIN
? ",R0,"XMAX?",R1
,"NO. OF POINTS?
",R2F
1: ENT "YMIN?",R12,
"YMAX",R13F
2: ENT "X TIC",R14,
"Y TIC",R15F
3: FXD 2;PRT "XMIN"
,"XMAX",R0,R1;
SPC F
4: PRT "YMIN","YMAX
",R12,R13;SPC F
5: PRT "X TIC","YTI
C",R14,R15;SPC 3
;GSB "DBP" F
6: ENT "LOG MW VS M
OB=1",R18,"LMW V
S LDU/U=2",R18,"
MW VS 1/MOB=3",R
18F
7: PEN ;CFG 13;ENT
"AXES? YES=1",Z;
IF FLG 13#0;GTO
+2F
8: SCL R0,R1,R12,R1
3;AXE R0,R12,R14
,R15F
9: CFG 13;ENT "TAPE
? NO=1",Z;IF
FLG 13=0;GTO 15F
10: IF R18=2;ENT "UM
",R19F
11: RED 1,Y,X;IF Y=0
;GTO +4F
12: GSB "MW" F
13: GSB "MOB" F
14: PEN ;PLT X,Y;
GTO -3F
15: PEN ;CFG 13;ENT
"HANDPLT PTS? Y=
1",Z;IF FLG 13#0
;GTO +4F
16: GSB "DBP" F
17: GSB "HENT" F
18: PLT X,Y;PEN ;IF
FLG 13=0;GTO -1F
19: CFG 13;ENT "PLT
MORE PTS N=1",Z;
IF FLG 13#0;GTO
9F
20: ENT "SLOPE",R10,
"INTERCEPT",R11,
"MOBILITY=1",R20
,"LOG(UM-U)/U=2"
,R20F
21: ENT "1/MOBILITY=
3",R20;IF R20=2;
ENT "UM (LSQRS )
",R21F
22: CFG 13;ENT "PLOT
NOW? NO=1",Z;
IF FLG 13=0;GTO
9F
23: SCL R0,R1,R12,R1
3;R0+X;(R1-R0)/R
2+Z F
24: GSB "PMOB" F
25: GSB "PF" F
26: GSB "PMW" F
27: PLT X,Y;IF (X+Z+
X)/R1;GTO -3F
28: PEN ;CFG 13;ENT
"BACK TO PT PLT=
1",Z;IF FLG 13=0
;GTO 7F
29: GTO 20F
30: "MW" F
31: IF R9=0;GTO +3F

```

Program "Plot Slope-Intercept Data in 3 Coordinate Systems (Cont.)

```

32: IF R18<2;LOG Y+Y
;RET F
33: RET F
34: 663Y+Y;GTO -2F
35: "MOB" F
36: IF R18=1;RET F
37: IF R18=3;1/X+X;
RET F
38: IF R18=2;(R19-X)
/X+X;LOG X+X;
RET F
39: "F" F
40: R10X+R11+Y;RET F
41: "PF" F
42: R10A+R11+B;RET F
43: "DBF" F
44: ENT "D=2 OR BP=0
",R9;RET F
45: "HENT" F
46: CFG 13;IF R9=2;
ENT "MW IN D",Y;
GTO +2F
47: ENT "MW IN BP",Y
F
48: IF FLG 13=1;RET
F
49: ENT "MOBILITY",X
;GSB "MW" F
50: GSB "MOB" F
51: RET F
52: "PMOB" F
53: IF R18=R20;X+A;
RET F
54: IF R18=2;IF R20=
2;1/X+A;RET F
55: IF R18=1;IF R20=
2;LOG ((R21-X)/X
)+A;RET F
56: IF R20=2;1/X+C;
LOG ((R21-C)/C)+
A;RET F
57: IF R18=2;R21/(
TN+ X+1)+A;IF R2
0=1;RET F
58: 1/A+A;RET F
59: "PMW" F
60: IF R18=R20;B+Y;
RET F
61: IF R18<2;IF R20<
2;B+Y;RET F
62: IF R20=3;LOG B+Y
;RET F
63: IF R18=3;TN+ B+Y
;RET F
64: END F
Σ15224
R994

```

Program "Optimize Vm"

0:	9:	16:	22:
CFG 13;ENT "TAPE	R(26+3R17)÷Y;IF	IF FLG 4=0;B÷R12	PRT " SUMS";
? NO=1",Z;IF	Y=0;0÷R17;GTO +3	;C÷R2;1+R0÷R0;	PRT "D=",R12,"DS
FLG 13=0;GTO 5F	F	SFG 4;GTO 8F	QR=",R2;SPC 8F
1:	10:	17:	23:
0÷R16;GSB "DBP" F	R(27+3R17)÷X;1+R	IF C≤R2;B÷R12;C÷	GTQ 0F
2:	17÷R17;LOG ((R0-	R2;R1+R0÷R0;R10÷	24:
RED 1,Y;IF Y=0;0	X)÷X)÷XF	R13;R11÷R14;CFG	"F" F
+R(26+3R16);GTO	11:	3;GTO 8F	25:
+3F	R5+Y÷R5;R8+YY÷R8	18:	R10X+R11÷Y;RET F
3:	;R4+X÷R4;R6+XY÷R	IF FLG 3=0;R0-R1	26:
IF R9=0;663Y÷YF	6;R7+XX÷R7;R3+1÷	-R1÷10÷R0;-R1÷10	"DBP" F
4:	R3;GTO -2F	+R1;SFG 3;GTO +2	27:
RED 1,X;LOG Y÷R(12:	F	ENT "D=2 OR BP=0
26+3R16);X÷R(27+	(R4R5-R3R6)÷(R4R	19:	",R9;RET F
3R16);1+R16÷R16;	4-R3R7)÷R10;(R4R	-R1÷R1;R0+R1÷R0;	28:
GTO -2F	6-R7R5)÷(R4R4-R3	GTO 8F	END F
5:	R7)÷R11F	20:	226044
CFG 13;ENT "LSQR	13:	IF R1R1>1E-5;	R1053
S? NO=1",Z;IF	IF R17>R16-1;0÷R	GTO 8F	
FLG 13=0;GTO 0F	17;GTO +3F	21:	
6:	14:	R0-R1÷R0;FXD 2;	
GSB "DBP" F	R(27+3R17)÷X;	PRT "UN=",R0;	
7:	LOG ((R0-X)÷X)÷X	SPC ;FLT 5;PRT "	
ENT "UM",R0;1÷R1	;XR10+R11÷Y;R(26	SLOPE=",R13,"INT	
;0÷B÷C;CFG 3;	+3R17)÷Z;(Y-Z÷A)	ERCEPT=",R14;	
CFG 4F	+B÷BF	SPC F	
8:	15:		
0÷R3÷R4÷R5÷R6÷R7	AA+C÷C;1+R17÷R17		
+R8÷R10÷R11÷B÷CF	;GTO -2F		

Program "YF Equations"

```

0:
ENT "DIA IN A?";
R3;"LAMBDA IN A?";
R4;"M SUB L?";
R5F
1:
CFG 13;ENT "SET
YF C? YES=1";Z;
GTO +3;IF FLG 13
=0;ENT "1.525?";
R21F
2:
ENT "V BAR ";X;
GTO +2;ENT "RHO"
,Y;R5(1-XY)+YF
3:
ENT "NU 20 W";X;
3*602.3/X+X;Y/X+
R21F
4:
R4R5+R6;R3/R4+R7
;R7R7+R8;R7R8+R9
;R8R8+R10F
5:
LOG (2.278R4R5)+
R22;1-.01412R8+.
00592R10+R11F
6:
.3863-.1667R7+.0
016R8-.0224R9-7E
-4R10+R12F
7:
.1667+.0222R8+.0
017R10+R13;.0188
3-.00789R8-.0003
8R10+R14F
8:
-.002039+.000805
R8+.000017R10+R1
5F
9:
(4/3)F(6/PI)+R16;
.1382+.6910R8+R1
8F
10:
-(1-.01412R8+.00
592R10)LN R7+R17
F
11:
R17-1.0561-.1667
R7-.19R8-.0224R9
+.019R10+R17F
12:
-(.04167R8+.0056
7R10)LN R7+R19F
13:
R19-.3301+.5R7-.
5854R8-.0094R9-.
0421R10+R19F
14:
-.0300+.1209R8+.
0259R10+R20F
15:
R12-R11LN (R6R7)
+R12;R13/R6+R13F
16:
R14/R6R6+R14;R15
/R6R6R6+R15F
17:
R16/R6+R16;R18F
R6+R18F
18:
R19R6+R19;R20R6R
6/R6+R20F
19:
CFG 13;ENT "PLOT
? NO=1";Z;IF
FLG 13=0;GTO 0F
20:
ENT "XMIN?";R0,"
XMAX?";R1;"NO. 0
F POINTS?";R2F
21:
CFG 13;ENT "YMIN
?";B;GTO +1;IF
FLG 13=0;ENT "YM
AX?";A;JMP 7F
22:
R0+X;(R1-R0)/R2+
Z;GSB "F"F
23:
Y+A+B;GTO +4F
24:
GSB "F"F
25:
IF Y>A;Y+AF
26:
IF Y<B;Y+BF
27:
IF (X+Z+X)<R1;
GTO -3F
28:
SCL R0,R1,B,A;
PRT " XMIN"
," XMAX",R0
,R1;SPC F
29:
PRT " YMIN"
," YMAX",B;
A;SPC 3F

```

Program "YF Equations" (Cont.)

30:	38:	46:
R0=X; (R1-R0)/R2+	CFG 13; ENT "MW I	R16TN+ (X/2)+R17
Z+	N BP"; X; LOG X+	+R18TN+ (-X/2)+R
31:	LOG 663+X; ENT "S	19TN+ (-X)+R20
GSB "F"+	20 W"; Y; CY+Y;	TN+ (-3X/2)+Y+
32:	PLT X, Y; PEN +	47:
PLT X, Y; IF (X+Z+	39:	GTO +2+
X) < R1; GTO -1+	IF FLG 13=0; GTO	48:
33:	-1+	XR11LN 10+R12+R1
PEN ; CFG 13; ENT	40:	3TN+ X+R14TN+ (2
"AXES?"; Z; IF	GTO +3+	X)+R15TN+ (3X)+Y
FLG 13=0; GTO 0+	41:	+
34:	CFG 13; ENT "MW I	49:
SCL R0, R1, B, A;	N D"; X; LOG X+X;	R21Y+Y; RET +
AXE R0, B, .5, 1+	ENT "S 20 W"; Y; C	50:
35:	Y+Y; PLT X, Y; PEN	END +
PEN ; CFG 13; ENT	+	25908
"PLT PTS? NO=1",	42:	R962
Z; IF FLG 13=0;	IF FLG 13=0; GTO	
GTO 0+	-1+	
36:	43:	
ENT "CORR TO S?"	GTO -8+	
; C+	44:	
37:	"F"+	
ENT "D=2 OR BP=0	45:	
", Z; IF Z=2; GTO +	IF X < R22; GTO +3+	
4+		